REMOVAL OF METHYLENE BLUE FROM AQUEOUS SOLUTIONS USING HIERARCHICAL ZSM-5

by

MBOKANE BAFANA NJABULO

DISSERTATION

Submitted in fulfilment of the requirements for the degree of

MASTER OF SCIENCE

in

CHEMISTRY

to the

FACULTY OF SCIENCE AND AGRICULTURE

(School of Physical and Mineral Sciences)

at the

UNIVERSITY OF LIMPOPO

SUPERVISOR: Prof. M. P. Mokhonoana

Co-SUPERVISOR: Prof R. Meijboom (UJ)

2017

DEDICATION

To my late brother Mathatha Solomon Mbokane, my parents, siblings and my girlfriend.

DECLARATION

I declare that the dissertation hereby submitted to the University of Limpopo, for the degree of Master of Science in Chemistry has not previously been submitted by me for a degree at this or any other institution; that this is my work in design and execution, and that all foreign material contained herein has been duly acknowledged.

…….. ……..

Mr B.N Mbokane **Date**

ACKNOWLEDGEMENTS

My sincerest and utmost gratitude goes to my supervisors Prof M.P. Mokhonoana and Prof R. Meijboom for their support, guidance and unrivalled patience during the course of this work. I would further like to extend much thanks to the following individuals and institutions for any and all help offered during this academic journey, without whom successful completion would have been near impossible:

- The Department of Chemistry at The University of Limpopo for affording me the opportunity to do a postgraduate degree in their institution.
- NRF-SASOL Inzalo Foundation for financial support.
- The University of Limpopo Geology Department for XRD analysis.
- Ms Batsile Mogadi and Mr Ndzondolelo Bingwa at The University of Johannesburg for BET surface area measurements and FTIR analysis.
- Dr P.B. Ramatsetse at The University of Pretoria for SEM micrographs.
- Mr M.B. Muluvhu, Mr N.M. Chauke and Mr C. Maswanganyi for encouragement and technical support.
- My lab mates and academic family Ms W. Monama and Mr R.L. Thubakgale for academic and social support.
- My family for their prayers, support and encouragement.
- Lastly and definitely most of all, the almighty God for the strength and endurance to complete this degree.

ABSTRACT

Pristine ZSM-5 zeolites with SARs of 25 and 50, together with their post-synthetically acid-dealuminated versions were prepared and characterised by a combination of physicochemical techniques: X-ray diffraction (XRD), Fourier-transform infrared (FTIR) spectroscopy, scanning electron microscopy (SEM), as well as nitrogen adsorption isotherms and BET surface area measurements. These materials were further evaluated for efficiency as adsorbents in the removal of the methylene blue, as a model textile contaminant, from simulated wastewater using a batch approach. XRD revealed that ZSM-5(50) retained its MFI framework structure throughout the dealumination duration, while ZSM-5(25) produced an additional non-MFI phase at dealumination times exceeding 3 hours. The relative XRD crystallinity for both series of zeolites decreased with increasing acid dealumination time, demonstrating the destructive nature of the acid treatment. It was also observed that the Scherrer crystallite size varied differently for the two series of zeolites: ZSM-5(25) and ZSM-5(50). A change from purely microporous to combined microporous-mesoporous hierarchies for both ZSM-5 series consequent to acid treatment was demonstrated by nitrogen adsorption isotherms. That is, pristine zeolites exhibited a Type I N_2 adsorption isotherm, while their acid-treated derivatives showed Type IV isotherms with a hysteresis loop, characteristic of mesoporous materials. The BET surface area (S_{BET}) of these zeolites improved remarkably with acid-dealumination treatment. For example, the S_{BET} of pristine ZSM-5(25) increased from 109 to 301 m^2/g after dealumination for 5 hours, while that of pristine ZSM-5(50) increased from 105 to 335 m^2/g after only 3 hours of acid-treatment. However, this latter material showed a reduced surface area (275 m^2/g) after a longer treatment time of 5 hours. In addition to coffin-shaped and rod-shaped crystals that are characteristic of ZSM-5 materials, the parent ZSM-5(50) material showed an atypical morphology, consisting of large deltoidal icositetrahedral crystals, previously observed for analcime zeolite. The dominance of these icositetrahedral crystals in MFI is spectacular, and marked the first appearance in the history of ZSM-5. Dealumination of ZSM-5(50) for different durations induced different changes in crystal morphology. A striking change in morphology was observed upon dealuminating this zeolite for 4.5 hours, producing a cylindrical stack of self-assembled longitudinally-packed nanorods, together with a

mixed-morphology consisting of agglomerated particles with ill-defined grain boundaries and coffin-shaped prismatic crystals.

MB adsorption studies on microporous ZSM-5 and its acid-dealuminated forms revealed that all materials perform best at pH ~8 (*i.e*., pH 7.91), with the removal efficiencies ranging from ~20 % to ~95 % in the case of ZSM-5(50) series, and ~22 % to ~95 % for ZSM-5(25). The corresponding MB adsorption capacity for ZSM-5(50) series ranged from ~5 to ~21.23 mg/g and ~8.33 to ~38 mg/g for ZSM-5(25).

The percentage MB removal efficiency increased consistently with increasing adsorbent dose and contact time, while it decreased as a function of initial MB concentration. The adsorption capacity of these adsorbent systems only showed a clear decreasing trend when the performance of these materials was studied as a function of adsorbent dose, and increased as a function of initial MB concentration. Notably, the 5 hour-long dealumination of the ZSM-5 zeolite series produced the best-performing adsorbent series though the lower SAR material consists of a mixture of different crystalline phases instead of one.

Table of Contents

LIST OF FIGURES

LIST OF TABLES

LIST OF ABBREVIATIONS

MB	Methylene blue
IZA	International Zeolite Association
MFI	Mobil Five
SAR	Silica-to-alumina ratio
XRD	X-ray diffraction
FTIR	Fourier transform infrared
BET	Brunauer-Emmett-Teller
SEM	Scanning Electron Microscopy
ZSM-5	Zeolite Socony Mobile-5
SDA	Structure-directing agent
TBABr	Tetrabutylammonium bromide
CTAB	cetyl trimethylammonium bromide
TPABr	Tetrapropylammonium bromide
TPAOH	Tetrapropylammonium hydroxide
EFAL	Extra-framework aluminium
RC	Relative crystallinity
S_{BET}	BET surface area

CHAPTER 1

General Introduction

1.1 Water contamination

The textile industry, through its various phases, constitutes a major source of water contamination [1, 2]. The presence of textile dyes in water, including their toxic nature, affects both aquatic ecosystems and human health negatively and mandate the need for efficient treatment of such water [3]. This occurs because the presence of coloured organic effluents in water also hinders the permeability of light and thus prevents processes such as underwater photosynthesis. Various methods are available for the treatment of textile dye-laden water for environmentally-sound disposal and/or reuse. These methods include coagulation/flocculation, ozonation, adsorption, photocatalytic degradation and many others [1 - 4]. The current dissertation considers adsorption as a method of choice for the removal of textile dyes from aqueous media, and uses methylene blue (MB) as a model textile dye while simultaneously exploring porosity-empowered ZSM-5 zeolites as potential adsorbents.

1.2 Technologies for removal of dyes from water

Various methods have been used to treat dye-contaminated wastewater. From these methods, several studies have shown adsorption to be the most efficient technology for the remediation of dyes from aqueous industrial effluents due to its simplicity and low cost of operation [2 - 5]. Several materials such as activated carbon [2], clays [3], mesoporous (2 nm < d < 50 nm) materials, as well as microporous (0 nm < d < 2 nm) zeolites, including ZSM-5, NH_4-Beta and MCM-22 [6], have been investigated as adsorbents for the removal of MB from water with good efficiencies. Although activated carbon has an established reputation as an adsorbent for MB, the high cost of its production and “no reusability” render its widespread use uneconomical [2]. The research focus has therefore shifted towards investigating the use of cheaper inorganic materials such as zeolites as alternatives to activated carbon for application as adsorbents in the rehabilitation of dye-contaminated wastewater [3, 4]. It was found that the use of mesoporous silicates such as SBA-15 as adsorbents

in the adsorptive removal of MB is highly efficient due to better diffusion of the bulky MB components within the cavities, exhibiting adsorption capacities as high as 300 mg/g [4]. A comparison of the adsorptive performance of microporous zeolites (ZSM-5, 20.68 mg/g [5]) and mesoporous silicates (SBA-15, 300 mg/g [4]) for MB led to the choice of adsorbent material in this study, *viz*., hierarchical ZSM-5. This class of zeolites contains both micro- and meso-pores within the same matrix [7, 8]. The hierarchical matrix of ZSM-5 creates a molecular sieving effect that can improve the removal of bulky dye contaminants. Textile dyes, including MB, have complex and sterically hindered structures that prevent their diffusion into microporous adsorbent matrices such as conventional zeolites. Thus, mesopore-containing adsorbents can form an important basis in the design of adsorbent materials for the efficient decontamination of these dyes from aqueous systems, due to the ease of percolation of the bulky fragments into their matrices and entrapment inside the pores. In this study, the adsorption of MB by different variations of ZSM-5 zeolite, obtained *via* an acid-mediated dealumination process, was investigated with respect to pH, contact time, adsorbent mass and initial concentration.

1.3 Description of zeolites

Zeolites are naturally-occurring and synthetic aluminosilicates characterised by a crystalline and microporous (0 nm < d < 2 nm) crystal structure. These materials are built by a matrix of channels and cages that consist of silicon (Si), aluminium (Al) and oxygen (O) ions together with various other cations in extra-framework sites [9 – 11]. Structurally, zeolites are complex inorganic polymers based on an infinitely extending 3-dimensional framework of $[SiO_4]^{4-}$ and $[AlO_4]^{5-}$ tetrahedra, linked to each other by sharing a vertex oxygen atom. The general formula for the composition of a zeolite is:

$$M_{x/n}[(AlO_2)_x(SiO_2)_y].mH_2O \qquad [9],$$

where *M* is a positively charged exchangeable ion of valence *n*, that electrically compensates for the negative charge on the negative aluminosilicate framework. This negative charge arises from the coordination of aluminium and silicon atoms (tetra-coordinated with oxygen atoms), with Al having a valency of 3 and Si a valency of 4. Zeolite cavities are connected by channels that give rise to a variety of microporous structures that are penetrated only by sufficiently small molecules. This

produces a “molecular sieving” effect, which is very important in separation applications [10], as well as shape-selectivity, which is important for acid catalysis. Compounds with bulky structures and/or long chains may not be able to percolate into the microporous zeolite cavities. Zeolites are cation exchangers, which are often ion-exchanged with ammonium ions that can be later decomposed into gaseous ammonia and a framework hydrogen proton [12]. Protonic forms of zeolites are very strong Brønsted solid acids. There are thousands of zeolite types that are recognised by the International Zeolite Association (IZA), and are differentiated using codes which identify the topology. These include about 40 naturally occurring and 150 synthetic zeolites. The most common zeolites in various applications include ZSM-48, ZSM-22 and ZSM-11 [13], as well as ZSM-5 [9].

1.4 ZSM-5 zeolite

Zeolite ZSM-5 was first prepared in 1972 by Mobil Oil Corporation researchers Argauer and Landolt [9], and is part of the pentasil family of zeolites. ZSM-5 has an MFI framework topology and is both highly crystalline and acidic. This zeolite ZSM-5 has other attractive properties such as tuneable pore sizes, as well as good thermal and chemical stability. These properties, and the flexibility of the material for use in a wide range of applications, led to its choice for use in this study. The range of applications of ZSM-5 can be extended by targeting a specific property and carrying out in-situ, or post-synthetic functionalisation in order to improve performance.

1.4.1 Properties of ZSM-5

The MFI framework typically crystallises in the *Pnma* orthorhombic space group with lattice constants a = 20.1, b = 19.9 and c = 13.4 Å. Figure 1.2(a) below shows the framework diagram of the (100) face of ZSM-5, where the 10-membered ring apertures serve as entrances to the intersecting channels [12, 14].

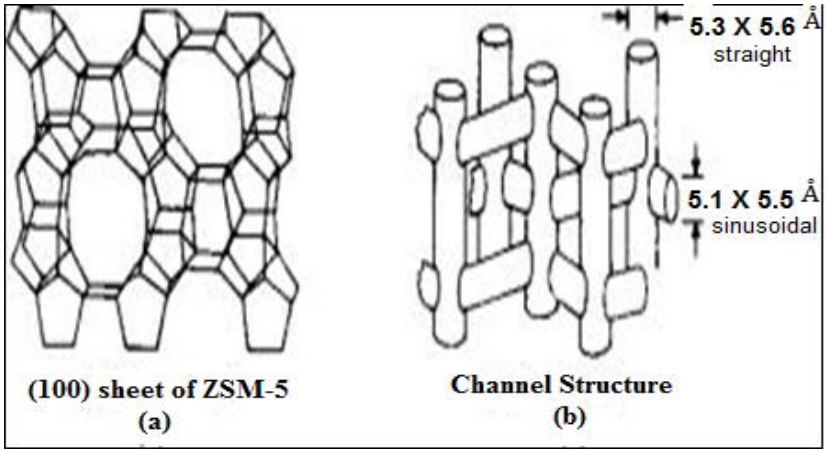

Figure 1.1: Structural connectivity in ZSM-5 zeolite [15].

The structure of ZSM-5 is characterised by the predominance of 5-membered ring cages [Figure 1.1(a)], where the vertices represent aluminium and/or silicon atoms with the lines representing oxygen atoms. The small cages join together to create 10-membered rings and the pore structure shown in Figure 1.1(b) above. The ZSM-5 framework contains two types of intersecting channel systems, *viz.*, straight channels with a nearly circular opening (5.3 × 5.6 Å), along (010) and a sinusoidal channel parallel to the (100) axis with an elliptical opening (5.1 × 5.5 Å) [15]. The surface of ZSM-5 consists of unbalanced negative charges, which are counter-balanced by H^+ ions to produce Brønsted adsorption sites, which enhance the affinity of ZSM-5 materials for the adsorption of cationic substrates [5]. It is reported that adsorption of cationic substrates occurs in two pathways, *viz*., a stepwise process or a concerted process. In the stepwise process, the substrate adsorbs one molecule at a time onto the adsorption site. In this case, the molecule binds to the adsorption site more strongly while other molecules bind to the first molecule. During the concerted process, individual molecules bind onto adsorption sites to form a larger ring with Brønsted sites and a zeolite framework. The simultaneous presence of micro- and meso-pores in hierarchical ZSM-5 is expected to enhance the adsorption and diffusion of bulky dye contaminants in ZSM-5 due to a molecular sieving effect. The Si/Al ratio of the framework controls the number of charge-balancing cations in the zeolite and hydrophilicity of a zeolite.

1.4.2 ZSM-5 as adsorbent for water contaminants

ZSM-5 is used in a number of industrial applications such as hydrocarbon cracking, adsorption, as well as purification of water and separation processes [14 – 18]. It is also used in agriculture to control soil pH and manure malodour [15], as well as to adsorb heavy metals such as lead and cadmium from the soil to limit their harmful availability to plants [16]. Furthermore, ZSM-5 enjoys widespread applications as an adsorbent for heavy metals and organic contaminants from water [17, 18]. Ali *et al*. [17] reported the use of ZSM-5 for the adsorptive removal of Pb^{2+} from aqueous solutions. The zeolite was modified and used with good efficiency, removing 85 % of Pb^{2+}. Hammed *et al.* [5] have recently reported the application of ZSM-5 as an adsorbent for the removal of MB from aqueous solutions. In their study, the zeolite was modified by coating with sugar solutions and impregnating with iron (Fe) to enhance MB removal performance. This novel modified ZSM-5 was found to have strong ion-exchange properties, and the removal of MB was improved from 20.68 mg/g for microporous ZSM-5 to 86.70 mg/g for the modified adsorbent. However, the modification of ZSM-5 *via* this method requires sophisticated experimental setups and excess reagents, making use of this material uneconomical. Moreover, Handreck and Smith [19] used hierarchical ZSM-5 zeolites prepared hydrothermally as adsorbents, and found the adsorptive removal of MB to be linearly proportional to the aluminium content in ZSM-5 as shown in Figure 1.2 below.

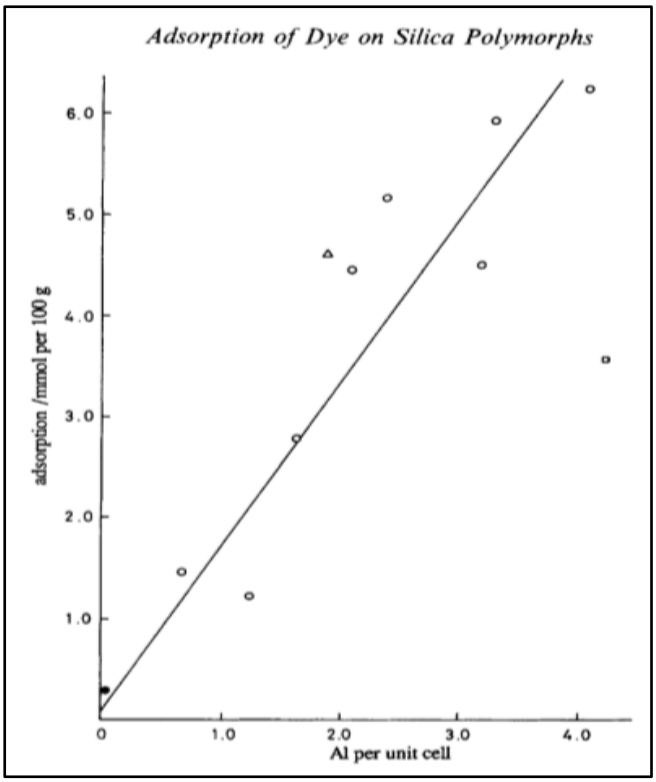

Figure 1.2: Variation of the MB adsorption capacity of pentasil zeolites with Al content: (○) ZSM-5, (●) silicates and (△) ZSM-11 [19].

Post-synthesis dealumination treatments of parent ZSM-5 zeolites are known to increase the porosity and surface area due to the extraction of aluminium ions from the zeolite framework [7, 20]. Well-known post-synthesis treatments include steaming at relatively high temperatures [20], acid-leaching [21] and alkaline treatment [18]. These treatments tailor the ZSM-5 properties for better efficiency in the adsorption of heavy metals and bulky organic contaminants. Acid-leaching selectively extracts framework aluminium atoms of ZSM-5, introducing mesopores in the intrinsically microporous framework of ZSM-5, and thus generating hierarchical ZSM-5 [8, 20, 21]. The co-existence of micro- and meso-pores in the ZSM-5 matrix creates a molecular sieving effect that will lead to bulky substrates being entrapped in the zeolite matrix. The acid-mediated dealumination of ZSM-5 was employed to produce adsorbent materials. This project mainly sought to investigate the potential of hierarchical ZSM-5, prepared *via* acid-mediated dealumination, in the adsorptive removal of MB (as a model organic dye) from aqueous solutions.

1.5 Aim and objectives

1.5.1 Aim

The aim of this study was to develop a hierarchical ZSM-5 adsorbent through controlled acid-mediated dealumination of pristine ZSM-5, and test its efficiency in the removal of MB from aqueous systems.

1.5.2 Objectives

The objectives of this study were to:

i. synthesise high-aluminium content pristine ZSM-5 zeolites with silica-to-alumina ratios (SARs) of 25 and 50,

ii. dealuminate the zeolites obtained in (i) above by acid-mediated treatment in order to produce hierarchical ZSM-5 derivatives with an additional level of porosity,

iii. characterise each zeolitic material using X-ray diffraction (XRD), Fourier-transform infrared (FTIR) spectroscopy, scanning electron microscopy (SEM), as well as N_2 adsorption isotherms and Brunauer-Emmett-Teller (BET) surface area measurements,

iv. investigate the adsorptive performance of each zeolitic material in the removal of MB from synthetic single-contaminant wastewater.

1.6 Dissertation structure

This dissertation consists of five chapters. Chapter 1 gives the background, aim and objectives associated with this work. A literature review on relevant research is compiled in Chapter 2. In Chapter 3, the details of methodology and experimental procedures for preparation of pristine ZSM-5 and its dealumination derivatives, physicochemical characterisation techniques, as well as procedure for MB adsorption studies are given. Chapter 4 presents and discusses the results obtained in this research. The summary and conclusions on the major findings of the work are given in Chapter 5, along with recommendations for future work. An appendix section, containing raw data of the results obtained, is at the end of the dissertation.

It is worth emphasising that each chapter contains its own references to limit their repetition and avoid confusion.

1.7 References

[1]] M.H. Zonoozi, M.R.A. Moghaddam, M. Arami; Removal of acid red 398 dye from aqueous solutions by coagulation/flocculation process; *Journal of Environmental Engineering Management* **7,** 695-699 (2008).

[2] M.A. Rahman, S.M. Rahul Amin, A.M.S Alam; Removal of methylene blue from wastewater using activated carbon prepared from rice husk ash; *Dhaka University Journal of Science* **60**, 185-189 (2012).

[3] I. Feddal, A. Ramdani, S. Taleb, E.M. Gaigneaux, N. Batis, N.Ghaffour; Adsorption capacity of methylene blue, an organic pollutant, by montmorillonite clay; *Journal of Desalination and Water Treatment* **52**, 2654-2661 (2014).

[4] Y. Dong, B. Lu, S. Zang, J. Zhao, X. Wang, Q. Cai; Removal of methylene blue from coloured effluents by adsorption onto SBA-15; *Journal of Chemical Technology and Biotechnology* **86**, 616-619 (2011).

[5] A.K. Hammed, N. Dewayanto, D. Du, M.H. Ab Rahim, M.R. Nordin; Novel modified ZSM-5 as an efficient adsorbent for methylene blue removal; *Journal of Environmental Chemical Engineering* **4**, 2607-2616 (2016).

[6] A.H. Karim, A.A. Jalil, S.Triwahyono, S.M. Sidik, N.H.N. Kamarudin, R. Jusoh, N.W.C. Jusoh, B.H. Hameed; Amino modified mesostructured silica nanoparticles for efficient adsorption of methylene blue; *Journal of Colloid and Interface Science* **386**, 307-314 (2012).

[7] C.S. Triatafillidis, A.G. Vlessidis, L. Nalbandian, N.P. Evmiridis; Effect of the degree and type of the dealumination method on the structural, compositional and acidic characteristics of H-ZSM-5 zeolites; *Journal of Microporous and Mesoporous Materials* **47**, 369-388 (2001).

[8] P.J. Kooyman, P. van der Waal, H. van Bekkum; Acid dealumination of ZSM-5; *Zeolites* **18**, 50-53 (1997).

[9] R.J. Argauer, G.R. Landolt; Crystalline zeolite ZSM-5 and method of preparing the same, *US Patent* **3** 702-886, (1972).

[10] M.E. Davis, R.F. Lobo; Zeolites and molecular sieve synthesis; *Chemistry of Materials* **4**, 756-768 (1992).

[11] S.C. Cundy; The hydrothermal synthesis of zeolites: History and development from the earliest days to the present time; *Chemical Reviews* **106**, 663-701 (2003).

[12] W. Song, R.E. Justice, C.A. Jones, V.H. Grassian, S.C. Larsen; Synthesis , characterisation and adsorption properties of nanocrystalline ZSM-5; *Langmuir* **20**, 8301-8306 (2004).

[13] Q. Yu, C. Cui, Q. Zhang, J. Chen, Y. Li, J. Sun, C. Li, Q. Cui, C. Yang, H. Shan; Hierarchical ZSM-11 with intergrowth structures: Synthesis, characterisation and catalytic properties; *Journal of Energy Chemistry* **22**, 761-768 (2013).

[14] M.A. Ali, B. Brisdon, W.J. Thomas; Synthesis, characterisation and catalytic activity of ZSM-5 zeolites having variable silicon-to-aluminium ratios; *Journal of Applied Catalysis A: General* **252**, 149-162 (2003).

[15] D.H. Olson, G.T. Kokotailo, S.L. Lawton, W.M. Meier; Structure of synthetic zeolite ZSM-5; *Journal of Physical Chemistry* **85**, 2238-2243 (1981).

[16] A.A. Mahabadi, M.A. Hajabbasi, H. Khademi, H. Kazemian; Soil cadmium stabilization using an Iranian zeolite; *Geoderma* **137**, 388-393 (2007).

[17] I.O. Ali, A.M. Hassan, S.M. Shaaban, K.S. Soliman; Synthesis of characterisation of ZSM-5 zeolite from rice husk ash and their adsorption of Pb^{2+} onto unmodified and surfactant-modified zeolite; *Journal of Separation and Purification Technology* **83**, 38-44, (2011).

[18] A. Ikhlaq, D.R. Brown, B. Kasprzyk-Hardern; Catalytic ozonation for the removal of organic contaminants in water on ZSM-5 zeolites; *Journal of Applied Catalysis B: Environmental* **154-155**, 110-122, (2014).

[19] P.G. Handreck, T.D. Smith; Adsorption of methylene blue from aqueous solutions by ZSM-5-type zeolites and related silica polymorphs; *Journal of Chemical Society, Faraday Transactions 1: Physical Chemistry in Condensed Phases* **84**, 4191-4201 (1988).

[20] M. Muller, G. Harvey, R. Prins; Comparison of the dealumination of zeolites beta, mordenite, ZSM-5 and ferrierite by thermal treatment, leaching with oxalic acid and treatment with $SiCl_4$ by ^{1}H, ^{29}Si and ^{27}Al MAS NMR; *Journal of Microporous and Mesoporous Materials* **34**, 135-147 (2000).

[21] S. Kumar, A.K. Sinha, S.G. Hedge, S. Sivasanker; Influence of mild dealumination on physicochemical, acidic and catalytic properties of H-ZSM-5; *Journal of Molecular Catalysis A: Chemical* **154**, 115-120 (2000).

CHAPTER 2

LITERATURE REVIEW

2.1 Textile organic water pollutants

Textile industries consume large volumes of water and chemicals for wet processing of textiles [1]. These industries further produce diverse types of coloured organic compounds, dyes, in effluents and their presence in water systems is undesirable. More than 70 000 tons of dyes are manufactured annually, and often find their way into various streams, dams and rivers. It is therefore essential to treat the aqueous industrial effluents in order to minimise the amount of coloured pollutants discharged into the environment. There are many structural varieties of dyes which include acidic, basic, disperse, azo, diazo, anthroquinone based and metal complex dyes [1 – 3]. Methylene blue (MB) is a cationic dye that is greenish in appearance and characteristically blue when dissolved in water. It is used in several industries such as textile, pharmaceutical, food, cosmetic and paper [1, 2], as well as an acid-base indicator in basic chemistry experiments. Many textile companies use MB as a pigment for the colour blue, which is often released along with the effluents from these industries. This cationic dye has recently also been used in the field of medicine to treat ailments such as methemoglobinema, schizophrenia, kidney stones and herpes infections [3]. The chemical structure of MB is shown in Figure 2.1.

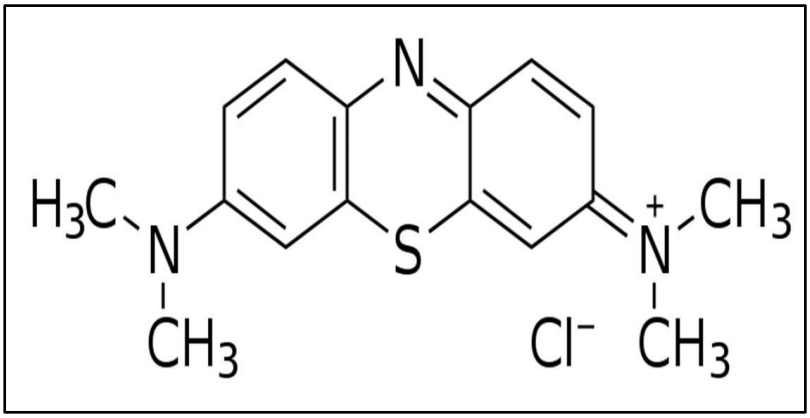

Figure 2.1: Chemical structure of MB, cited from [4].

The complex chemical structure of MB (Figure 2.1) and other dyes make them resistant to breakdown by numerous chemical, biological, as well as physical

treatments and it becomes difficult to efficiently decontaminate MB and other organic dyes from water. The MB dye is toxic in water at levels exceeding 5 mg/L [4].

2.2 Environmental effects of textile dyes

Effluents generated from daily routines and various industries contain numerous water pollutants such as organic dyes and these constitute major sources of global water pollution. Due to their aromatic rings, textile dyes are highly toxic and very difficult to degrade and remove from water. The discharge of these organic dyes from their sources into water systems disturbs the metabolic processes of aquatic organisms since they weaken the permeability of light [2]. Furthermore, industrial effluents with organic coloured effluents cause the formation of toxic and carcinogenic breakdown products.

Figure 2.2: Effect of methylene blue on aquatic ecosystems [5].

The effect of MB and other dyes is apparent in Figure 2.2 above, whereby numerous fish and other aquatic species die in the dye-contaminated water. This could be due to the lack of penetration of light which retards photosynthesis and limits the availability of oxygen in water for aquatic organisms. Several methods have been developed for the decontamination of coloured organic pollutants from water. Biological methods such as biodegradation have been proposed, but are less efficient due to the low

biodegradability of cationic dyes. Chemical treatment processes such as ozonation, coagulation/flocculation and chlorination are more effective [2 – 4]. Adsorption is the most frequently used method due to its high efficiency and low cost of operation. Low-cost materials are preferred for use as adsorbents for the adsorptive removal of textile dye compounds from water.

2.3 Adsorption of MB from wastewater

Aqueous effluents from several industries, including the textile sector, as well as everyday life contain coloured organic contaminants in the form of dyes and these constitute one of the major sources of worldwide water pollution. The presence of textile dyes in water, including their toxic nature, affects both aquatic ecosystems and human health negatively and warrant the need for efficient treatment of contaminated water. This toxicity occurs because the presence of coloured organic effluents in water prevents the permeability of light and thus hinders processes such as photosynthesis. Organic dyes have characteristic bulky chemical structures, which make them resistant to being broken down or removed by water treatment technologies such as bio-degradation, ozonation [6], electro-coagulation, advanced oxidation and coagulation-flocculation [7]. Furthermore, the maintenance of the abovementioned processes remains costly with limited efficiency. Several disadvantages of some water treatment methods are summarised in Table 2.1:

Table 2.1: Disadvantages of the common methods of dye removal from industrial effluents [8].

Physical/chemical methods	**Disadvantages**
Ozonation	Short half-life (20 min)
Membrane filtration	Concentrated sludge production
Electro-coagulation	High sludge production
Photochemical	Formation of toxic by-products
Electrochemical destruction	High cost of electricity

Thus, there is a need for alternative efficient and economical processes for the purification of water. Adsorption is a process where a solute is removed from a liquid phase through contact with a solid adsorbent having affinity for the solute [9]. It is considered an effective method for removing bulky organic molecules from aqueous solutions due to its simplicity of design, insensitivity to toxic substances and low cost of operation [9 – 12]. Adsorption is considered the most efficient technology for the removal of dyes using low-cost materials [2, 8]. Research has expanded towards low-cost materials with large adsorption capacities. A wide range of adsorbents have recently been evaluated for efficiency in the remediation of dyes. Several materials including clays [2], activated carbon [3], zeolites [9] and agricultural products have been used in the remediation of MB from aqueous solutions. Activated carbon is the most used adsorbent for the removal of dye contaminants from wastewater due to its high surface area. This adsorbent can be prepared from different abundant sources of carbon. However, the activation of the carbon sources requires sophisticated equipment operating in the presence of N_2 gas, which raises the production costs. Despite activated carbon having very high adsorption capacity (>120 mg/g), the high cost of production and lack of regeneration makes it uneconomical [3]. Advancements have been made to produce low-cost adsorbents having improved efficiency in the removal of dyes from wastewater and also with ease of regeneration. Recently, inorganic adsorbents with high surface areas have been used as alternatives to costly carbon adsorbents [9, 13]. These include synthetic zeolites and siliceous materials, with unique surfaces and pore properties, as well as high thermal and chemical stabilities, which are increasingly used in the adsorption [10] of dissolved pollutants from aqueous systems. Dong *et al*. [14] investigated the efficiency of several zeolites in removing dyes from aqueous effluents. Materials such as NH_4-ZSM-5, NH_4-Beta, MCM-22 and SBA-15 were all evaluated as potential MB adsorbents in their work. They found that the microporous NH_4-ZSM-5, NH_4-Beta and MCM-22 were ineffective in quickly lowering the MB concentrations of the effluents. NH_4-ZSM-5 in particular showed rapid reaction with the dye solution since the equilibrium point of the experiment was reached very quickly [13].

Mesoporous materials, such as MCM-41, are demonstrating a higher efficiency in the removal of organic contaminants from aqueous effluents [8, 13, 14], because of their larger pore sizes (2 – 50 nm) and surface areas (>1000 m^2/g), achieving high

adsorption capacities (300 – 800 mg/g) [7, 14]. Eftekhari *et al*. [7] observed a high removal efficiency in the decontamination of rhodamine B from aqueous solutions using mesoporous Al-MCM-41 as adsorbent. Conventional MCM-41 has an adsorption capacity for methylene blue of 54 mg/g [13]. However, MCM-41 has a low stability in aqueous environment and is prone to structure collapse [7, 8]. Thus, it is not viable for applications in water. Dong *et al.* [14], tested SBA-15 in the remediation of MB from aqueous effluents, and found an outstanding adsorption performance (adsorption capacity ~300 mg/g). Their material could be easily regenerated through calcination, and reused at least ten times. Furthermore, regenerated SBA-15 exhibited an XRD pattern consistent with that of the parent material. Inorganic aluminosilicates, such as zeolites, have great potential for use in the remediation of dye-containing wastewater [15]. Hammed *et al.* [9] reported the application of modified ZSM-5 zeolites in water purification, as an adsorbent for MB. However, microporous materials consist of significantly smaller pore sizes that cannot accommodate the bulky MB molecules (dimension: 0.4 nm x 0.61 nm x 1.43 nm), shown in Figure 2.1 [4]. Sugar-coating ZSM-5, followed by impregnation with iron precursor solution improved the MB adsorption capacity of ZSM-5 from 20.68 to 86.70 mg/g. The current dissertation focusses on the flexibility of zeolite ZSM-5 as a low-cost material with potential in water decontamination processes. Particular attention is directed to the removal of organic dyes, modelled by MB, from synthetic wastewater. From a consideration of the microporous nature of ZSM-5 (pore size 5.3 – 5.6 Å), together with the bulky and sterically-hindered nature of MB, it became imperative in this research to empower microporous ZSM-5 with an additional level of porosity through a post-synthesis acid-mediated dealumination treatment. The properties of ZSM-5 as an efficient adsorbent for MB, as a model textile dye, are highlighted in the subsequent sections.

2.4 The ZSM-5 zeolite

Zeolites are crystalline microporous aluminosilicate materials, consisting of high specific surface areas and nanometer-sized channels, which are used for many crucial industrial reactions. Zeolite Socony Mobil-5 (ZSM-5) is a synthetic subclass of these materials which finds widespread applications in oil refining and in water treatment as adsorbents [4, 6, 15]. Zeolite ZSM-5 was first prepared by Mobil Oil Corporation researchers Argauer and Landolt in 1972 [16], and belongs to the pentasil family of

zeolites, and has since demonstrated to be one of the most important classes of zeolite catalysts. There are thousands of zeolite types that are recognised by the International Zeolite Association (IZA) and each is differentiated using three-letter code which identifies the zeolite framework topology. For example, ZSM-5 is a highly crystalline zeolite with an MFI topology.

2.4.1 Physicochemical characterisation of ZSM-5

ZSM-5 possesses attractive characteristics, including high internal surface area, good thermal stability, intrinsic acidity and tuneable pore sizes. The structure of this zeolite consists two types of intersecting channels, both formed by 10-membered silicate rings as shown in Figure 2.3 and is classified as a medium-pore zeolite [16].

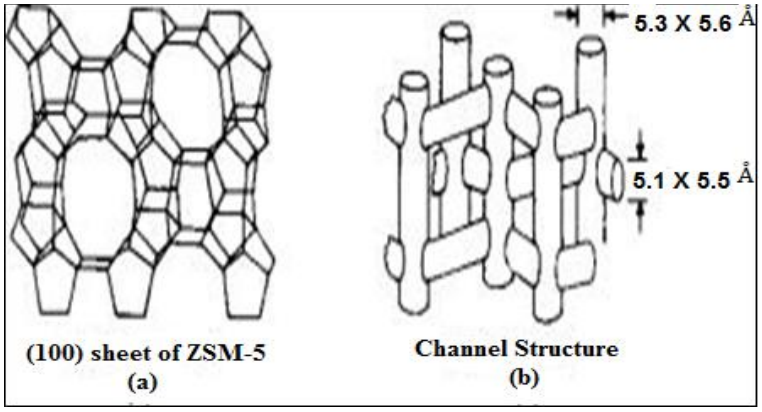

Figure 2.3: Structural connectivity in ZSM-5 zeolite [17].

Figure 2.3 illustrates the layout of the ZSM-5 channels. The skeletal diagram of (100) face of ZSM-5 is depicted on Figure 2.3(a), where the 10-membered ring apertures constitute the entrances to the sinusoidal channels. Some of these channels are straight and have a nearly circular opening (5.3 x 5.6 Å) along (010), while the others are sinusoidal with an elliptical opening (5.1 x 5.5 Å) along (100) [18, 19], as shown on Figure 2.3(b).

The zeolite matrix consists of Si-O-Si and Si-O-Al chain linkages that make up the pores, aligned in a geometry governed by a structure-directing agent (SDA) used in the synthesis. There are also bridging hydroxyl groups that induce a single band that shifts from 3595 to 3620 cm^{-1} on the FTIR spectrum, by varying the silica-to-alumina ratio (SAR). Furthermore, the IR spectrum of ZSM-5 also provides confirmatory information regarding the identity of this zeolite by a characteristic MFI band at 550

cm^{-1}. The characteristics of ZSM-5 samples produced are strikingly similar, irrespective of the synthesis method. XRD patterns normally show seven characteristic peaks: two in the region 8 – 10° 2θ, three in the region 24 – 26° 2θ and a doublet at 45° 2θ. The surface of ZSM-5 consists of unbalanced negative charges, which are counter-balanced by cations. These extraframework cations are responsible for the ion-exchange properties of ZSM-5 and other zeolites. When these cations are exchanged with protons (H^+), the Brønsted acid form, H-ZSM-5, is generated. The framework of negative charges can play a role in the adsorption of cationic substrates. [16]. Many other different techniques have been used for the characterisation of ZSM-5 zeolites such as NH_3-TPD to determine acid sites and strength, transmission electron microscopy (TEM) and scanning electron microscopy (SEM) for morphological studies, N_2 adsorption isotherms and BET surface area measurements, as well as ^{27}Al NMR for the types of aluminium species in zeolites. In this study, however, N_2 adsorption isotherms were used to confirm the preparation of hierarchical ZSM-5 by the appearance of a pronounced hysteresis loop with respect to the parent material after dealumination, XRD, FTIR and SEM to probe the morphology of synthesised samples. ZSM-5 zeolites have characteristic coffin-shaped particles with intergrowth crystals.

2.4.2 Synthesis of ZSM-5

The original method for synthesising this zeolite is based on the hydrothermal crystallisation of reactive alkali metal aluminosilicate gels at high pH and temperatures exceeding 100 °C [16]. These gels are prepared using recipes consisting of a silica source, an alumina source, mineralising agents such as OH^- or F^-, a solvent, and optionally organic molecules as SDAs. The complexity of the crystallisation process makes ZSM-5 synthesis dependent on parameters such as synthesis gel aging, stirring, temperature, pH, nature of template, composition and order of reagents addition, all of which have a bearing on the structural integrity of this zeolite. The hydrothermal synthesis approach, under the influence of TPABr as an organic SDA, has been chosen for the production of ZSM-5 in this study. These as-synthesised ZSM-5 samples will be post-synthetically dealuminated to prepare hierarchical ZSM-5 (see section 2.4.2 and Chapter 3). The most important part in zeolite synthesis is

structure direction, which is normally facilitated by various organic amines. This is described in the next section.

2.4.2.1 Templating agents

The role of organic molecules in the synthesis of zeolites can be in various forms such as space filling, structure-directing and templating. ZSM-5 is commonly synthesised using organic SDAs such as tetrapropylammonium hydroxide (TPAOH), TPABr [18], carbon black pearls [15], triethylammonium, tripropylammonium, ethyldiamine, n-butylamine, ethylamine, ethanol, isopropylamine [19], 1,5-diaminopentane, 1,6-diaminohexane or under organic template-free conditions [16 – 18, 20]. The TPA^+ ion is universally used as structure-directing template, since it promotes the synthesis of MFI over a wide range of compositions, and eventually gets entrapped in the channels of the final zeolite [16]. Laboratory synthesis methods are varied, and include crystallisation under hydrothermal conditions [15, 18], microwave-assisted syntheses [15] and sol-gel route [21]. Compared with other methods, the hydrothermal route is a useful and attractive method for the preparation of pristine ZSM-5 zeolites, since it produces pure and highly crystalline powders with controlled morphology [22].

Most organic SDAs are very costly to acquire and recent advances have been made to prepare ZSM-5 materials without the use of a template. Argauer and Landolt [16] reported the synthesis of pristine ZSM-5 with and without a template. The structural stability of ZSM-5 samples synthesised without a template was found to be lower when compared to the samples obtained from templated methods [16]. Further production of ZSM-5 *via* organic-free synthesis gels was evaluated and reported by Shiralkar and Clearfield [23]. They found that the structural stability of the organic-free samples is significantly lower than that of samples prepared in the presence of organics. The lack of stability is attributed to excess sodium atoms occluded within the zeolite framework [16, 23, 24]. A comparatively inexpensive synthesis method was explored by Koo *et al*. [15], where microwave irradiation was used to enhance the growth of carbon-templated ZSM-5. Additional dielectric heating of the synthesis gel is advantageous in producing samples with larger crystals, as well as higher chemical and thermal stability. However, syntheses using this route is not viable since very sophisticated equipment is required. Recently, non-ionic surfactants have been shown to be effective in reducing cost implications aligned with ZSM-5 syntheses. Narayanan *et al*.

[22] identified an inexpensive non-ionic surfactant Triton X-100 as a template for producing hierarchical ZSM-5 materials with different SARs. This surfactant produced materials consisting of micro-, meso- and macro-pore size ranges. However, materials produced in their study had relatively low crystallinity, which limited their lifetime and stability. Moreover, samples obtained through the use of the surfactant were not phase-pure, and the method was not reproducible. A potentially beneficial method for the production of hierarchically-structured ZSM-5 was reported by Ge *et al*. [25]. It uses a single micropore template, TPAOH, to direct the formation of the product zeolite at moderate temperatures. However, not all the materials prepared through this route were hydrothermally stable, and they showed no ordered mesoporosity. Generally, the use of organic SDAs is an acceptable to prepare highly crystalline and ordered materials with enhanced physicochemical properties. Furthermore, TPA^+ ions compounds are very popular for the synthesis of ZSM-5, since they produce materials with highly defined crystal structures, high internal surface areas, uniform pores, as well as good thermal stability [16].

2.4.2.2 Zeolite synthesis variables

Primary variables that play a role in the synthesis of ZSM-5 and other zeolites include alumina and silica sources, alkalinity, SAR, synthesis temperature, aging and crystallisation time, water content, presence of seed crystals, alkalinity, nature of cations in the synthesis medium and template(s) [16 – 19, 21-25].

Particle size and size distribution of MFI-type zeolites are influenced by all of these variables. Prolonged gel aging before hydrothermal crystallisation, along with the type of aluminium source, affect the crystal sizes of ZSM-5 [24, 25]. For example, crystals increase in size when the aging time preceding crystallisation is relatively short and inorganic aluminium salts are used as alumina sources [25]. Aly *et al*. [26] have investigated the influence of different alumina sources on the properties of ZSM-5 zeolites. It was found that highly crystalline ZSM-5 materials are obtained in synthesis with sodium aluminate. Furthermore, the average crystal size increased in the order sodium aluminate (78.56 nm) < aluminium nitrate (104.87 nm) < aluminium chloride (112.3 nm). Aluminium nitrate produces materials with high surface area (212.4 m^2/g) that crystallise in hexagonal and spherical shape crystal morphology. Moreover,

synthesis of ZSM-5 at low SAR *i.e*., high aluminium content, has the tendency to produce analcime zeolites [27].

The alkalinity of reaction system also has a strong influence on the average crystal size, but can change the topology of an envisaged material if not managed correctly. A lower synthesis pH of 11 is advantageous for the crystallisation of samples as compared to a more basic pH 14. It has been reported that lowering the pH can significantly lower the probability of having ZSM-5/ZSM-11 intergrowths in the products [16]. Moreover, smaller crystal sizes are obtained at lower pH and a suppression of the intergrowth morphology is achieved. Water content in synthesis mixture also affects the crystallised products [16 -19, 22]. When the amount of water is high at a constant pH, the average crystallite sizes of MFI materials is large while the yield of produced material is low. Figure 2.4 summarises the effect of some synthesis parameters on the production of ZSM-5 zeolites.

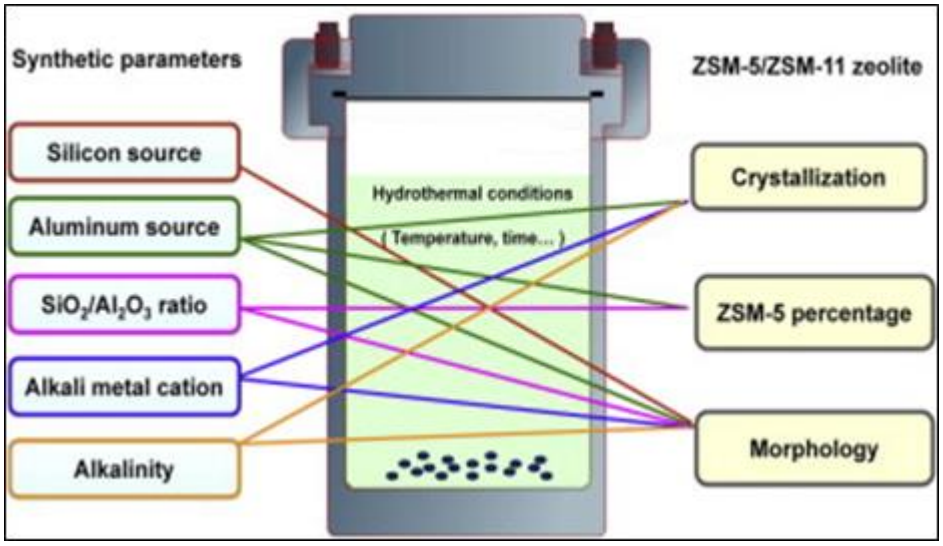

Figure 2.4: The effect of synthesis parameters on physicochemical properties of ZSM-5 materials [19].

The amorphous silicate intermediates formed during the process of silica dissolution play an important role in zeolite formation and are influenced by the nature of the silica source used. Silica sources can also influence specific features of zeolitic materials because the impurities introduced by the sources into a gel composition can also affect the morphology and chemical properties [28]. Tetraethyl orthosilicate (TEOS), fumed silica, colloidal silica and sodium metasilicate have previously been studied as different silica sources in the synthesis of ZSM-5 [28]. Highly crystalline materials are obtained using fumed and colloidal silica, as well as TEOS, but a quartz silica phase exists

when sodium metasilicate is used. Furthermore, zeolites obtained using fumed silica crystallise in cuboidal shaped crystals and the samples which were prepared from TEOS and colloidal silica crystallise in twinned and intergrowth crystal morphology. Fumed silica, TEOS and colloidal silica have been reported as the best sources to use for zeolite synthesis [17].

The composition of the zeolite framework can be varied by changing the SAR of the reaction mixture. Synthesis of ZSM-5 materials with very low SARs require more effort to prevent the formation of adventitious extra-framework aluminium (EFAL) species forming [15, 25]. Furthermore, it has proved extremely difficult to produce ZSM-5 from reaction mixtures with SARs less than 20, which could produce crystals with correspondingly lower framework silica to alumina molar ratio. The problem of producing ZSM-5 with a low silica to alumina molar ratio has been particularly pronounced in the case of small crystal materials [29]. Beck *et al*. [29] pioneered a method of preparing ZSM-5 materials with SARs in the range 15 – 100. This method produces highly crystalline ZSM-5 materials with very small crystals (1 μm).

Hydrothermal crystallisation time is directly related to the synthesis temperature used. Argauer and Landolt [16] have reported the synthesis of ZSM-5 within 24 – 144 hours. However, many researchers have reported that induction time decreases as synthesis temperature is increased [15 - 17]. The synthesis of ZSM-5 has further been reported for the temperature range 150 – 180 °C [16, 27, 28]. Moreover, the synthesis of ZSM-5 at synthesis temperatures below 100 °C has also been reported [15, 16]. A previous study by Mintova *et al*. [30] illustrated the use of temperature to study the growth process of ZSM-5 crystals and optimise product yields during synthesis, as well as alter the morphology of samples. Analysis of their kinetic data shows that the growth mechanism is independent of temperature and maximal crystallinity was reached in a shorter time at higher temperatures. Furthermore, it was observed that synthesis time decreased with increasing temperature, and fewer crystals are formed at higher temperatures [30].

2.5 Hierarchical ZSM-5

Hierarchical ZSM-5 zeolites are zeolites that consist of both micro- ($0\ nm < d < 2\ nm$) and meso-pores ($2\ nm < d < 50\ nm$) within the same matrix. Consequently, they combine the advantages of the two pore regimes. These materials show an enhanced

accessibility, leading to improved catalytic activity in reactions suffering from steric and/or diffusional limitations [31, 32]. The secondary porosity offers an ideal space for the deposition of additional active phases and for functionalisation with organic moieties. The channel system of bulk ZSM-5 restricts diffusion within the cavities, but the presence of mesopores in hierarchical ZSM-5 makes it capable of adsorbing and processing bulky organic molecules [9]. Hierarchical zeolites exhibit zeolitic properties similar to those of conventional zeolites in terms of acidity, hydrophobic/hydrophilic character, confinement effects, shape-selectivity and hydrothermal stability [23]. Hierarchical zeolites can be prepared by a direct hydrothermal method under the influence of polyquartenary ammonium surfactants, and also through post-synthesis treatments of pre-formed microporous zeolites such as acid- and base-treatments. Furthermore, it has been demonstrated that hierarchical zeolites, prepared by post-synthesis treatments, not only retain most properties of the parent materials, but also show vast advantages of easy separation and fast mass-transport [33, 34]. Thus, hierarchical ZSM-5 is a promising material for the remediation of bulky organic molecules from water and catalysis of reactions restricted by diffusion limitations.

Pristine ZSM-5 zeolites have severe diffusion limitations and confinement effects that impose mass transport constraints on the products upon application [21]. Tailoring the shape, size and connectivity of the framework channels is an important aspect of zeolite synthesis. The effective post-synthetic methods for tailoring zeolite properties continue to be indispensable to enable the preparation of materials with application-specific properties [35]. Hierarchical ZSM-5 is the subject of larger surface area, special pore structure, improved mass transfer, shape selectivity and high thermal stability [31, 36]. These hierarchical materials are commonly produced from post-synthesis treatments such as acid/base leaching by dealumination/desilication, synthesis with hard/soft templates, as well as thermal treatments using steam [31, 33, 35, 36]. There are two main routes leading to hierarchical ZSM-5 products, *viz.,* template and non-template methods [25]. The former centres on the use of soft bulky templating agents or dual templates that work constructively to direct the synthesis of hierarchical materials [25]. In the “constructive”/hard-templating method, large amounts of organic or inorganic templates are used which makes thermal treatments and/or acid washing somewhat inevitable to open the porous structures. To avoid the occurrence of phase separation between microporous crystals and amorphous

mesoporous species in this method, carefully selected or specially designed dual pore-making templates are usually necessary [25]. This increases the cost of materials manufacturing and reduces large-scale industrial applications. The latter non-templated methods use already synthesised zeolites followed by post-synthesis treatments such as acid/base leaching or thermal treatment [31, 33]. This "deconstructive" method is a multi-step process, consisting of either acid treatment for dealumination or alkaline treatment for desilication, with a rare combination of these processes to generate additional mesoporous structures [32]. For this acid-leaching post-synthesis process, there is a SAR limitation which ranges from 25 to 50 for ZSM-5 zeolites [37].

Synthesis of high aluminium-content ZSM-5 can encourage modifications of the structural connectivity. Leaching out the Al atoms from within the zeolite framework improves the surface area, modifies crystallite sizes and generates irregularly dispersed mesopores [33, 34, 38]. The true nature of the mechanism of mesopore formation is not clear, but several plausible theories have been put forward to elucidate the understanding of post-synthesis treatments [33]. The dealumination process is influenced by the zeolite structure, the distribution of the framework aluminium within, as well as its ability to stabilise the resulting defect sites. Proposed dealumination models are often based on zeolites with high aluminium content which contain, primarily, aluminium tetrahedra that are less stable against hydrolysis and dealumination [34]. The figure below shows a schematic representation of perceived mesopore generation in pristine ZSM-5 zeolites *via* post-synthesis treatment.

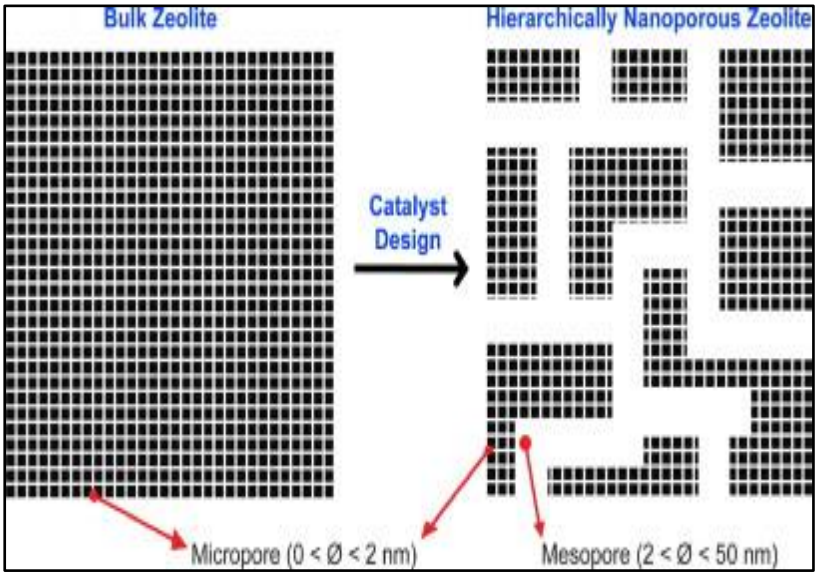

Figure 2.5: Schematic depicting mesopore formation from bulk zeolite [34].

Research has demonstrated that alkaline desilication of zeolites is one of the most important strategies for the synthesis of hierarchical zeolites [33]. However, its destructive nature usually causes a reduction in microporosity and acid sites, resulting in the decreased activity and stability of the zeolites [39]. Low aluminium content zeolites have greater stability, which makes the zeolite desilication process particularly difficult to control. The current dissertation is based on acid-mediated dealumination as a post-syntheses route to hierarchical ZSM-5 zeolites.

2.5.1 Thermal dealumination

The most prominent technique for the dealumination of ZSM-5 remains thermal treatments at elevated temperatures. This is traditionally achieved using steam [38]. Dealumination through steaming is the most common technique for preparing industrially-important catalysts of high activity, selectivity and stability [38, 39]. Water is able to hydrolytically remove Al from their tetrahedral coordination in the lattice of the zeolite [38]. Treating ZSM-5 with steam produces larger mesopores compared to those obtained from acid leaching and alkaline treatment. This is because aluminium atoms are easily extracted from the framework of ZSM-5 at elevated temperatures (>500 ^{o}C), producing thermally and chemically stable materials that are hierarchical in nature [38, 39]. Different EFAL/amorphous phases with disordered mesoporosity are typically observed in the thermally-dealuminated samples. The formation of Lewis acid EFAL is known to enhance the catalytic activity in hydroxylation reactions [40]. In order to control the degree of dealumination using steam, the technology requires constant monitoring of the treatment temperature and time, as well as the steam pressure [9, 29, 10]. This makes the technique uneconomical and time-consuming. Thermal dealumination produces materials with significantly large mesopores but disadvantages include:

- Requiring elevated temperatures and being temperature sensitive.
- Producing excess EFAL.
- Leading to significant structural damage.
- Difficult to control.
- Demands constant supervision and monitoring.

Therefore, thermal dealumination of ZSM-5 is associated with numerous disadvantages and, is therefore, not very straightforward to use. Hence, this approach was not considered in the current dissertation.

2.5.2 Acid dealumination of ZSM-5

The framework Si/Al ratio of zeolites is an important factor governing properties such as catalytic activity, selectivity, strength of Brønsted acid sites and hydrothermal stability. Dealumination of ZSM-5 selectively extracts Al from within the zeolite framework, thereby generating surface defects and mesopores. Generally, zeolites containing a low Al concentration are chemically and thermally more stable [37]. Dealumination can be achieved *via* either acid-leaching or thermal treatments at high temperatures with/without steam [34, 37, 39 - 42]. The chemical leaching technique is a prominent method since it introduces irregularly dispersed mesopores within the zeolite cavities. Dealumination of zeolites was first reported by Barrer *et al.* [43] in 1964 on their study of clinoptilolite. This method gives rise to EFAL species in and around the zeolite cavities [37, 43 - 45]. The EFAL species are mostly cationic, but can in some cases be neutral. Their formation can be seen as a change in coordination mode of the framework aluminium as it is removed from the matrix. The presence of the EFAL, however, enhances the acid strength of ZSM-5 materials [34, 38]. Both the mechanism of formation and nature of these species is still unclear and their characterisation requires expensive techniques. Removal of Al atoms from the zeolite framework has been agreed to occur *via* a penta-coordinated aluminium species, identified by a signal at 30 ppm on the ^{27}Al MAS NMR spectrum [38, 39].

Kooyman *et al*. [35] were the first to explore a wide range of dealumination acids, and the effect of their concentrations on the extent of dealumination. The strength of an acid can largely influence the formation and dispersion of the mesopores. Organic acids such as acetic and oxalic acid [40], ammonium hexafluorosilicate (AHFS), chelating agents such as ethylenediamine tetraacetic acid (EDTA), as well as mineral acids such as hydrochloric acid (HCl) [39, 45], sulfuric acid (H_2SO_4) [37] and nitric acid (HNO_3) [35, 36] have all been previously evaluated as suitable dealuminating agents. The organic acids are classified as mild dealuminating agents due to their inferior acid strength. Dealumination using organic acids achieves minimal removal of aluminium from the zeolite framework and uneven distribution of the mesopores [33]. Mineral

acids, on the other hand, have since enjoyed extensive interest in the dealumination of particularly ZSM-5 due to the superior acid strength [33, 36]. In this regard, HNO_3 has been shown to be the most suitable and effective mineral acid in the dealumination of ZSM-5. This acid removes aluminium, inducing regularly dispersed mesopores within the zeolite matrix [36]. However, in the study reported by Kooyman *et al*. [35], no significant dealumination is found when aqueous solutions of H_2SO_4 and HBr are used [35]. Only HCl treatment led to mild dealumination of ZSM-5 as the concentration was increased, but produced non-uniform hierarchical pores [35]. The temperature, acid concentration and Si/Al ratio of the zeolite was found to not have a significant effect in the removal of the framework aluminium. Ammonium hexafluorosilicate has also been investigated as a zeolite dealuminating agent [46]. Though it is a mild dealuminating agent, it has the advantage of producing samples that are relatively free of any EFAL. The mechanism of this dealumination was postulated by Silaghi *et al*. [33] to generally consist of a net replacement of the framework aluminium by Si atoms. This stabilises the zeolite, but reduces its activity in processes such as hydrocracking. The technique is difficult and costly to maintain because it requires high temperature conditions to take effect [38, 39]. The acid-mediated dealumination method has shortfalls such as producing large amounts of highly acidic waste products that must be disposed properly and being difficult to control. However, this method is associated with several advantages such as:

- Yields no significant structural damage.
- Produces less EFAL.
- Small EFAL species are easily removed.
- Induces evenly dispersed mesopores.
- Does not require persistent monitoring.

The limited number of disadvantages of the acid-dealumination of zeolites makes this method suitable for application, compared to other techniques, for post-synthesis mesopore generation. Therefore, the current dissertation is based on acid-mediated dealumination of ZSM-5 in an attempt to expand its level of porosity and thereby increase its adsorption capacity for water pollutants.

2.6 Applications of hierarchical ZSM-5

Hierarchical ZSM-5 zeolite has attracted attention in applications such as isomerisation [47], catalytic hydrocracking [48] and water purification [9]. This attraction stems from its known and controlled physicochemical properties such as surface area and acidity. A consequence of the porous organisation in hierarchical ZSM-5 is the high surface area, which can vary from several hundred to several thousand square meters per gram (m^2/g). Intrinsic ZSM-5 acidity, shape selectivity as well as other flexible physicochemical properties make the material sought after for different applications. Recent studies on zeolite synthesis are concentrated on tailoring the shape, size and connectivity of intra-framework channels. It has been envisaged that shortening the diffusion path length of the micropores would lead to an improved mass-transport [16]. Ali *et al*. [10] reported the use of hierarchical ZSM-5 for the adsorptive removal of Pb^{2+} from aqueous solutions. Pristine ZSM-5 zeolites were secondarily modified using mesopore-directing templates, and used with good efficiency for the adsorption of heavy cations removing 85 % of Pb^{2+}. Hierarchical ZSM-5 has also been used by Ikhlaq *et al*. [6] for the catalytic ozonation of organic contaminants for their decontamination in water. Ozonation of cumene and Ibuprofen by ZSM-5 was found to be efficient, with 100 % and 79 % decontaminated, respectively. Similar studies other have been carried out for the adsorption of dyes by ZSM-5 zeolites. Lamia *et al*. [11] investigated the adsorption of methyl green onto hierarchical ZSM-5 zeolites. In this work, pyrrolidine was incorporated onto ZSM-5 and was found to greatly improve the adsorption capacity. However, the performance was low with increasing dye concentrations which was attributed to less accessibility to active sites at high concentrations. Furthermore, Handreck and Smith [12] have found the adsorptive removal of MB by ZSM-5 zeolites to be linearly proportional to the aluminium content in ZSM-5.

2.7 References

[1] H. Kariminezhad, M. Habibi, N. Mirzababayi; Nanosized ZSM-5 will improve photodynamic therapy using methylene blue; *Journal of Photochemistry and Photobiology B: Biology* **148**, 107-112 (2015).

[2] I. Feddal, A. Ramdani, S. Taleb, E.M. Gaigneaux, N. Batis, N.Ghaffour; Adsorption capacity of methylene blue, an organic pollutant, by montmorillonite clay; *Journal of Desalination and Water Treatment* **52**, 2654-2661, (2014).

[3] M.A. Rahman, S.M. Ruhul Amin, A.M. Shafiqul Alam; Removal of methylene blue from wastewater using activated carbon prepared from rice husk; *Dhaka University Journal of Science* **60**, 185-189, (2012).

[4] P. Sevcik, T. Mackul'ak, P. Olejnikova, G. Cik; Study of antimicrobial effect of methylene blue incorporated in ZSM-5 zeolite; *Acta Chimica Slovaca* **1**, 238-249, (2008).

[5] www.fewresources.org/toxicchemical Accessed: 18 October 2016

[6] A. Ikhlaq, D.R. Brown, B. Kasprzyk-Hordern; Catalytic ozonation for the removal of organic contaminants in water on ZSM-5 zeolites; *Journal of Applied Catalysis B: Environmental* **154-155**, 110-122, (2014).

[7] S. Eftekhari, A. Habibi-Yangjeh, S. Sohrabnezhad; Application of Al-MCM-41 for competitive adsorption of methylene blue and Rhodamine B: Thermodynamic and kinetic studies, *Journal of Hazardous Materials* **178**, 349-355, (2010).

[8] T. Robinson, G. McMullan, R. Marchant, P. Nigam; Remediation of dyes in textile effluents: a critical review on current treatment technologies with a proposed alternative; *Bioresource Technology Journal* **77**, 247-255, (2000).

[9] A.K. Hammed, N. Dewayanto, D. Du, M.H. Ab Rahim, M.R. Nordin; Novel modified ZSM-5 as an efficient adsorbent for methylene blue removal; *Environmental Chemical Engineering Journal* **4**, 2607-2616, (2016).

[10] I.O. Ali, A.M. Hassan, S.M. Shaaban, K.S. Soliman; Synthesis of characterisation of ZSM-5 zeolite from rice husk ash and their adsorption of Pb^{2+} onto unmodified and

surfactant-modified zeolite; *Journal of Separation and Purification Technology* **83**, 38-44, (2011).

[11] M. Lamia, D. Fatiha, B, Mohammed, D. Ayada; Adsorption of methyl green onto zeolite ZSM-5(pyrr.) in aqueous solutions; *Oriental Journal of Chemistry* **32**, 171-180, (2016).

[12] P.G. Handreck, T.D. Smith; Adsorption of methylene blue from aqueous solutions by ZSM-5-type zeolites and related silica polymorphs; *Journal of Chemical Society, Faraday Transactions 1: Physical Chemistry in Condensed Phases* **84**, 4191-4201, (1988).

[13] K.Y. Ho, G. McKay, K.L. Yeung; Selective adsorbents from ordered mesoporous silica; *Langmuir* **19**, 3019-3024, (2003).

[14] Y. Dong, B. Lu, S. Zang, J. Zhao, X. Wang, Q. Cai; Removal of methylene blue from coloured effluents by adsorption onto SBA-15; *Journal of Chemical Technology and Biotechnology* **86**, 616-619, (2011).

[15] J.B. Koo, N. Jiang, S. Saravanamurugan, M. Bejblova, Z. Musilova, J. Cejka, S.E Park; Direct synthesis of carbon-templating mesoporous ZSM-5 using microwave heating; *Journal of Catalysis* **276**, 327-344, (2010).

[16] R.J. Argauer, G.R. Landolt; Crystalline zeolite ZSM-5 and method of preparing the same; *US Patent* **3** 702 886, (1972).

[17] P.K. Dutta, M. Puri; Synthesis and structure of zeolite ZSM-5: a Raman spectroscopic study; *Journal of Physical Chemistry* **91**, 4329-4333, (1987).

[18] J. Houzvicka, J.G. Nienhuis, S. Hansildaar, V. Ponec; The shape selectivity in the skeletal isomerisation of n-butene to isobutene; *Journal of Applied Catalysis A: General* **154**, 443-449, (1997).

[19] S. Sang, F. Chang, Z. Liu, C. He, Y. He, L. Xu; Difference of ZSM-5 zeolites synthesised with various templates; *Catalysis Today* **93-95**, 729-734, (2004).

[20] A.K. Hammed, N. Dewayanto, D. Du, M.H. Ab Rahim, M.R. Nordin; Novel modified ZSM-5 as an efficient adsorbent for methylene blue removal; *Journal of Environmental Chemical Engineering* **4**, 2607-2616 (2016).

[21] S.S. Kim, J. Shah, T.J. Pinnavaia, Colloid-imprinted carbons as templates for the nanocasting synthesis of mesoporous ZSM-5 zeolite, *Journal of Chemistry Materials* **15**, 1664-1668, (2003).

[22] S. Narayanan, J.J Vijaya, S, Sivasanker, L.J Kennedy, S.K Jesudoss; Structural, morphological and catalytic investigations on hierarchical ZSM-5 zeolite hexagonal cubes by surfactant assisted hydrothermal method; *Journal of Powder Technology* **274**, 338-348, (2015).

[23] V.P. Shiralkar, A. Clearfield; Synthesis of the molecular sieve ZSM-5 without the aid of templates; *Zeolites* **9**, 363-370, (1989).

[24] F. Pan, X. Lu, Y. Wang, S. Chen, T. Wang, Y. Yan; Organic template-free synthesis of ZSM-5 zeolites from coal-series kaolinite; *Material Letters* **115**, 5-8, (2014).

[25] T. Ge, Z. Hua, X. He, Y. Zhu, W. Ren, L. Chen, L. Zhang, H. Chen, C. Lin, H. Yao, J. Shi; One-pot synthesis of hierarchically structured ZSM-5 zeolites using single micropore-template; *Chinese Journal of Catalysis* **36**, 866-873, (2015).

[26] H.M. Aly, M.F. Moustafa, E.A. Abdelrahman; Influence of aluminium source on the gel synthesis of nanosized ZSM-5 zeolite; *Der Chemica Sinica* **2**, 166-173, (2011).

[27] Z.G.L.V. Sari, H. Younesi, H. Kazemian; Synthesis of nanosized ZSM-5 zeolite using extracted silica from rice husk without adding any alumina source; *Journal of Applied Nanoscience* **5**, 737-745, (2015).

[28] R.M. Mohammed, H.M. Aly, M.F. El-Shahat, I.A. Ibrahim; Effect of silica sources on the crystallinity of nanosized ZSM-5 zeolite; *Journal of Microporous and Mesoporous Materials* **79**, 7-12, (2005).

[29] J.S. Beck, C.L. Kennedy, W.J. Roth, D.L. Stern; Small crystal ZSM-5, its synthesis and use; *US Patent 6180550* **B1**, (2001).

[30] S. Mintova, V. Valtchev, E. Vultcheva, S. Veleva; Crystallisation kinetics of zeolite ZSM-5; *Zeolites* **12**, 210-215, (1992).

[31] L.H Ong, M. Domok, R. Olindo, A.C van Veen, J.A Lercher; Dealumination of H-ZSM-5 via steam treatment; *Journal of Microporous and Mesoporous Materials* **164**, 9-20, (2012).

[32] L. Jin, T. Xie, S. Liu, Y. Li, H. Hu; Controllable synthesis of chainlike hierarchical ZSM-5 templated by sucrose and its catalytic performance; *Catalytic Communications* **75**, 32-36, (2016).

[33] M.C Silaghi, C. Chizallet, P. Raybaud; Challenges on the molecular aspects of dealumination and desilication of zeolites; *Journal of Microporous and Mesoporous Materials* **191**, 82-96, (2014).

[34] C.S. Triantafillidis, A.G. Vessidis, L. Nalbandian, N.P. Evmiridis; Effect of degree and type of the dealumination method on the structural, compositional and acidic characteristics of H-ZSM-5 zeolites; *Journal of Microporous and Mesoporous Materials* **47**, 369-388, (2001).

[35] P.J Kooyman, P. Van der Waal, H. van Bekkum; Acid dealumination of ZSM-5; *Zeolites* **18**, 50-53, (1997).

[36] M.D Gonzales, Y. Cesteros, P. Salarge; Comparison of dealumination of zeolites beta, mordenite and ZSM-5 by treatment with acid under microwave irradiation; *Journal of Microporous and Mesoporous Materials* **144**, 162-170, (2011).

[37] L. Jin, H. Hu, S. Zhu, B. Ma; An improved dealumination method for adjusting acidity of H-ZSM-5; *Catalysis Today* **149**, 207-211, (2010).

[38] V. Valtchev, G. Majano, S. Mintova, J. Perez-Ramirez; Tailored crystalline microporous materials by post-synthesis modification; *Chemical Society Reviews* **42**, 263-290, (2013).

[39] C.S. Mei, P.Y. Wen, Z.C Liu, H.X. Liu, Y.D. Wang, W.M. Yang, Z.K. Xie, W.M. Hua, Z. Gao; Selective production of propylene from methanol: Mesoporosity development in high silica HZSM-5; *Journal of Catalysis* **258**, 243-248, (2008).

[40] M. Muller, G. Harvey, R. Prins; Comparison of the dealumination of zeolites beta, mordenite, ZSM-5 and ferrierite by thermal treatment, leaching with oxalic acid and treatment with $SiCl_4$ by ^{1}H, ^{29}Si and ^{27}Al MAS NMR; *Journal of Microporous and Mesoporous Materials* **34**, 135-147, (2000).

[41] M. Mulina, S. Mitchell, N.L. Michels, J. Kenvin, J. Perez-Ramirez; Interdependence between porosity, acidity and catalytic performance by post-synthetic modification; *Journal of Catalysis* **308**, 398-407, (2013).

[42] M. Yao, N. Yao, B. Liu, S. Li, L. Xu, X. Li; Effect of SiO_2/Al_2O_3 ratio on the activities of CoRu/ZSM-5 Fischer-Tropsch synthesis catalysts; *Journal of Catalysis Science and Technology* **5**, 2821-2828, (2015).

[43] R.M. Barrer, M.B. Makki; Molecular sieve sorbents from clinoptilolite; *Journal of Chemistry* **42**, 1481-1487, (1964).

[44] S. Kumar, A.K. Sinha, S.G. Hedge, S. Sivasanker; Influence of dealumination on physicochemical, acidic and catalytic properties of H-ZSM-5; *Journal of Molecular Catalysis A: Chemical* **154**, 115-120, (2000).

[45] J. Kim, M. Choi, R. Ryoo; Effect of mesoporosity against the deactivation of MFI zeolite catalyst during the methanol-to-hydrocarbon conversion process, *Journal of Catalysis* **269**, 219-228, (2010).

[46] J.M. Muller, G.C. Mesquita, S.M. Franco, L.D. Borges, J.L. de Macedo, J.A. Dias, S.C.L. Dias; Solid-state dealumination of zeolites for use as catalysts in alcohol dehydration; *Journal of Microporous and Mesoporous Materials* **204**, 50-57, (2015).

[47] M. Bjorgen, F. Joensen, M.S. Holm, U. Olsbye, K.P. Lillerud, S. Svelle; Methanol to gasoline over zeolite H-ZSM-5 Improved catalyst performance by treatment with NaOH, *Journal of Applied Catalysis A: General* **345**, 43-50, (2008).

[48] H. Mochizuki, T. Yokoi, H. Imai, R. Watanabe, S. Namba, J.N. Kondo, T. Tatsumi; Facile control of crystallite size of ZSM-5 catalyst for cracking of hexane, *Journal of Microporous and Mesoporous Materials* **145**, 165-171, (2011).

CHAPTER 3

Experimental

3.1 Brief Introduction

This chapter describes experimental procedures for the synthesis of microporous ZSM-5 zeolite and its subsequent conversion into hierarchically porous derivatives *via* acid-mediated dealumination, together with the physicochemical characterisation techniques used. Characterisation techniques included X-ray powder diffraction (XRD), Fourier-transform infrared (FTIR) spectroscopy, scanning electron microscopy (SEM), as well as N_2 adsorption isotherms and Brunauer-Emmett-Teller (BET) surface area measurements. The procedure for the removal of MB from aqueous solutions, and expressions for quantitation are also described.

3.2 Synthesis of zeolite ZSM-5 and post-synthesis treatment

3.2.1 Materials and supplies

The zeolites were synthesised hydrothermally using a 1 L Parr 4848 high pressure reactor, fitted with a magnetic drive and a turbine-type impeller to allow overhead stirring. All chemical reagents were used as received, without further purification, and are listed in Table 3.1. The list includes colloidal SiO_2 (Ludox HS-40), aluminium sulphate octadecahydrate [$Al_2(SO_4)_3.18H_2O$], sodium hydroxide (NaOH), tetrapropylammonium bromide (TPABr), ammonium nitrate (NH_4NO_3) and nitric acid (HNO_3).

Table 3.1: Chemicals and reagents used for the preparation of adsorbent materials in this study.

Material	**Role**	**Supplier**
Ludox HS-40 (40% SiO_2, 60% H_2O)	Silica source	Sigma-Aldrich
$Al_2(SO_4)_3 \cdot 18H_2O$, (98%)	Alumina source	Sigma-Aldrich
NaOH, (97%)	Mineraliser	Rochelle Chemicals
TPABr, (99%)	Template	Acros Organics
NH_4NO_3, (98%)	Acidification	Fisher Chemicals
HNO_3, (70%)	Al extraction	Sigma-Aldrich

3.2.2 Synthesis of parent ZSM-5 zeolites

ZSM-5 zeolite was synthesised to two levels of silica-to-alumina ratio (SAR), *viz*., 25 and 50, and the resulting zeolites were designated as ZSM-5(25) and ZSM-5(50).

3.2.2.1 Synthesis of ZSM-5(50)

The synthesis of ZSM-5(50) zeolites was carried out following a method previously reported by Yu *et al.* [1], using a synthesis gel of initial molar composition

9.0 Na_2O : 1.0 Al_2O_3 : 50 SiO_2 : 0.53 $(TPA)_2O$: 1300 H_2O.

The general synthesis procedure involved the preparation of two solutions, *viz*., solution A and solution B. Solution A was prepared by dissolving *ca*. 20.40 g of NaOH and 22.04 g of $Al_2(SO_4)_3 \cdot 18\ H_2O$ in 317 mL of distilled water. The mixture was stirred for 0.5 h using an overhead stirrer to obtain a clear solution. Solution B was prepared by dissolving 8.64 g of TPABr in 20 g distilled water, followed by addition of 173.31 mL of Ludox HS-40 colloidal SiO_2, and consequent homogenisation by stirring. Solution A was then slowly added to solution B under stirring, and the mixture was further stirred for 2 h to form a homogeneous gel (pH ~14). The resulting gel was transferred into a 1 L Parr 4848 high pressure reactor and heated under hydrothermal conditions with stirring at 170 ^oC for 72 h. The as-synthesised ZSM-5 solid products were filtered from the mother liquor using a Buchner funnel, fitted with a glass microfiber filter paper (Whatman GF/C) of 12.5 cm diameter. They were then washed with distilled water until all Br^- ions were removed (confirmed by the $AgNO_3$ test). Subsequent to the washing, the zeolites were dried overnight in an oven (Labotech Ecotherm^e) at 85 ^oC, and the template was removed by calcination in a Carbolite-type S30 furnace at 550 ^oC for 5 h. The calcination process was carried out by increasing the temperature from room temperature, in steps of 50 ^oC at 15 min intervals, to 550 ^oC, and maintained at this temperature for 5 h.

3.2.2.2 Synthesis of ZSM-5(25)

This zeolite composition was synthesised according to the method reported by Nicolaides *et al.* [2], using a synthesis gel of initial molar composition

$$25\ SiO_2: Al_2O_3: 13\ Na_2O: 3\ (TPA)_2O: 3978\ H_2O$$

The synthesis procedures, including the calcination step, were the same as those used for the synthesis of ZSM-5(50) materials above, except that the hydrothermal treatment was carried out at 150 °C for 48 h.

3.2.3 Conversion of Na-ZSM-5 into H-ZSM-5

The Na-ZSM-5 zeolites obtained in Sections 3.2.2.2 and 3.2.2.3 above were ion-exchanged with a 1 M NH_4NO_3 solution in the solid-to-liquid ratio of 1 g : 20 mL. The suspension, contained in a round-bottom flask, was heated at 65 ^oC under reflux for 1 h without stirring. At the end of 1 h, the aqueous solution was decanted and a fresh NH_4^+ solution was added. This ion-exchange procedure was carried out three times. The resulting NH_4^+-ZSM-5 zeolites were thoroughly washed with distilled water until a negative nitrate test (brown-ring test) and dried overnight in an oven at 85 ^oC. Subsequently, these NH_4^+-forms of ZSM-5 zeolites were converted into H^+-forms by calcination at 550 ^oC for 4 h.

3.2.4 Dealumination of H-ZSM-5 zeolites

The dealumination of H-ZSM-5 was achieved by acid-mediated treatment following a method reported by Kooyman *et al*. [3]. In a typical procedure, approximately 5 g of H-ZSM-5 was added to 100 mL of 1 M HNO_3 solution in a 250 mL round-bottom flask. The suspension was then heated under reflux at 90 °C using a heating mantle without any stirring. Dealumination times ranged from 0.5 to 6 h. At the end of each treatment step, the mixture was left to settle and cool to room temperature, followed by filtering to recover the zeolite residue using a glass funnel fitted with a Macherey-Nagel (MN 615) filter paper with a diameter of 7.0 cm. The recovered solid product was washed thoroughly with distilled water until the pH of the filtrate was *ca*. 7. The samples were then dried overnight in a Labotech™ Ecotherm^e oven at 85 °C. Subsequently, the dealuminated H-ZSM-5 products were calcined at 550 ^oC for 4 h.

3.3 Physicochemical characterisation of ZSM-5 derivatives

3.3.1 X-ray powder diffraction

The XRD patterns of the ZSM-5 zeolites synthesised in this study were recorded on a Philips PW1830 diffractometer using Cu-K_α radiation (λ = 1.5405 Å), operated at a voltage of 40 kV and a tube current of 40 mA. The diffractometer was equipped with a primary beam Göbel mirror, a radial Soller slit and a Vanatec-1 detector. About 1 g of each zeolite was finely-ground with a mortar and pestle. The ground zeolite was mounted on an acetone-cleaned aluminium plate sample-holder. After loading the sample into the sample compartment, the diffractometer was switched on to allow the X-rays to strike the sample at different angles. The scanning speed was 0.025° per second over a 2θ range of 4 – 63°. In addition to structural confirmation, the XRD patterns were further used to determine the relative crystallinity and the crystallite size of the resulting zeolites. The relative % crystallinity of each material was calculated from the intensities of the characteristic diffraction peaks using equation 3.1 [4]:

$$\text{Relative \% crystallinity} = \frac{\sum I\,(sample)}{\sum I\,(reference)} \times 100\% \qquad 3.1$$

where $I_{(sample)}$ and $I_{(reference)}$ are the intensities of the characteristic peaks of the sample and reference material, respectively. The reference material was chosen as the sample with the highest XRD peak intensities synthesised in this work.

The crystallite size of ZSM-5 was calculated using the Scherrer equation, given by equation 3.2 [5]:

$$L = \frac{K\lambda}{\beta cos\theta} \qquad 3.2$$

where L is the crystallite size of the crystalline domains; K is a dimensionless shape factor, with a value close to 1; λ is the X-ray wavelength (1.5405 Å); β is the full-width at half maximum intensity in radians, and θ is the diffraction angle.

3.3.2 Fourier-transform infrared spectroscopy

Room-temperature FTIR spectra were recorded using an Agilent Cary 600 series FTIR spectrophotometer (equipped with Agilent Resolutions Pro software) in the wavenumber range 500 - 4000 cm^{-1}. ZSM-5 samples were ground to a fine powder using a mortar and pestle. Approximately 0.05 g of the sample was packed into the

hole of the crystal plate sample holder. The sample was pressed sufficiently and covered atop with a crystal plate. Thereafter, a crystal plate clamp was pinned in place, followed by closing the instrument cover in order to collect the FTIR spectra of the samples for about 20 min per sample. For every sample, 100 scans were collected using a resolution of 4 cm^{-1}.

3.3.3 N_2 adsorption analysis

N_2 adsorption/desorption experiments were carried out using a Micrometrics Tristar II Surface Area and Porosity Analyser 3000 instrument. For the sorption measurements, approximately 0.1 g of sample was degassed overnight (using N_2 gas) at 400 °C to completely remove the water inside the pores and subsequently cooled to room-temperature. After the degassing process, the sample holder containing the zeolite was loaded on the analysis station for the determination of the adsorption isotherms. The BET surface areas were calculated from the N_2 isotherms at -196 °C.

3.3.4 Scanning electron microscopy

Samples for SEM analysis were prepared as follows:

A 40.0 mm x 20.4 mm aluminium stub was covered with 12 mm double-sided carbon tape (S-05082-AB, SPI Supplies, USA). The carbon tape was also attached to a transparency paper, which was subsequently cut into small pieces (12 mm x 3 mm) to strengthen the carbon tape. These pieces were dipped into the zeolite sample resulting in small quantities of powder attaching to the carbon tape. About 6 to 8 of these small carbon tape pieces containing different samples were placed on the double sided carbon tape that was attached to the aluminium stub. Excess powder was removed by using a single blast of compressed dry nitrogen gas. The samples were then coated with gold under argon gas using an Emitech K550X sputter-coater (Ashford, England). They were then viewed on a JEOL JSM-5800LV (JEOL, Tokyo, Japan) scanning electron microscope. The samples were imaged at 5 kV and lowest beam current that would achieve the optimum resolution of a specific magnification. The low beam intensity was used as a precaution to avoid sample damage.

3.3.5 Methylene blue adsorption studies

The performance of the bulk and dealuminated ZSM-5 zeolites in the adsorption of MB from aqueous solutions was investigated by adopting a method reported by Gong *et al*. [5]. A batch-type experimentation was carried out at room temperature for this study. In a typical procedure, ZSM-5 zeolites were added to 250 mL conical flasks containing 50 mL of MB solutions with concentrations in the range 50 – 250 mg/L, and agitated at 300 rpm for 0.5 – 6 h. After each experiment, the solid materials were filtered off from the liquid solutions using a Whatman™ filter paper with a diameter of 11.0 cm. The final concentrations of MB in the filtrates were determined by using a UV-Vis spectrophotometer (Shimadzu UVmini-1240) at, λ = 660 nm. The percentage MB removal was calculated using the equation:

$$\% \text{ MB Removal} = \frac{(Ci - Ceq)}{Ci} \times 100 \qquad 3.3$$

where C_i is the initial concentration (mg/L) and C_{eq} is the equilibrium concentration (mg/L).

The adsorption capacity of each zeolitic adsorbent for MB (in mg/g) was calculated using the equation:

$$q_e = \frac{(Ci - Ceq)V}{m} \qquad 3.4$$

where q_e is the amount of MB adsorbed (mg/g), m is the mass of the adsorbent used (g) and V is the volume of the analysed solution (L). The influence of process variables such as pH, initial concentration, contact time and adsorbent dose on MB uptake by the different zeolites was investigated.

3.4 References

[1] Q. Yu, C. Cui, Q. Zhang, J. Chen, Y. Li, J. Sun, C. Li, Q. Cui, C. Yang, H. Shan; Hierarchical ZSM-11 with intergrowth structures: Synthesis, characterisation and catalytic properties; *Journal of Energy Chemistry* **22**, 761-768, (2013).

[2] C. P. Nicolaides, M. Waplennik, K. I. G. Weis, H. Van Der Akker, B. Van Zalk, P. Wielaard; Alkali metal cation exchange of ZSM-5 and the catalytic properties of alkylised zeolites; *Journal of Applied Catalysis* **68**, 31-39, (1991).

[3] P.J. Kooyman, P. van der Waal, H. van Bekkum; Acid dealumination of ZSM-5; *Zeolites* **18**, 50-53, (1997).

[4] S.S. Rayalu, J.S. Udhoji, S.U. Meshram, R.R. Naidu, S. Devotta; Estimation of crystallinity in fly ash-based zeolite-A using XRD and IR spectroscopy; *Current Science Journal* **89**, 2147-2151, (2005).

[5] J. Gong, J. Liu, Z. Jiang, X. Wen, E. Mijowska, T. Tang, X. Chen; A facile approach to prepare porous cup-stacked carbon nanotubes with high performance in adsorption of methylene blue; *Journal of Colloid and Interface Science* **445**, 195-204, (2015).

CHAPTER 4

RESULTS AND DISCUSSION

4.1 Introduction

In this chapter, the results obtained from the physicochemical characterisation of ZSM-5 zeolitic materials, as well as their performance in the adsorptive removal of methylene blue (MB) from aqueous solutions are presented and discussed. The major characterisation techniques used in this study were X-ray diffraction (XRD), Fourier-transform infrared (FT-IR) spectroscopy, Brunauer-Emmett-Teller (BET) surface area measurements and scanning electron microscopy (SEM). No elemental analysis was done on the final zeolites. Therefore, the silica-to-alumina ratio (SAR) quoted for each sample was determined directly from the synthesis gel composition, and is consequently nominal. Two pristine ZSM-5 zeolites were synthesised to SARs of 25 and 50, respectively, and were further dealuminated *via* treatment with aqueous HNO_3 solutions to influence their structural as well as their MB adsorption properties. For ease of reference, the different sets of parent zeolites are designated as ZSM-5(x), where *x* is the nominal SAR, a notation that was also held for dealuminated materials.

4.2 XRD patterns

The parent ZSM-5 zeolites and their dealumination derivatives were examined using XRD for phase confirmation and crystallinity elucidation. The figure below shows the XRD patterns of the pristine ZSM-5(25), synthesised at 150 °C for 72 h, and its derivatives obtained by HNO_3 acid dealumination for different lengths of time.

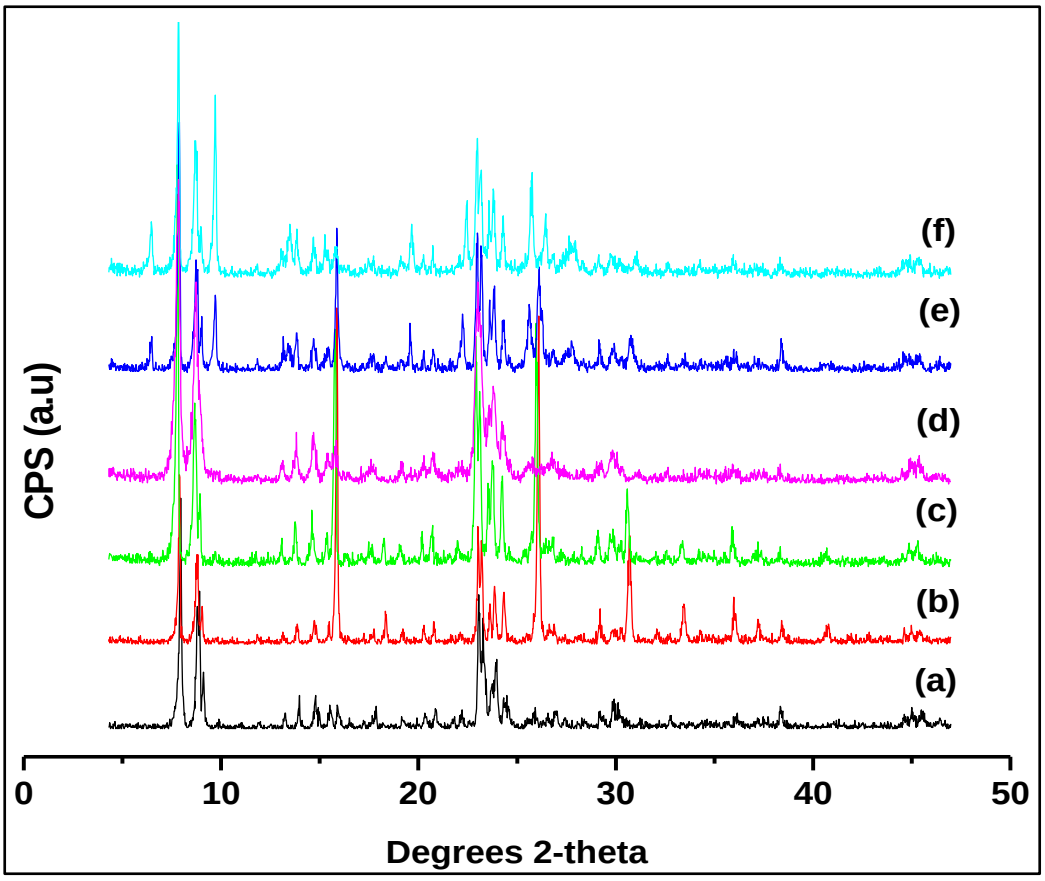

Figure 4.1: XRD patterns of the ZSM-5(25) sample synthesised at 150 °C for 72 h and its dealumination derivatives: (a) Parent, (b) 0.5 h, (c) 2.5 h, (d) 3 h, (e) 4 h and (f) 5 h.

It follows from Figure 4.1(a) that the parent ZSM-5 zeolite was successfully synthesised in this study, as evidenced by sets of peaks at ~8 - 10°, 24 - 26°and 45° 2θ which are characteristic of the MFI topology [1]. The material obtained by dealuminating for 0.5 h [Figure 4.1(b)] possesses all the characteristic MFI peaks, but shows enhanced intensities of the XRD peaks at ~16°, ~26.4° and 31° 2θ. Triantafilidis *et al*. [2] attributed the increase in intensity of peaks to relatively small changes occurring in the unit cell of a ZSM-5 zeolite after dealumination. They reasoned that the removed aluminium species may form extra-framework aluminium (EFAL) fragments, which change the framework arrangement of ZSM-5 and lead to intense signals in the XRD patterns. Furthermore, the intensity of the peak at ~23° 2θ decreases slightly as a result of the dealumination treatment leading to a decrease in relative crystallinity. Dealumination for 2.5 h [Figure 4.1(c)] showed a similar effect, with intense peaks at ~16°, ~26.4° and 31° 2θ. However, the intensities of these peaks are slightly lower compared to those of the material acid-treated for 0.5 h [Figure

4.1(b)]. A further increase in the dealumination time to 4 h and higher [Figures 4.1(e) and (f)] produces additional non-MFI XRD peaks at ~6.4°, 9.7° and 22.19° 2θ. These additional signals closely resemble those of analcime zeolite, by analogy with the findings by Sari *et al*. [3]. Notably, the MFI structure of the pristine zeolite was maximally retained, regardless of the coexistence of additional phase.

Figure 4.2 illustrates the variation of the relative crystallinity (RC) of ZSM-5(25) samples with dealumination time. RC value are tabulated in Appendix (Table A1).

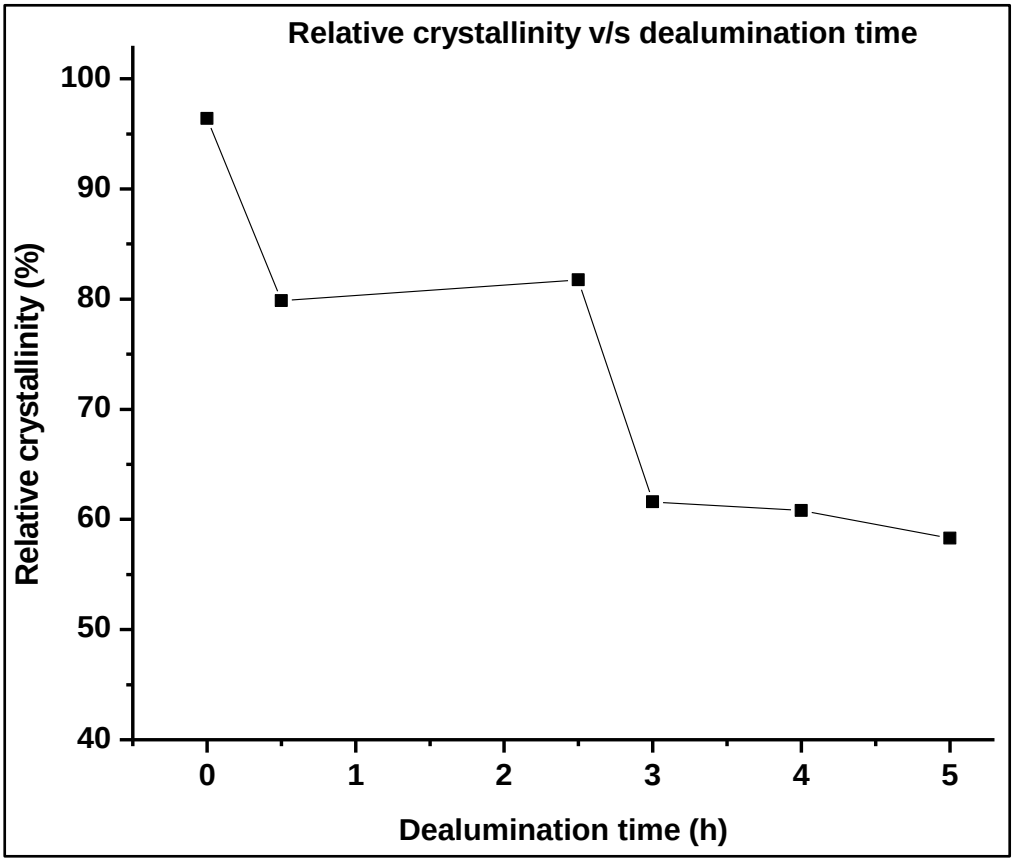

Figure 4.2: Variation of the relative crystallinitiy of ZSM-5(25) samples with dealumination time. The intensities were normalised to those of the ZSM-5(50) sample used as a reference, and the dealumination time of 0 h corresponds to the pristine ZSM-5(25) zeolite.

The RC of these materials decreases as the dealumination time increases. A breakdown in the trend is observed as the dealumination treatment time is increased to 2.5 h. Within the dealumination period of 0 – 5 h, all samples were found to exhibit relative crystallinity values of ≥60 %. Fan *et al.* [4] also studied the dealumination of H-ZSM-5 and found that the RC decreased as a result of the formation of an additional phase. Furthermore, dealumination of zeolites has been reported by other researchers to be associated with partial loss of relative crystallinity [4, 5]. Moreover, the

dealumination of aluminium-rich zeolites was also found to produce multiple lattice defects, resulting in a lower stability of the crystal structure.

The corresponding crystallite sizes of the ZSM-5(25) derivatives, as calculated using the Scherrer equation, are shown in Figure 4.3. Crystallite sizes tabulated in Table A1.

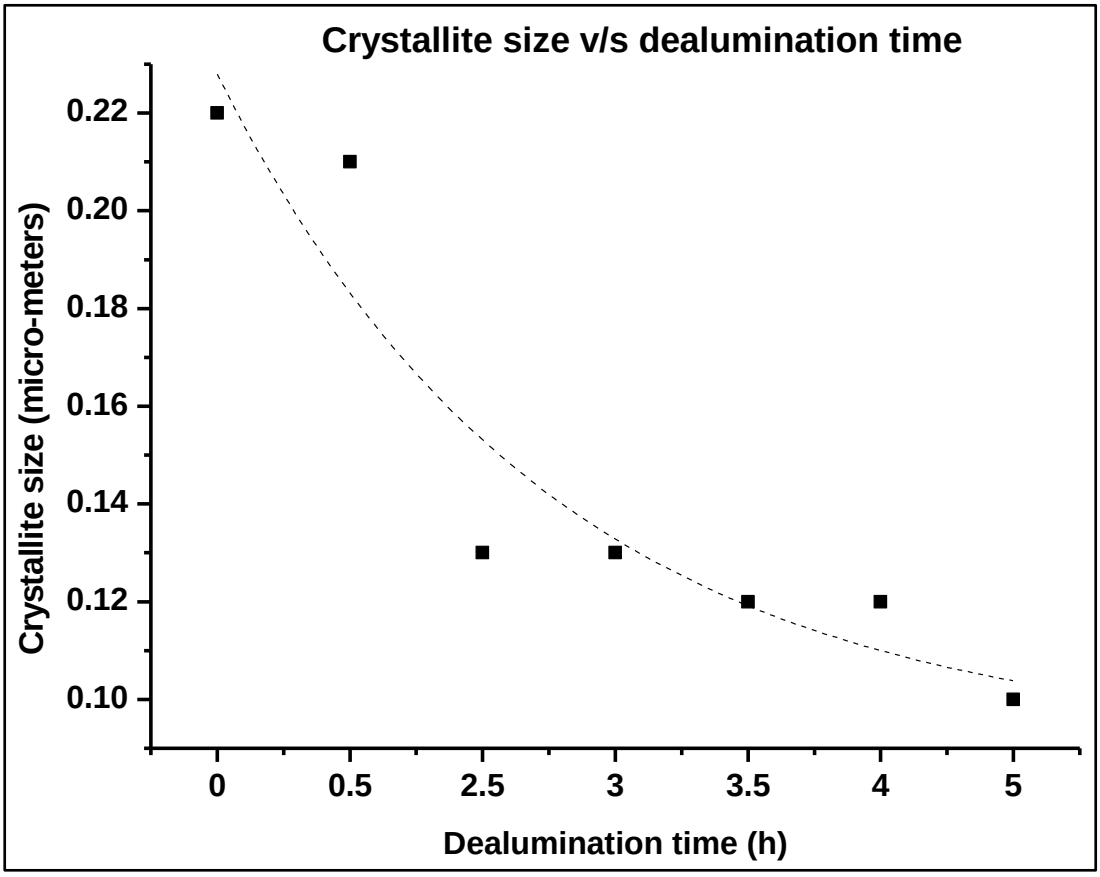

Figure 4.3: Variation of the crystallite size of ZSM-5(25) samples with dealumination time. The dealumination time of 0 h corresponds to the pristine ZSM-5(25) zeolite.

The Scherrer crystallite sizes of the ZSM-5(25)-based zeolites decrease with dealumination time. A 54.5 % reduction in the Scherrer crystallite size is attained after 5 h of HNO_3-mediated dealumination of the pristine zeolite. This decrease in the Scherrer crystallite sizes of ZSM-5 materials has also been previously reported [4, 6].

A pristine ZSM-5(50) sample, synthesised using the same protocol as ZSM-5(25) discussed above, was similarly dealuminated and the XRD patterns of the resulting series of zeolites are shown in Figure 4.4.

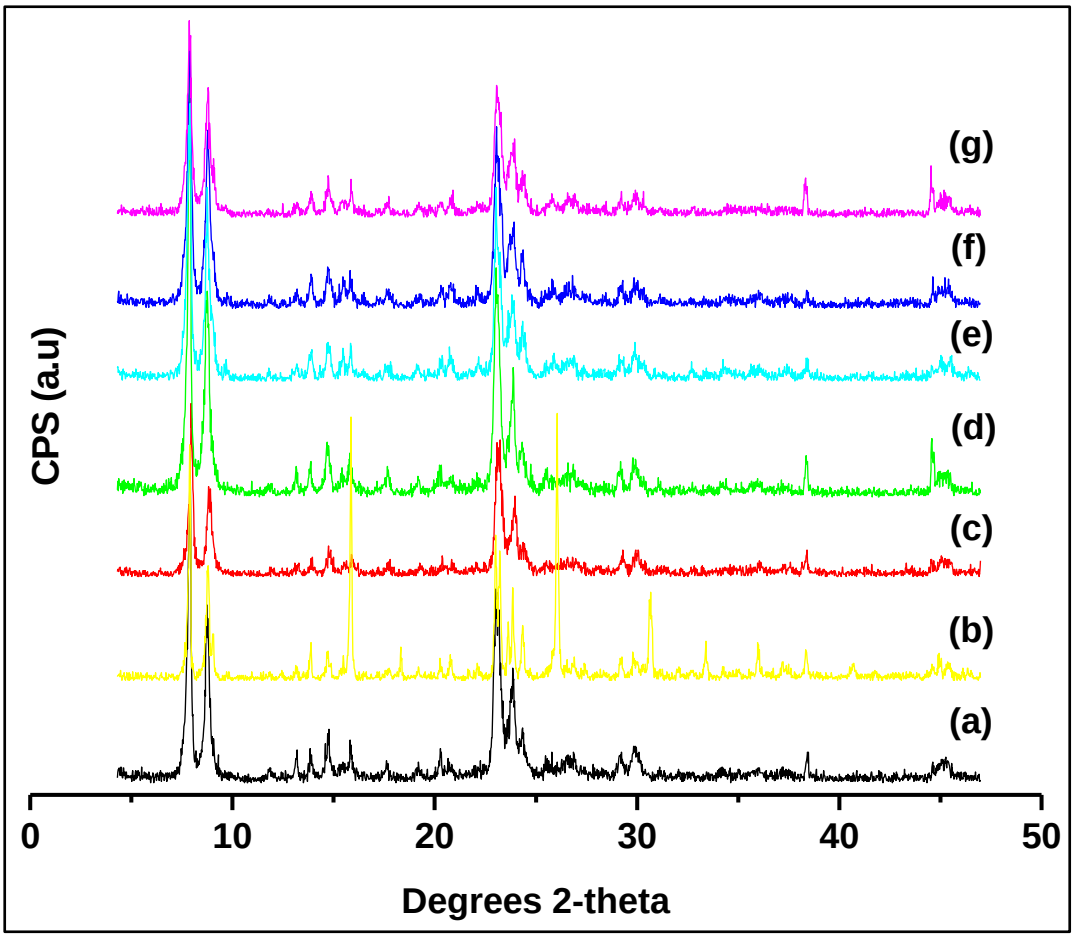

Figure 4.4: XRD patterns of the ZSM-5(50) sample synthesised at 150 °C for 72 h and its dealumination derivatives: (a) Parent (0 h) (b) 0.5 h, (c) 1.5 h, (d) 2 h, (e) 3 h, (f) 4 h and (g) 5 h.

A successful synthesis of the pristine material is highlighted by Figure 4.4(a). Interestingly, the pristine MFI framework structure was totally maintained throughout the dealumination treatment up to 5 h as evidenced by the absence of non-MFI peaks. This observation suggests the resistance of ZSM-5(50) to structural collapse through acid-mediated dealumination over the treatment-time range studied. However, the shortest dealumination time (0.5 h) was accompanied by enhancement of certain MFI reflections (Figure 4.4(b)) relative to the pristine zeolite, especially the ones at 2θ values of ~16. ~26.4 and ~31°. This observation is analogous to that in the ZSM-5(25) counterpart in Figure 4.1(b) above. The ZSM-5(50) series of zeolites is more resistant, compared with ZSM-5(25) samples, to structural degradation by the corrosive treatment.

Figure 4.5 illustrates the effect of dealumination time on the relative crystallinity of the pristine ZSM-5(50). RC values are tabulated in Table A3 of Appendix section.

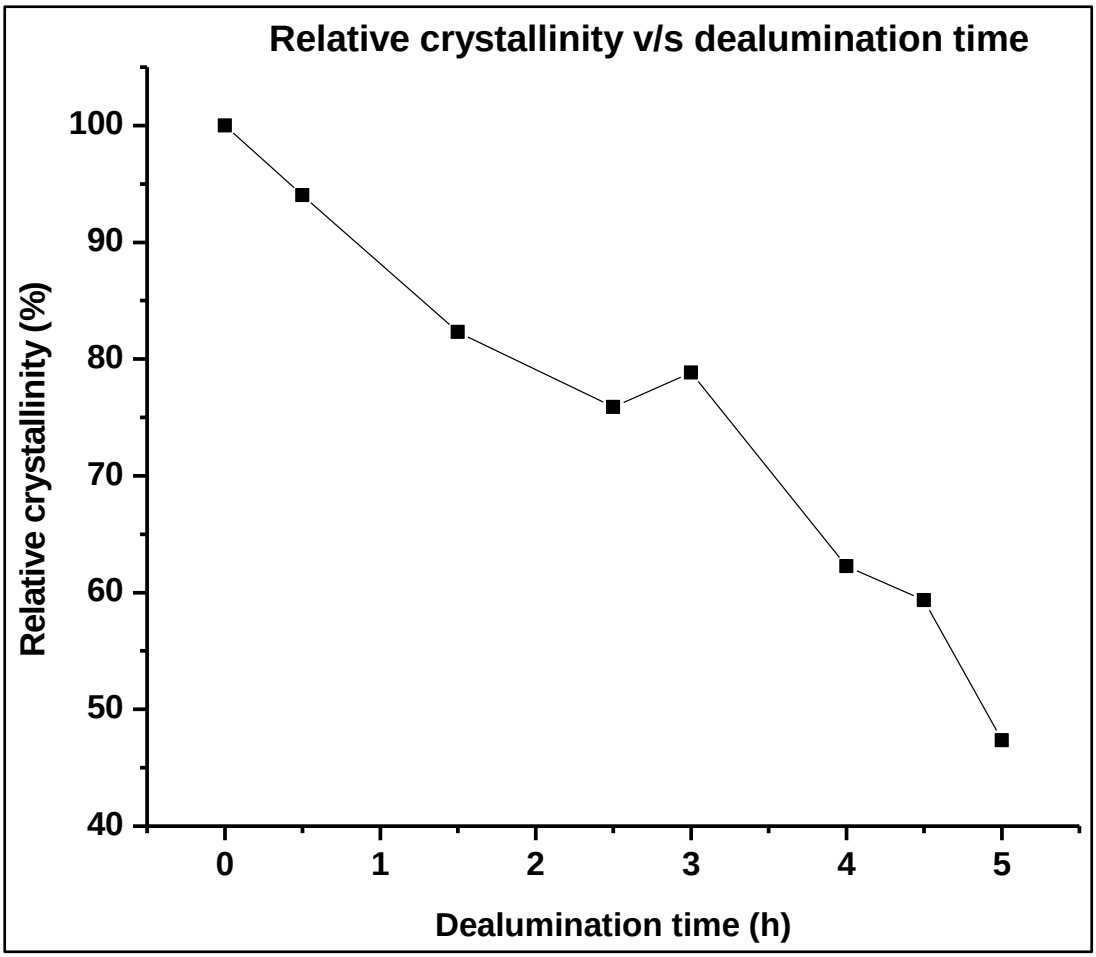

Figure 4.5: Variation of the relative crystallinitiy of ZSM-5(50) samples with dealumination time. The intensities were normalised to those of the pristine sample used as a reference, and the dealumination time of 0 h corresponds to the pristine ZSM-5(50) zeolite.

The RC of ZSM-5(50) also shows a general decrease with HNO_3-aided dealumination time, with a slight breakdown in the trend at 3 h. This observed fluctuation may arise from a dealumination-realumination cycle taking place during this treatment. The general decrease observed may be a result of lattice contractions as aluminium species are extracted from the pristine zeolite framework. Previous studies have also found that dealumination of zeolites produces a partial loss of their crystallinity [4 – 6].

The change in the crystallite size of ZSM-5(50) was also studied as a function of the duration of acid-mediated dealumination, and the results are shown in Figure 4.6. The crystallite sizes that were calculated are tabulated in Table A3 of Appendix section.

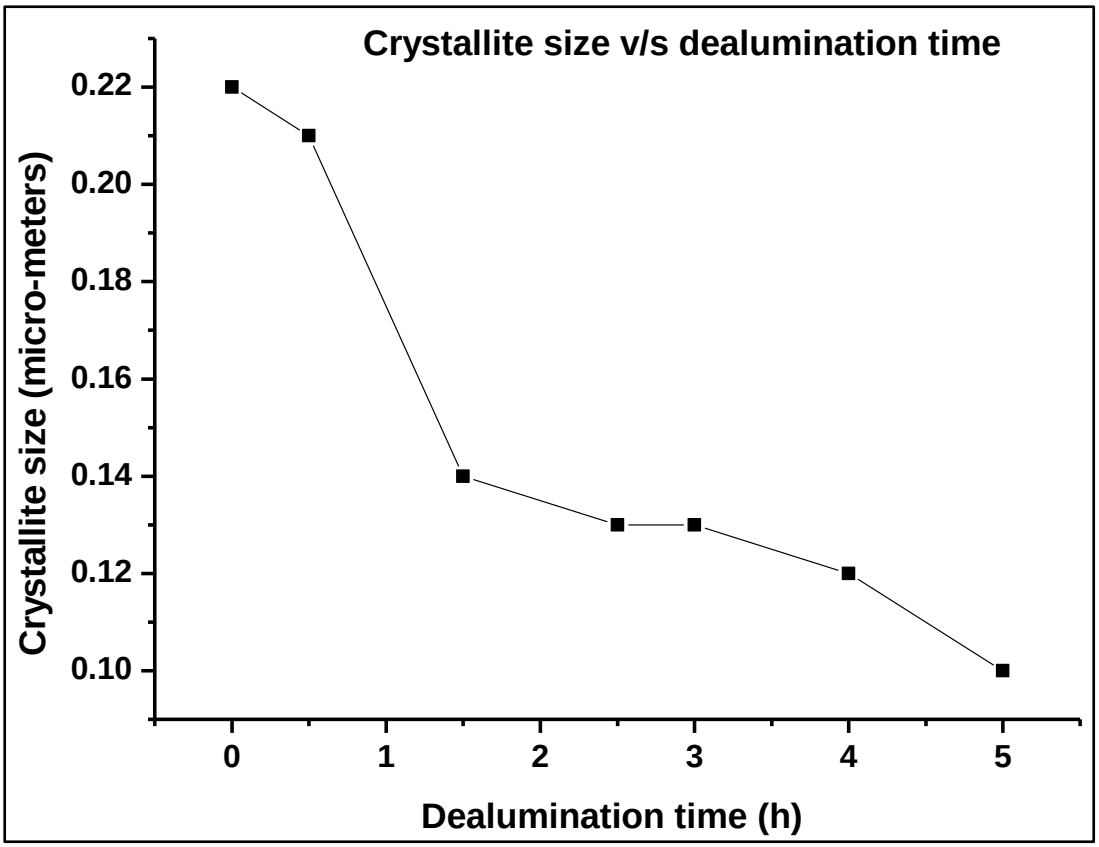

Figure 4.6: Variation of the crystallite size of ZSM-5(50) samples with dealumination time. The dealumination time of 0 h corresponds to the pristine ZSM-5(50) zeolite.

It follows from Figure 4.6 that the Scherrer crystallite size also decreases with HNO_3 treatment time, decreasing from ~0.22 μm in the parent zeolite to ~0.11 μm after a 5 h treatment. This 50 % decrease in the crystallite size is less than that found for the ZSM-5(25) series of zeolites (54%) over the same period of treatment, and further highlights the resistance of this material to structural collapse. Previous studies have also found the dealumination in ZSM-5 to be accompanied by a decrease of the Scherrer crystallite size [4, 6].

4.3 FTIR spectroscopy

The figure below shows IR spectra of the ZSM-5(25) series of zeolites obtained by acid-mediated dealumination.

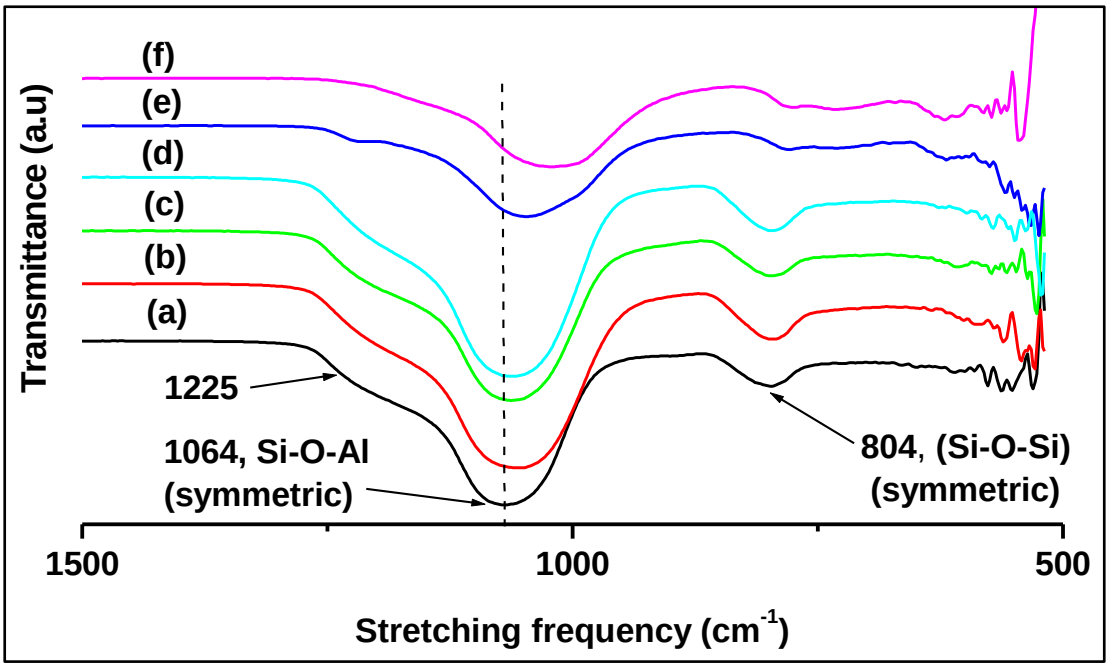

Figure 4.7: Framework IR spectra of ZSM-5(25) recorded as a function of dealumination time: (a) Parent, (b) 0.5 h, (c) 2.5 h, (d) 3 h, (e) 4 h and (f) 5 h.

The spectrum of the parent ZSM-5(25) material [Figure 4.7(a)] shows characteristic zeolitic vibration bands at ~1064 cm^{-1} (with a shoulder at ~1225 cm^{-1}) and ~800 cm^{-1}, which are attributed to symmetric Si-O-Al vibrations and symmetric Si-O-Si vibrations, respectively [1]. The intensity of the Si-O-Al band is indicative of the aluminium content found in a zeolitic sample [7]. Upon dealumination for 0.5 h [Figure 4.7(b)], 2.5 h [Figure 4.7(c)] and 3 h [Figure 4.7(d)], the intensity of the characteristic bands is similar with those of the parent zeolite spectrum. Further extending the dealumination time to 4 h [Figure 4.7(e)] shows a significant decrease in the intensity of the symmetric Si-O-Al vibration. The removed aluminium species have a tendency to form EFAL species [8, 9], which may account for the increase in the intensity of this band. Extending the dealumination treatment further to 5 h [Figure 4.7(f)] led to a decrease in the intensity of the symmetric Si-O-Al band. This is accompanied by the disappearance of the symmetric Si-O-Si band with respect to the parent. The zeolitic functional groups of ZSM-5(25) are more resistant to degradation by the dealumination treatment to different extents.

Figure 4.8 shows the FTIR spectra in the framework region of ZSM-5(50) series of zeolites obtained by acid-mediated dealumination.

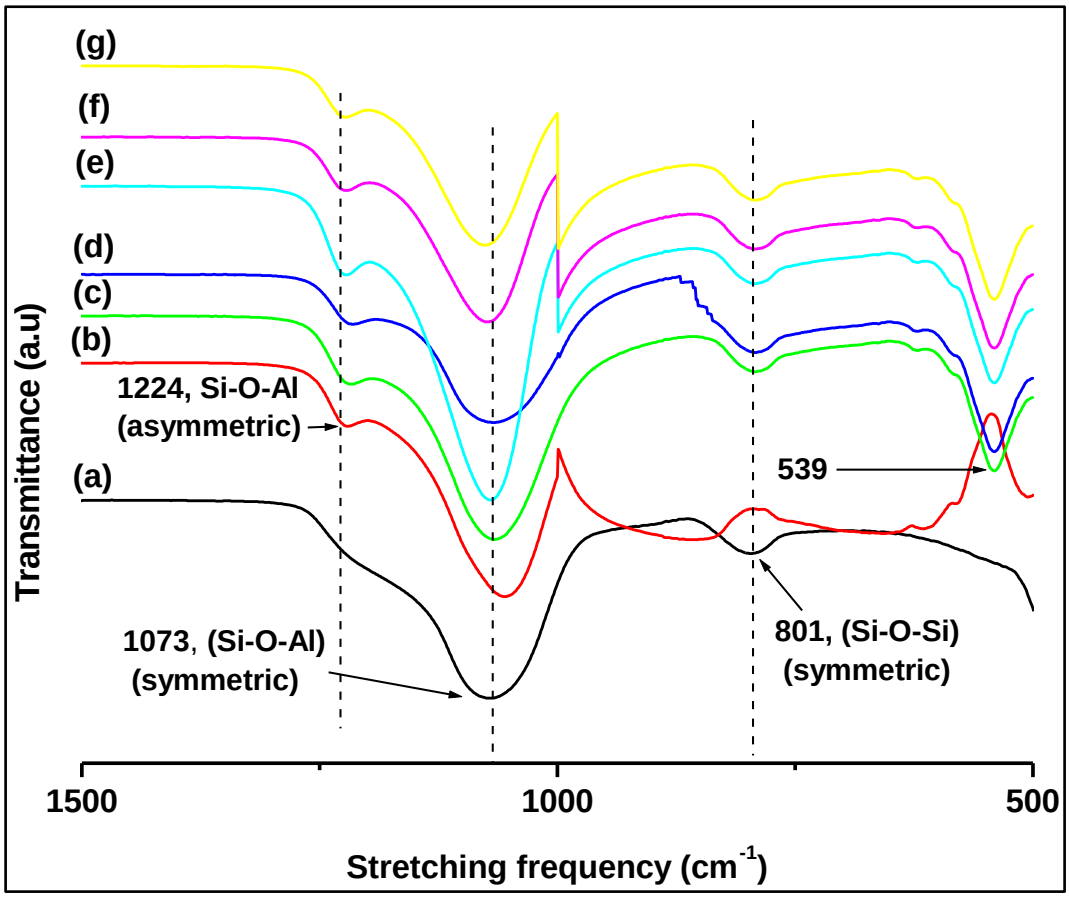

Figure 4.8: Framework IR spectra of ZSM-5(50) recorded as a function of dealumination time: (a) Parent, (b) 0.5 h, (c) 1.5 h, (d) 2 h, (e) 3 h, (f) 4 h and (g) 5 h.

The spectrum of the parent material [Figure 4.8(a)] shows characteristic zeolitic vibration bands at ~1224 cm^{-1}, ~1073 cm^{-1} and ~801 cm^{-1}, which are attributed to asymmetric Si-O-Al, symmetric Si-O-Al and symmetric Si-O-Si vibrations, respectively [1]. The intensity of the symmetric Si-O-Al band is indicative of aluminium content in the zeolite sample while the crystalline ZSM-5 structure is indicated by a band at ~539 cm^{-1} [3]. As the ZSM-5 material was dealuminated for 0.5 h [Figure 4.8(b)], the intensity of the symmetric Si-O-Al band decreased. However, the band at 1224 cm^{-1} is more pronounced on this derivative compared to the parent zeolite. This vibration is observed as a shoulder on the spectrum of the parent sample. As the dealumination treatment was increased to 1.5 h [Figure 4.8(c)], a decrease in the intensity of the symmetric Si-O-Al band is observed. The intensity of the asymmetric vibration at 801 cm^{-1} increases compared to that of the parent ZSM-5(50). Further increasing the dealumination time to 2 h [Figure 4.8(d)] shows a more pronounced decrease in the intensity of the symmetric Si-O-Al band. Further increase of the dealumination time to 3 h results in an increase in the intensity of the symmetric Si-O-Al band at 1073 cm^{-1}.

Increasing the treatment time from 4 to 5 h [Figure 4.8(f) – (g)] resulted in no significant changes compared to the spectrum of the parent. The spectra of the dealuminated ZSM-5(50) variants show a general shift in the position of the symmetric Si-O-Al vibration compared to that of the parent.

4.3 N_2 sorption isotherms

The ZSM-5(25)-derived materials were characterised using adsorption-desorption isotherms and the results are shown in Figure 4.9.

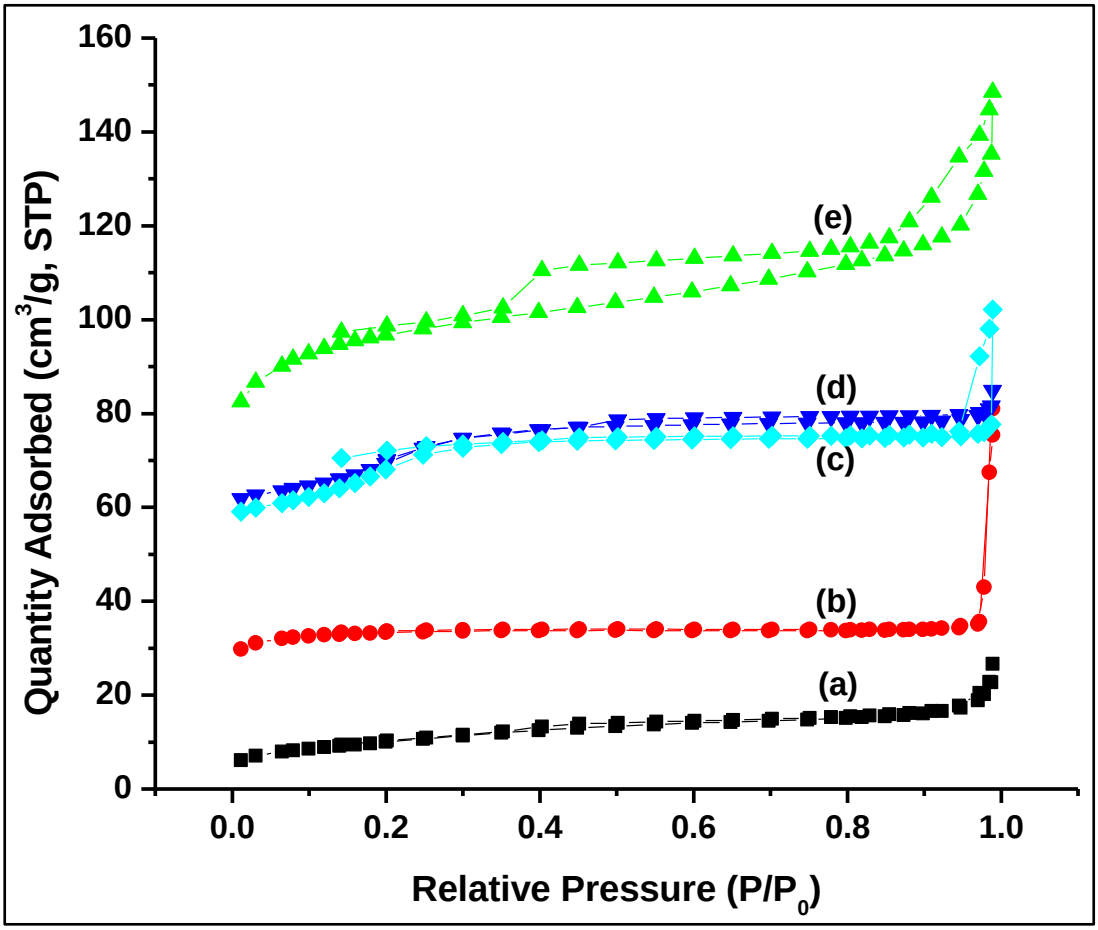

Figure 4.9: N_2 adsorption/desorption isotherms of pristine ZSM-5(25) and its dealuminated variants: (a) Parent, (b) 0.5 h, (c) 3.5 h, (d) 4 h and (e) 5 h. 0 h represents pristine ZSM-5(25).

It is apparent from Figure 4.9 that the parent material exhibits a Type I isotherm, a characteristic feature of microporous materials [1, 4]. The lowest N_2 adsorption capacity was observed for this material and increased with dealumination time in the dealuminated derivatives. The largest increase in N_2 adsorption was obtained in the material that was dealuminated for 5 h. The development of a hysteresis loop is also observed in the dealuminated samples in the partial pressure range $0.4 < P/P_0 < 0.8$.

The hysteresis loop signals the presence of mesopores in the dealuminated ZSM-5(25) samples, and is more pronounced in the derivative obtained after 5 h dealumination. It is interesting to remember that this ZSM-5(25) derivative also showed the co-existence of an additional non-MFI phase in Figure 4.1(e). The increased uptake of N_2 at higher relative pressure, coupled with the pronounced hysteresis loop confirms a hierarchically porous system containing both micro- and meso-pores within the same zeolite matrix [3, 4]. It is apparent that the dealumination of ZSM-5(25) affects the structure of the material by improving its porosity.

The figure below shows the variation of the surface area of ZSM-5(25) samples with increasing dealumination time. Textural properties of ZSM-5(25) materials are tabulated in Table A2 of Appendix section.

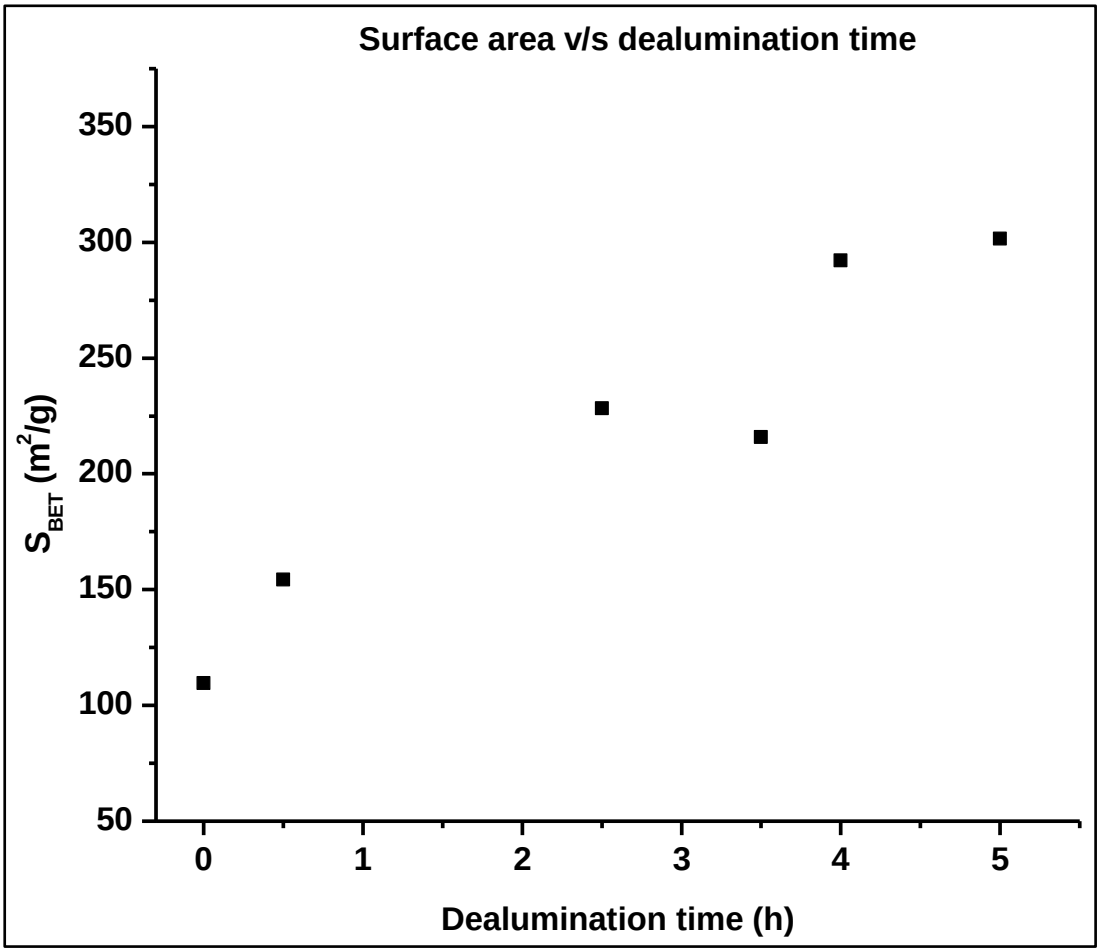

Figure 4.10: Variation of the BET surface area of ZSM-5(25) samples with dealumination time.

The surface area of the materials obtained by dealumination of ZSM-5(25) seems to increase with dealumination time, with a tendency to level off beyond 5 h. A maximum BET surface area of 301 m^2/g was reached at 5 h of HNO_3 treatment, making 5 h a

requisite treatment time for achieving high surface area materials, though resulting in mixed zeolite phases. Other researchers have also reported an increase of surface area with dealumination time [4, 6].

Below is a depiction of the relationship between the BET surface area of ZSM-5(25) materials and the relative crystallinity, achieved by dealuminating the parent zeolite for different periods of time.

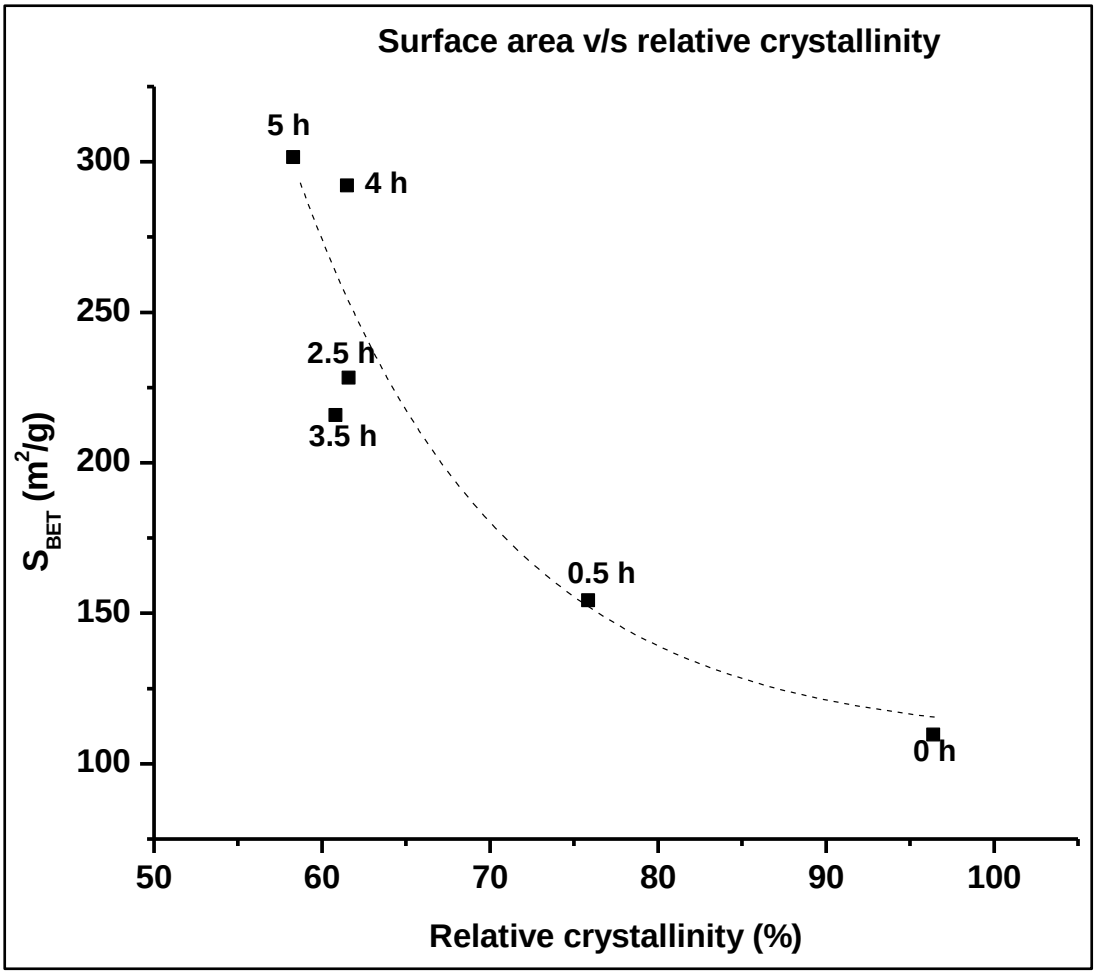

Figure 4.11: Variation of the BET surface area of ZSM-5(25) samples. The dealumination time used to achieve each S_{BET}/RC pair is indicated inside the plot area.

The general trend suggests that the BET surface area of the ZSM-5(25) series of zeolites decreases asymptotically with RC. This figure also suggests that highly crystalline materials possess low BET surface areas. It is interesting to note from this plot that high surface area derivatives with moderate crystallinity are obtained at high dealumination times. Therefore, to obtain high surface area materials, the RC range between 50 and 65% should be targeted in the preparation of these zeolites.

The nitrogen adsorption-desorption isotherms of the ZSM-5(50) series of zeolites related by acid dealumination are depicted in Figure 4.12.

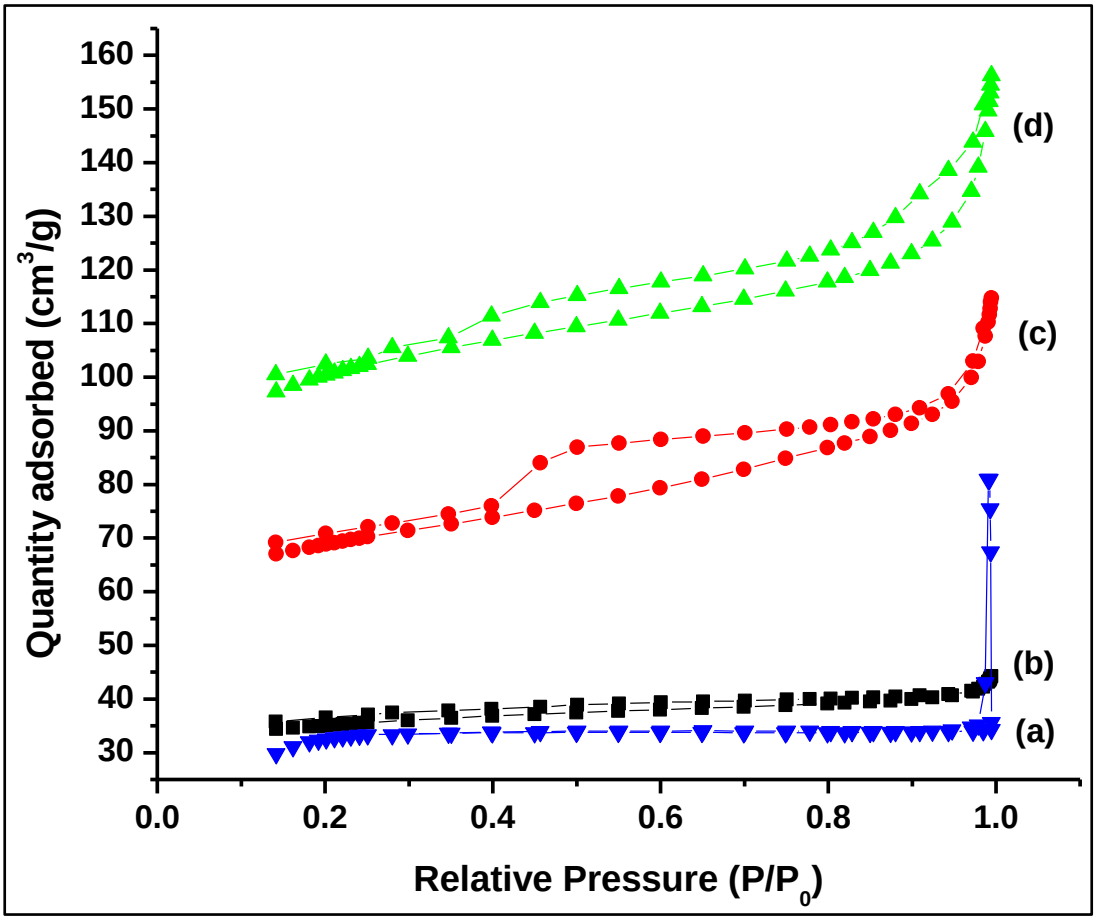

Figure 4.12: N_2 adsorption/desorption isotherms of pristine ZSM-5(50) and its dealuminated variants: (a) Parent, (b) 0.5 h, (c) 2.5 h and (d) 3 h. 0 h represents the parent material.

The parent ZSM-5(50) material exhibits a Type I N_2 adsorption isotherm, a characteristic feature of microporous materials [1, 4]. Upon dealumination, improvements are observed in the N_2 adsorption capacity, accompanied by the appearance of an obscure hysteresis at P/P_0 0.3 – 0.9. The hysteresis loop is more pronounced for materials acid-treated for ≥ 2.5 h. The increased uptake of N_2 at higher relative pressure, coupled with the pronounced hysteresis loop confirms a hierarchically porous system containing both micro- and meso-pores within the same zeolite matrix [4, 5]. However, the hysteresis loops of the isotherms cannot be assigned to any significant ordered mesoporosity that develops after dealumination of the parent ZSM-5(50) due to the unpredictability of dealumination [2].

The relationship between BET surface area and dealumination time for the ZSM-5(50) series of zeolites is depicted below. Textural properties of ZSM-5(50) samples are compiled in Table A4 in Appendix section.

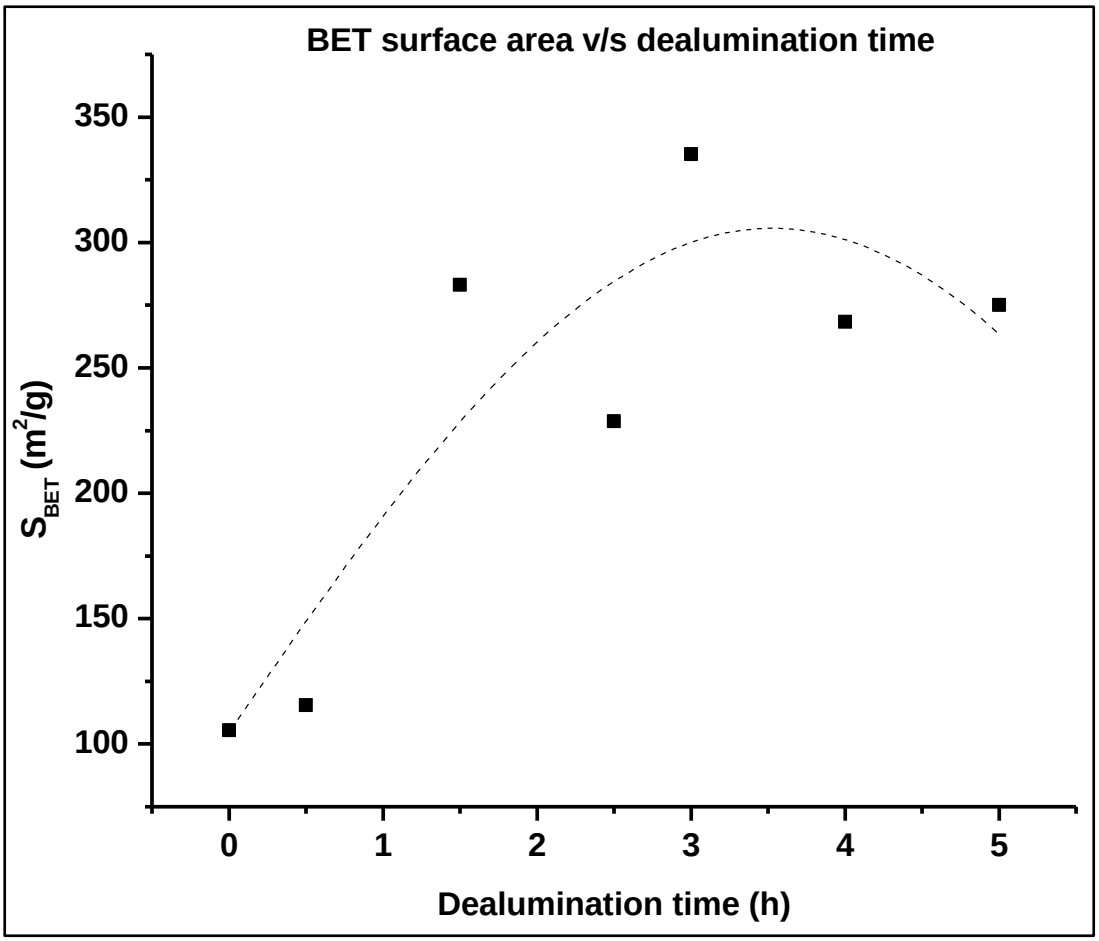

Figure 4.13: Variation of surface area of ZSM-5(50) zeolites with dealumination time.

As the dealumination time increases, the surface area of the materials is observed to increase relative to that of the parent material. The surface area of this series of zeolites was found to increase from 105 m^2/g in the parent ZSM-5(50) to a maximum of 335 m^2/g in the sample obtained after 3 h of HNO_3 acid treatment. This is higher than the 302 m^2/g surface area recorded for ZSM-5(25). Figure 4.13 suggests that the specific surface area increases through a maximum as the HNO_3-treatment time is increased, making 3 h an optimal treatment time. The data points are spread above and below the trend line

The variation of BET surface area with the relative crystallinity of ZSM-5(50), induced by different dealumination times, is shown in Figure 4.14

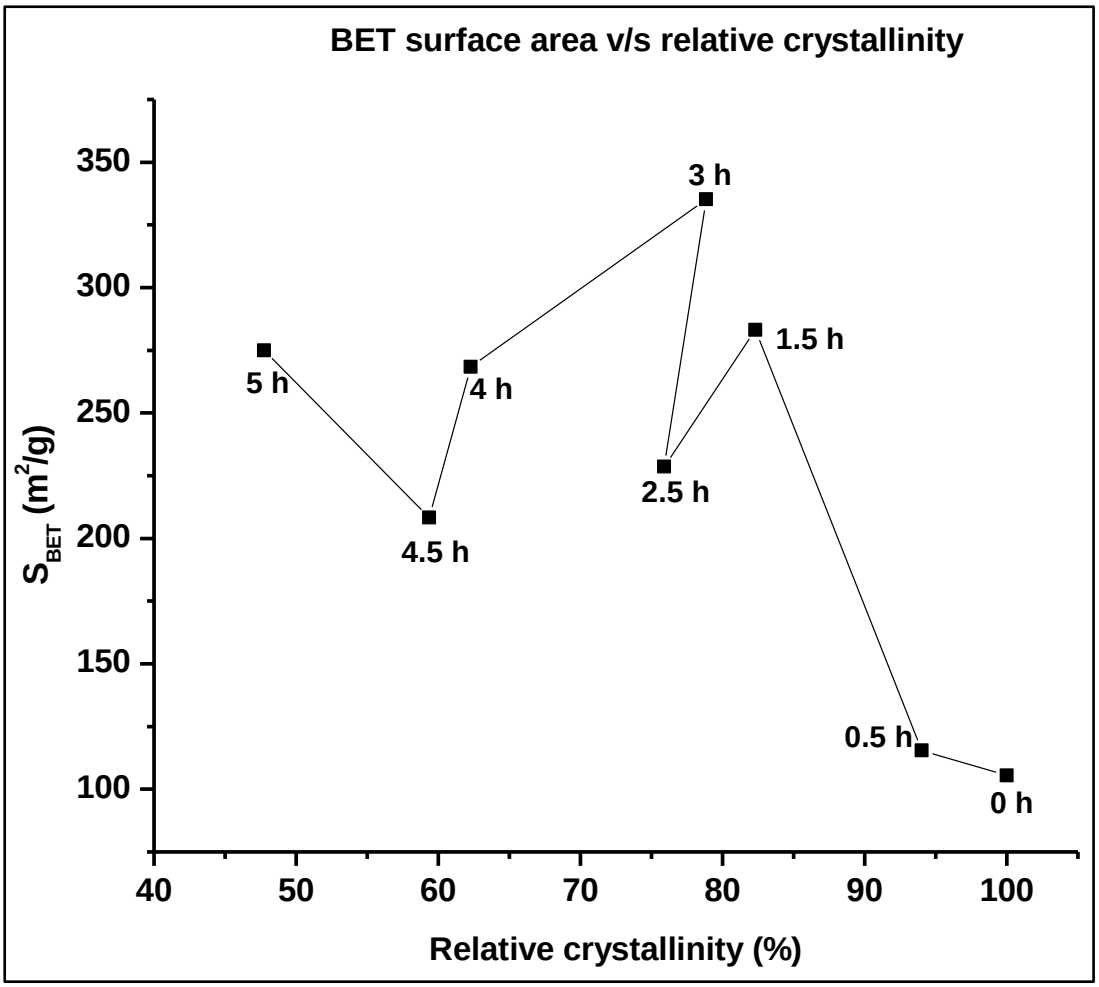

Figure 4.14: Variation of BET surface area and relative crystallinity of ZSM-5(50) with dealumination time. The dealumination time used to achieve each S_{BET}/RC pair is indicated in the plot area.

The data points in this figure do not follow a clear general trend, but suggest that highly crystalline products have the lowest specific surface areas. In terms of the dealumination time responsible for the observed RC/S_{BET} pairs, it can be concluded that longer treatment times (≥ 1.5 h) are necessary to produce high surface area materials with reasonable retention of crystallinity. Interestingly, the MFI structure for this series of zeolites was maximally retained, with no evidence of a "foreign" phase in the XRD patterns (Figure 4.4). Therefore, it can be safely concluded in this work that 3 h dealumination is recommendable for achieving a high surface area derivatives of reasonable crystallinity.

4.4 SEM micrographs

The surface morphology of ZSM-5 zeolites prepared in this work was studied using scanning electron microscopy (SEM). Several areas of each sample were imaged at

different magnifications to zoom into the different shapes present. Only the ZSM-5(50) series of zeolites prepared in this work was studied by SEM because of its maximal retention of the MFI structure throughout the dealumination time range investigated, in contrast with ZSM-5(25) (see XRD patterns in Figures 4.1 and Figure 4.4) The SEM micrographs of the parent ZSM-5(50) zeolite, synthesised by hydrothermal treatment of the pertinent precursor gel, are shown in Figure 4.15.

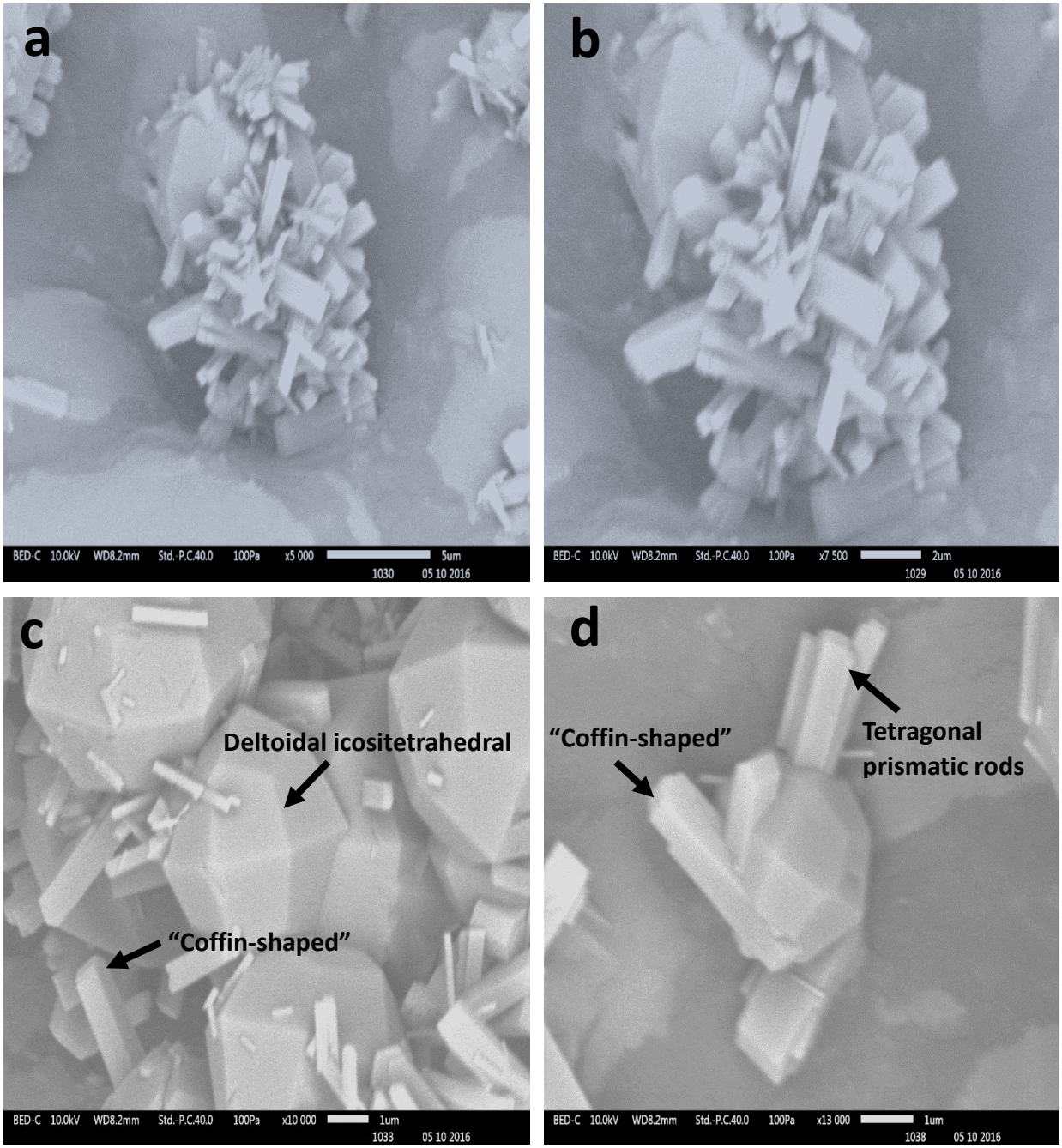

Figure 4.15: SEM micrographs of parent ZSM-5(50) zeolite calcined at 550 ° C for 5 h. The micrograph are arranged in order of increasing magnification: (a) x1500, (b) x3000, (c) x10000 and (d) x20000. Arrows in (c) and (d) highlight key morphological features.

The morphology of this sample is dominated by large deltoidal icositetrahedral crystals, in the proximity of randomly-aligned rod-like prismatic particles including coffin-shaped crystals. The large crystals appear with multiple faces of trapezohedral form [illustrated by arrows on Figure 4.15(c)], which are unusual for ZSM-5 materials, and have never been reported in the literature. Such a morphology has been commonly-observed in zeolite analcime [6]. Moreover, the parent ZSM-5(50) material is observed to consist of well-defined crystals with smooth surfaces [clearly apparent in Figure 4.15(d)]. These latter features may be indicative of the crystallinity of this material as suggested by the corresponding XRD pattern.

Dealumination of ZSM-5(50) using HNO_3 at 90 °C for 0.5 h was found to change the morphology of this zeolite significantly as shown in Figure 4.16.

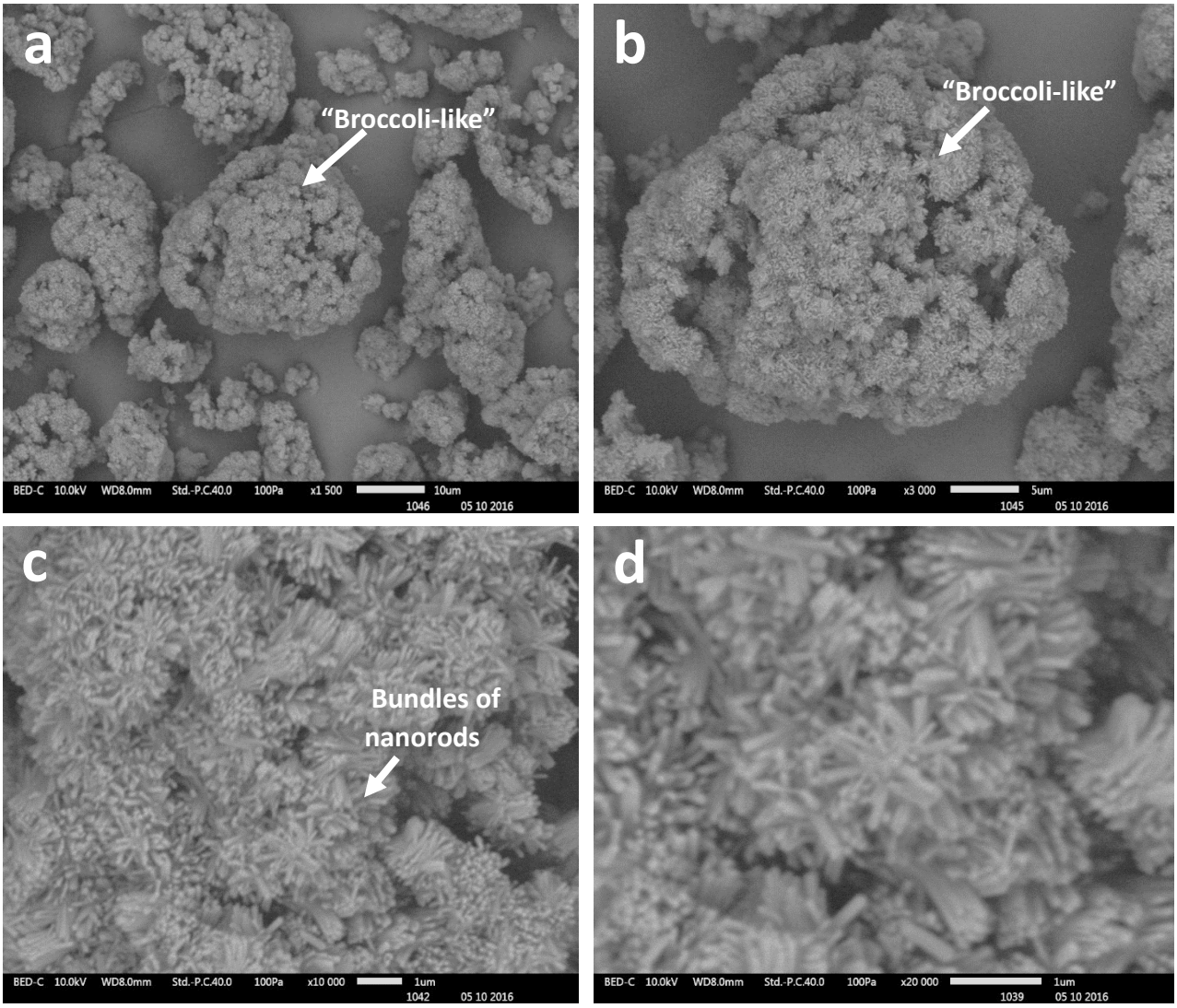

Figure 4.16: SEM micrographs of ZSM-5(50) acid-treated for 0.5 h, arranged in order of increasing magnification: (a) x1500, (b) x3000, (c) x10000 and (d) x20000.

Large chunks of “broccoli-like” structures are observable in Figure 4.16(a) and (b). As the sample is zoomed into, small agglomerated rod-like crystals are visible in Figure 4.16(c) and (d) with a random alignment. These rod-like crystals are different from the tetragonal prismatic crystals observed in the parent material in Figure 4.15(c) above. The deltoidal icositetrahedral crystals of the parent material are no longer visible in the derivative obtained after 0.5 h of acid-treatment. Instead, randomly aligned agglomerated cylindrical nanorod particles are observed [Figure 4.16(c)]. This change in morphology differs from what has been previously reported by other authors, where the morphology of ZSM-5 was maintained after dealumination treatments [7, 8]. However, Fujita *et al*. [9] found the sizes of the ZSM-5 crystals to be decreasing after dealumination relative to the parent materials.

A further increase in the dealumination time to 1.5 h brought about additional changes in the surface morphology of the ZSM-5(50) zeolite as illustrated in Figure 4.17.

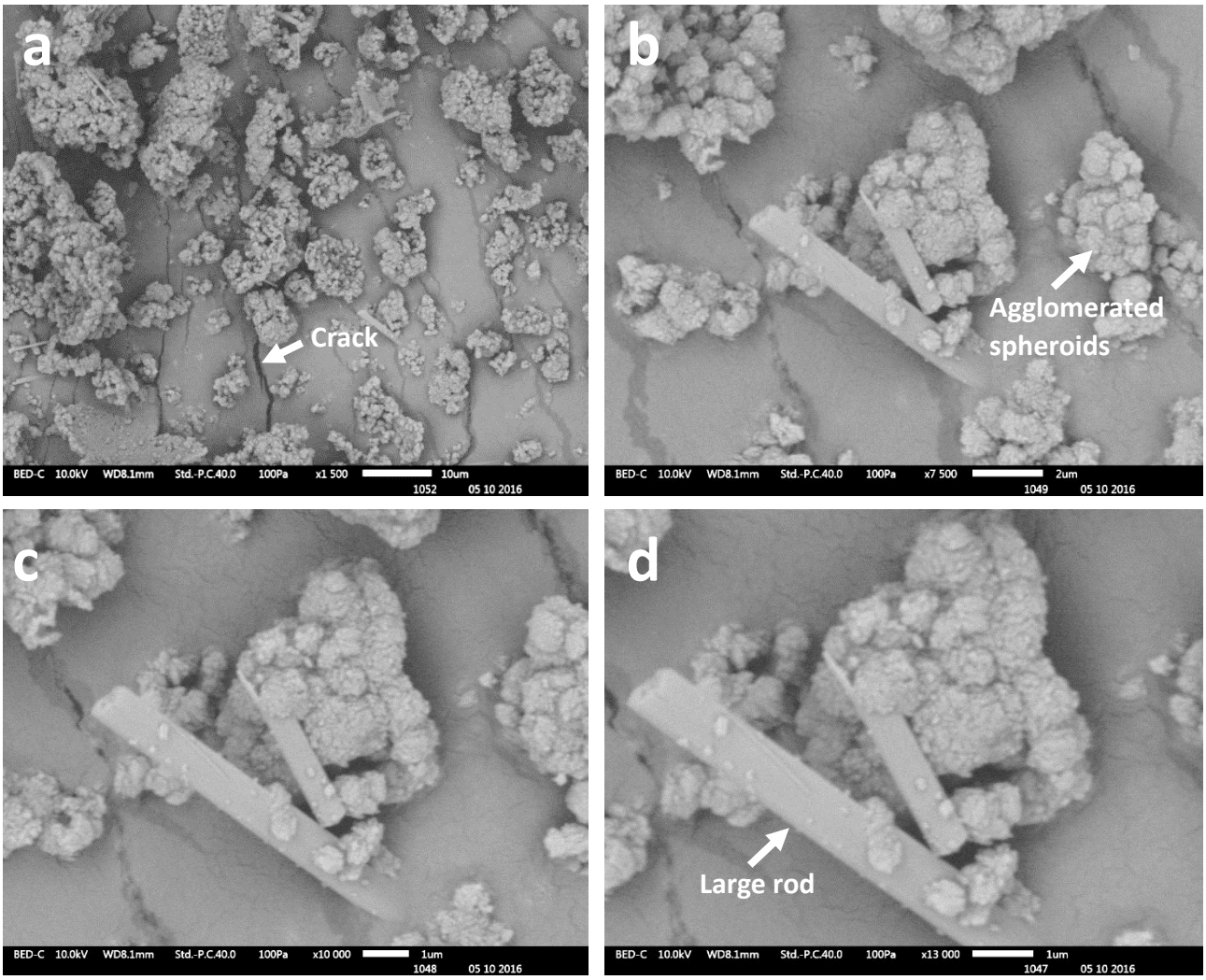

Figure 4.17: SEM micrographs of ZSM-5(50) acid-treated for 1.5 h, arranged in order of increasing magnification: (a) x1500, (b) x7500, (c) x10000 and (d) x13000. The arrows highlight the main morphological features observed.

A change in morphology accompanying the 1.5 h acid treatment manifests itself by the appearance of larger rod-like crystals, co-existing with small agglomerated spheroidal crystals. These rod-like crystals [Figure 4.17(b)] appear longer and fewer than those observed in the micrograph of the parent ZSM-5(50) and the related derivative obtained after 0.5 h acid treatment [Figure 4.16(d)], deposited on a cracked amorphous surface [Figure 4.17(a) – (d)]. Moreover, the large rods appear corroded on the surface of the smaller face or ends.

When the dealumination treatment time was further increased to 2 h, additional changes in morphology of ZSM-5(50) were observed. These are illustrated in Figure 4.18.

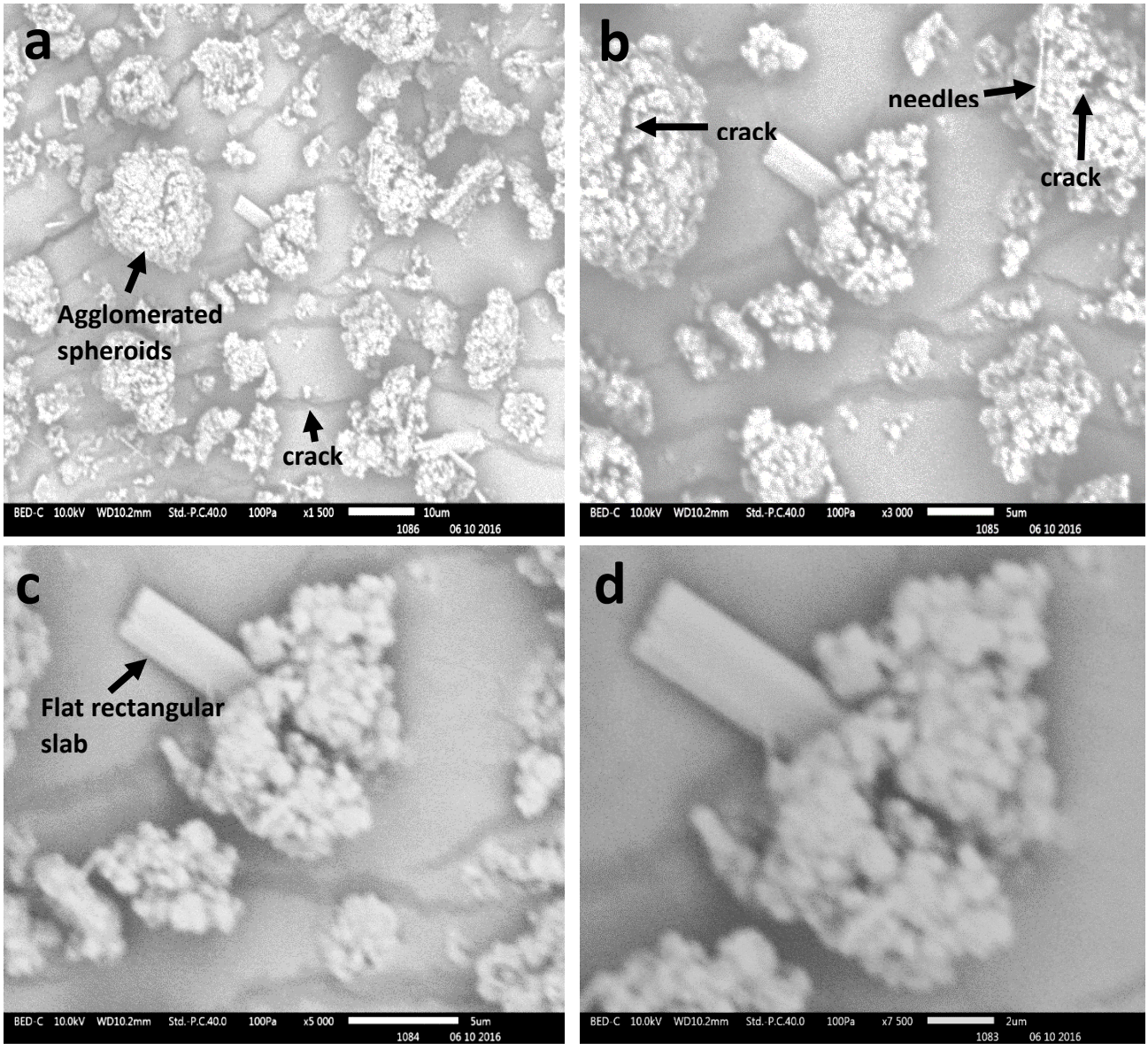

Figure 4.18: SEM micrographs of ZSM-5(50) zeolite dealuminated for 2 h, recorded at different magnifications: (a) x1500, (b) x3000, (c) x5000 and (d) x7500.

Acid treatment of the ZSM-5(50) material for 2 h produced a mixture of thick, flat and smooth rectangular rods, and predominant small agglomerated spheroidal particles. The agglomerated spheroidal crystals appear cracked in the middle of the large chunk [Figure 4.18(a)], together with rod-like particles [indicated by arrows on Figure 4.18(b)]. Furthermore, the flat rectangular particles have corroded edges which can be attributed to the corrosive nature of the treatment. The particles are deposited onto an amorphous cracked surface.

Dealumination of ZSM-5(50) for 3 h produced a material with SEM features illustrated in Figure 4.19 below.

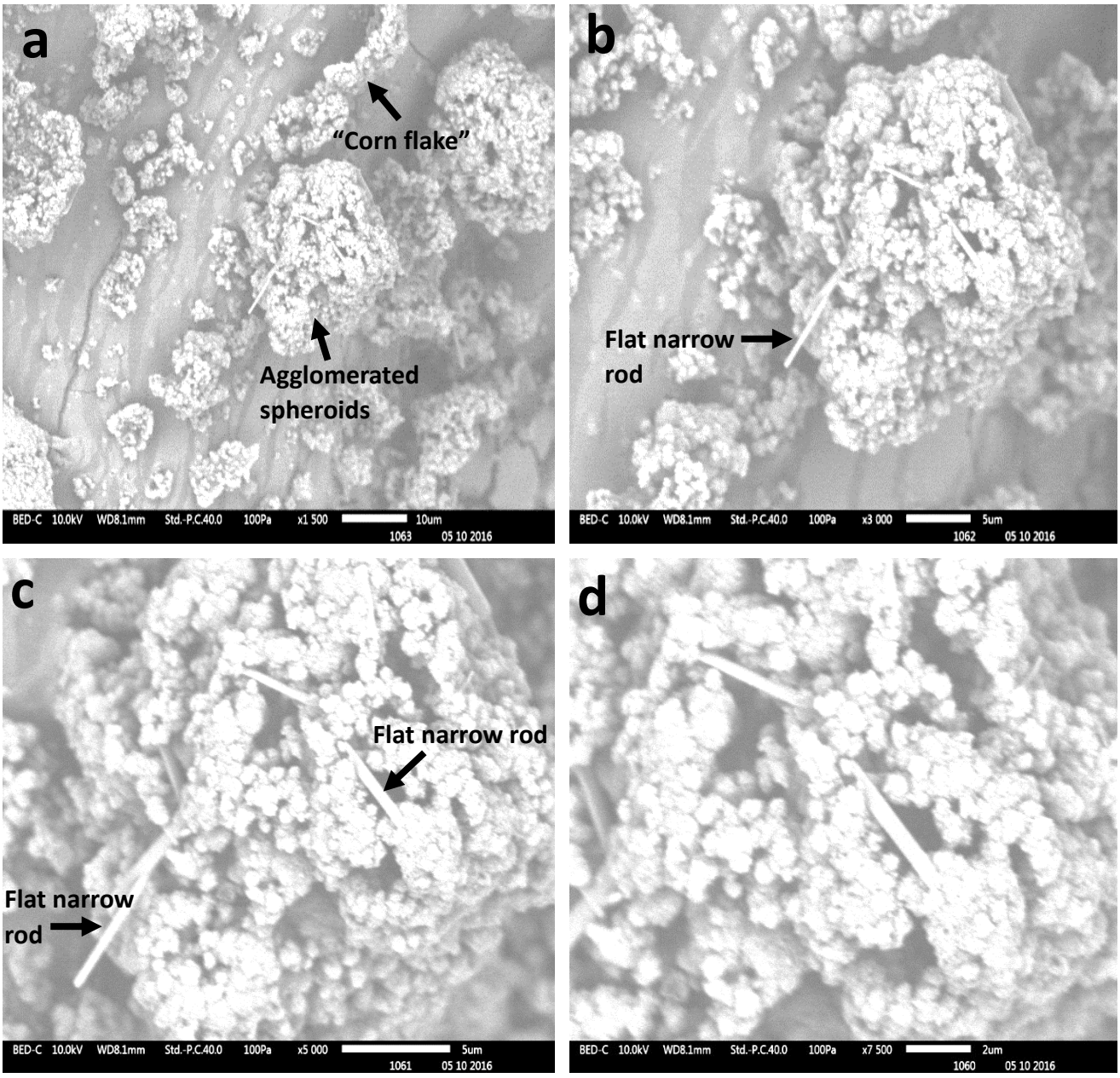

Figure 4.19: SEM micrographs of ZSM-5(50) after acid-dealumination for 3 h, and imaged at different magnifications: (a) x1500, (b) x3000, (c) x5000 and (d) x7500.

Irregularly dispersed lumps of agglomerated spheroidal crystals are observed with a non-uniform morphology. The large chunks observed seem to be made of small irregularly-shaped spheroids. Additionally, flat narrow rods are visible [indicated by arrows in Figure 4.19(b)] fused with the agglomerated spheroidal crystals. Small flake-like particles are also visible as indicated in Figure 4.19(a). The crystals are deposited onto an amorphous cracked surface. Gonzalez *et al*. [7] reported no significant change in the morphology of ZSM-5 after dealumination in HCl medium. However, dealumination of mordenite and zeolite beta in the same conditions produced samples that appear less agglomerated, with densely packed crystallites similar to what was found in this study.

Upon increasing the dealumination time to 4 h, additional changes in particle morphology of the ZSM-5(50) zeolites were also observed. Figure 4.20 shows representative micrographs of this sample.

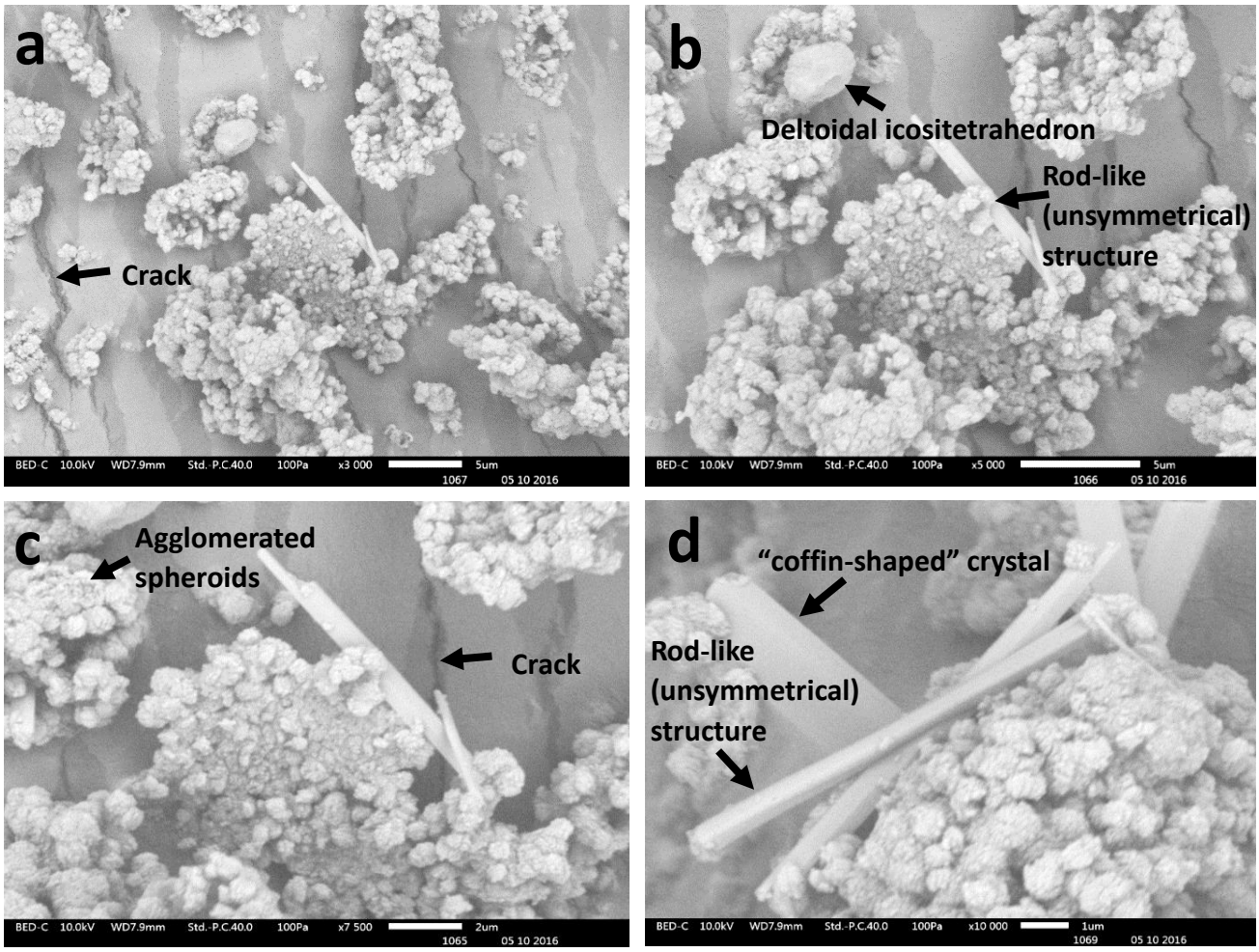

Figure 4.20: SEM micrographs of ZSM-5(50) acid-treated for 4 h, recorded at different magnifications, as well as regions of the same sample: (a) x3000, (b) x5000, (c) x7500 and (d) x10000.

A different change in the morphology for this derivative is manifested by agglomerated spheroidal and rod-like particles deposited on a cracked surface. The small spheroidal crystals are connected to larger rod-like unsymmetrical particles [illustrated with arrow in Figure 4.20(d)], as well as “coffin-shaped” crystals. The compact arrangement of particles for this derivative [illustrated by arrows in Figure 4.20(c)] is identical to that seen in the micrographs of the other derivatives (Figures 4.17 – 4.19). Furthermore, a well-defined deltoidal icositetrahedral particle is observed amongst the small agglomerated spheroids in Figure 4.20(b). A larger icositetrahedral crystal was observed in Figure 4.15 of the parent ZSM-5(50), and the appearance here is evidence that the material can withstand the corrosive acid treatment, as corroborated by the XRD patterns. Moreover, the decrease in the size can be attributed to the corrosive nature of the acid treatment in harsh conditions (90 °C for 4 h)

A spectacular morphology was observed in the material obtained from nitric acid-mediated dealumination of ZSM-5(50) for 4.5 h. This is depicted in Figure 4.21.

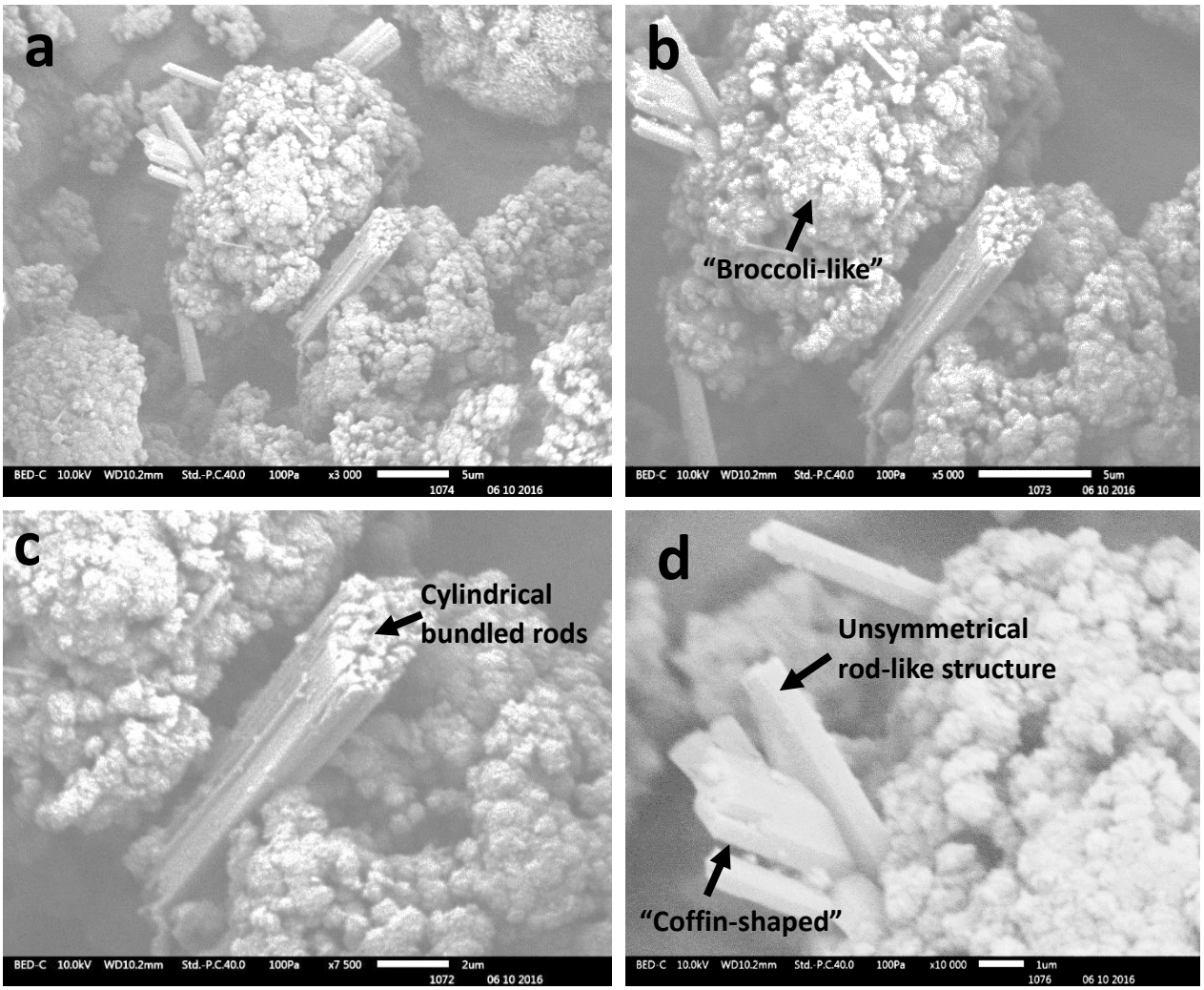

Figure 4.21: SEM micrographs of ZSM-5(50) dealuminated for 4.5 h, recorded at different magnifications: (a) x3000, (b) x5000, (c) x7500 and (d) x10000.

The representative morphology of this ZSM-5(50) derivative, depicted in Figure 4.21, is dominated by agglomerated spheroidal particles with ill-defined grain boundaries. Co-existent with these groups of agglomerated spheroids are coffin-shaped and rectangular prismatic rods with smooth surfaces [Figure 4.21(d)], as well as a tightly-packed structure consisting of self-assembled longitudinally-stacked cylindrical rods near the centre of Figure 4.21(a – c). This morphology is rather unique compared to that of similar materials obtained by dealuminating the parent ZSM-5(50) zeolite for ≤ 4 h. Interestingly, this morphology is also different from that of the material produced by dealuminating for 5 h (see Figure 4.22 below). Notably, no cracks are observable on the supporting surface of Figure 4.21, which was consistently observed on Figures 4.15 - 4.20.

When the dealumination time for the pristine ZSM-5(50) was further increased to 5 h, the morphological changes depicted in Figure 4.22 were observed.

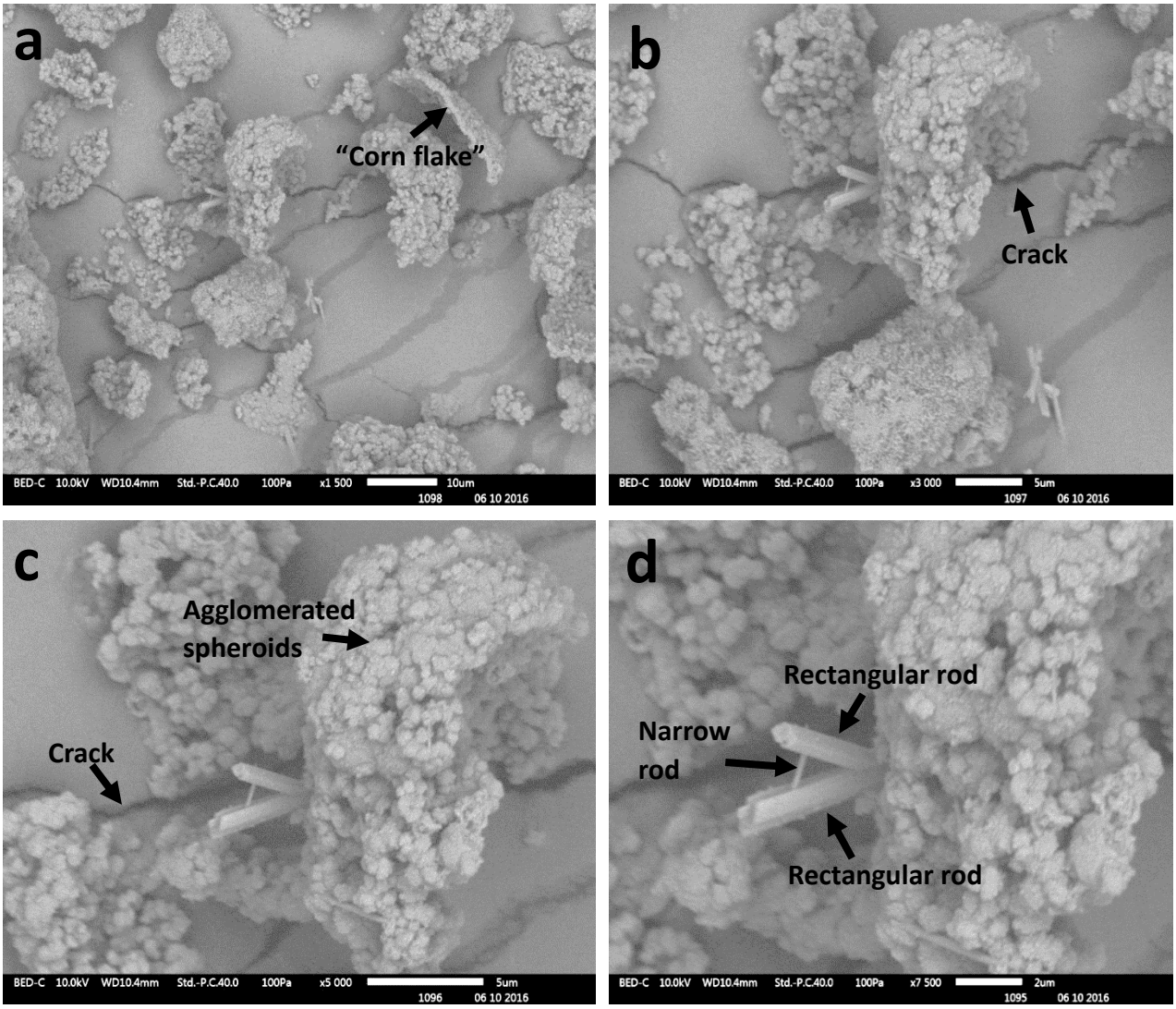

Figure 4.22: SEM micrographs of ZSM-5(50) zeolite acid-dealuminated for 5 h and imaged at different regions and magnifications: (a) x1500, (b) x3000, (c) x5000 and (d) x7500.

This treatment produced materials with a non-uniform arrangement of agglomerated spheroidal particles. This irregular dispersion of the particles is significantly different from the morphology observed in Figure 4.21 above for ZSM-5(50) treated for 4.5 h, but similar in the type of agglomeration observed in Figures 4.17 – 4.19 above. Furthermore, two rectangular rod-like particles are observed surrounded by the agglomerated spheroidal particles. To generalise, in addition to the agglomerated spheroidal morphology observed in the series of zeolites in this study, this sample also shows “corn-flake” type of particles, and a strange arrangement of two rods “propped” by a third narrow rod to define a “capital A” shape. The morphology of the derivatives prepared in this study is closely related, with a visible agglomeration of particles, while the acid treatment carried out induced evident changes in the morphology and crystal shapes from the parent zeolite. It is clear that the surface morphology of ZSM-5(50) is greatly influenced by acid-mediated dealumination.

4.5 Adsorption of MB on ZSM-5(25)-based adsorbents

Both the parent and dealuminated derivatives of ZSM-5(25) were evaluated as potential adsorbents for the removal of methylene blue (MB) from aqueous solutions. Four process variables were investigated for their influence on the adsorptive removal of this dye, namely solution pH, adsorbent dose, contact time, MB initial concentration. The results obtained from this investigation are systematically presented and discussed below. Supplementary information on the adsorption results is tabulated in Appendix section in Figure A1 and Tables A5 - A20.

4.5.1 Solution pH

The influence of the initial pH of MB solutions on the removal efficiency of the dye from aqueous solutions using ZSM-5(25) derivative was evaluated. Evaluation of the pH of a solution is important because it determines the surface charge of the adsorbent material, thus affecting the adsorption affinity or preference for the adsorbate. This study was carried out at room temperature using a solution with concentration 50 mg/L in contact with 0.1 g of the zeolitic adsorbent and contact time of 1 h. The pH was measured using a pH meter (AOWA AD 111) for all the solutions. Figure 4.23 summarises the results obtained from the ZSM-5(25) series of zeolites.

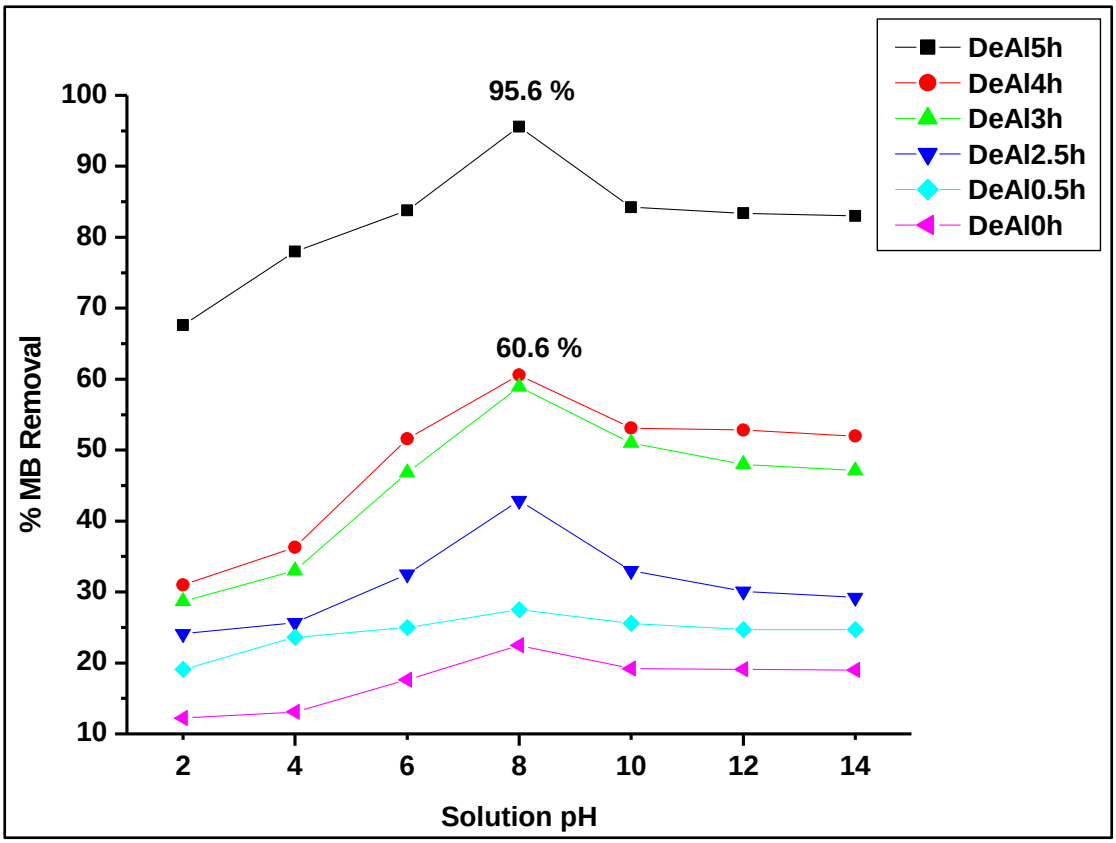

Figure 4.23: The effect of solution pH on MB removal by the dealuminated ZSM-5(25) series of zeolitic materials. The designation DeAlYh means ZSM-5(25) dealuminated for Y hours and 0 h represents the parent material; conditions: dose = 0.1 g, contact time = 1 h).

Figure 4.23 shows a general increase in MB removal with solution pH up to a pH value of 8, beyond which the MB removal decreases. However, the decreased MB removal seems to remain stable/constant above pH 10. This performance pattern is observed for all the ZSM-5(25) series of zeolites investigated in this work. Hammed *et al*. [13] also observed a similar pattern of performance in their study. It is also striking to note that the adsorptive performance of the ZSM-5(25) derivatives increases with increasing dealumination time, with the largest improvement in MB removal observed upon increasing the dealumination time from 4 h to 5 h. This enhanced MB adsorption by these materials seems to agree with their high BET surface areas 301 m^2/g, but can also arise from the co-existence of an additional crystalline phase suggested by their XRD patterns [Figure 4.1(e + f)]. This sample (dealuminated for 5 h) attained the highest value of 95 %.

The corresponding MB adsorption capacity data for the ZSM-5(25) series of zeolitic adsorbents is plotted in Figure 4.24.

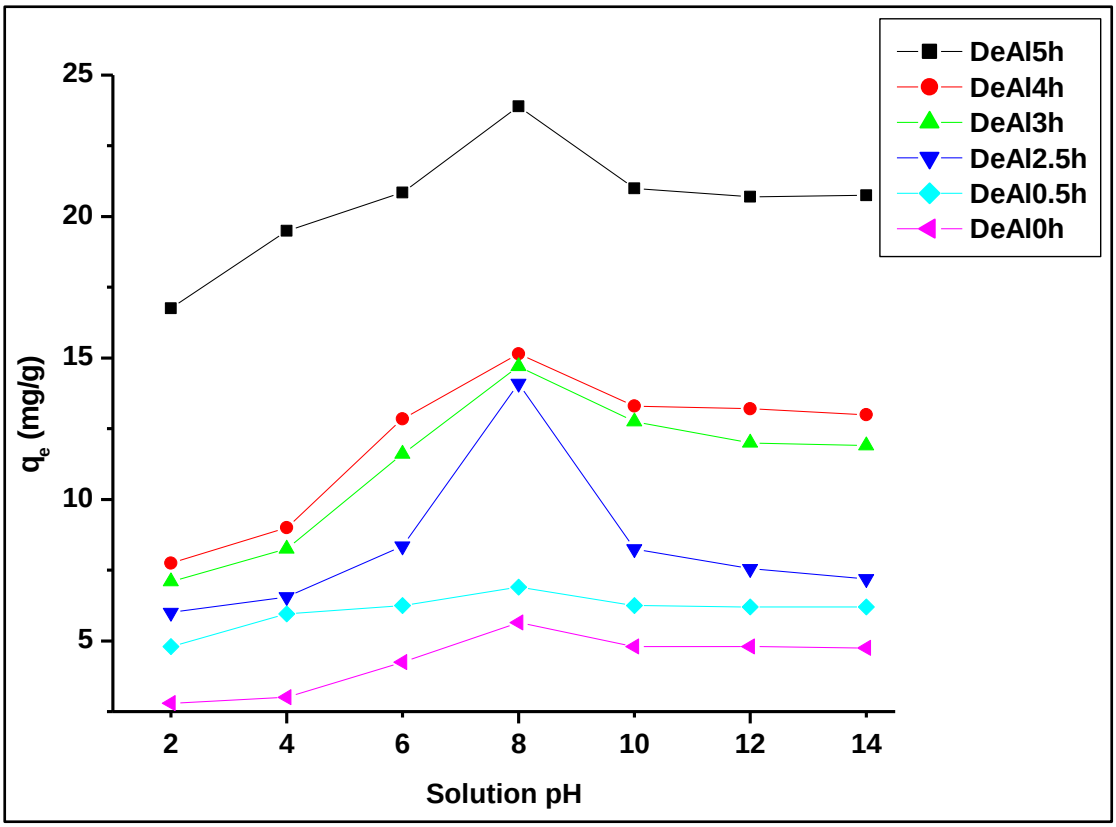

Figure 4.24: The effect of solution pH on MB adsorption capacity of the dealuminated ZSM-5(25) series of adsorbents. The designation DeAlYh means ZSM-5(25) dealuminated for Y hours and 0 h represents the parent material; conditions: dose = 0.1 g, contact time = 1

The adsorption capacity of the ZSM-5(25) series of adsorbents demonstrates a similar trend to the % MB removal observed in Figure 4.23 above. The highest performing sample with the BET surface area of 301 m^2/g and co-existence of an additional non-MFI phase, also demonstrated the highest MB adsorption capacity (24.8 mg/g) in this series of adsorbents. It is interesting to note that the dealumination treatment increase the adsorption capacity from 5.65 mg/g in the parent zeolite to ~24.8 mg/g in the derivative obtained after 5 h of dealumination. Since the BET surface areas of these materials increase from 109 m^2/g in the parent to 301 m^2/g in the derivative obtained after a 5 h acid treatment, it can be concluded that the adsorption capacity increases with increasing S_{BET}.

In a similar study, Jin *et al*. [15] reported MB adsorption studies by commercial microporous and surfactant-modified ZSM-5 zeolites. They found very low MB adsorption capacities in both the unmodified and modified ZSM-5 zeolites, increasing with an increase in pH and reaching maximum adsorption capacities of 6.1 and 12.42 mg/g, respectively. In this study, however, MB adsorption studies on parent ZSM-5

and its acid-dealuminated forms showed that all materials perform best at pH ~8 (*i.e.*, pH 7.91), with MB adsorption capacities ranging from ~8.33 to ~38 mg/g for ZSM-5(25) adsorbents.

4.5.2 Adsorbent dose

The effect of adsorbent dose on MB removal was investigated using a solution of initial concentration 50 mg/L at pH 7.91. Figure 4.25 illustrates the observed trends.

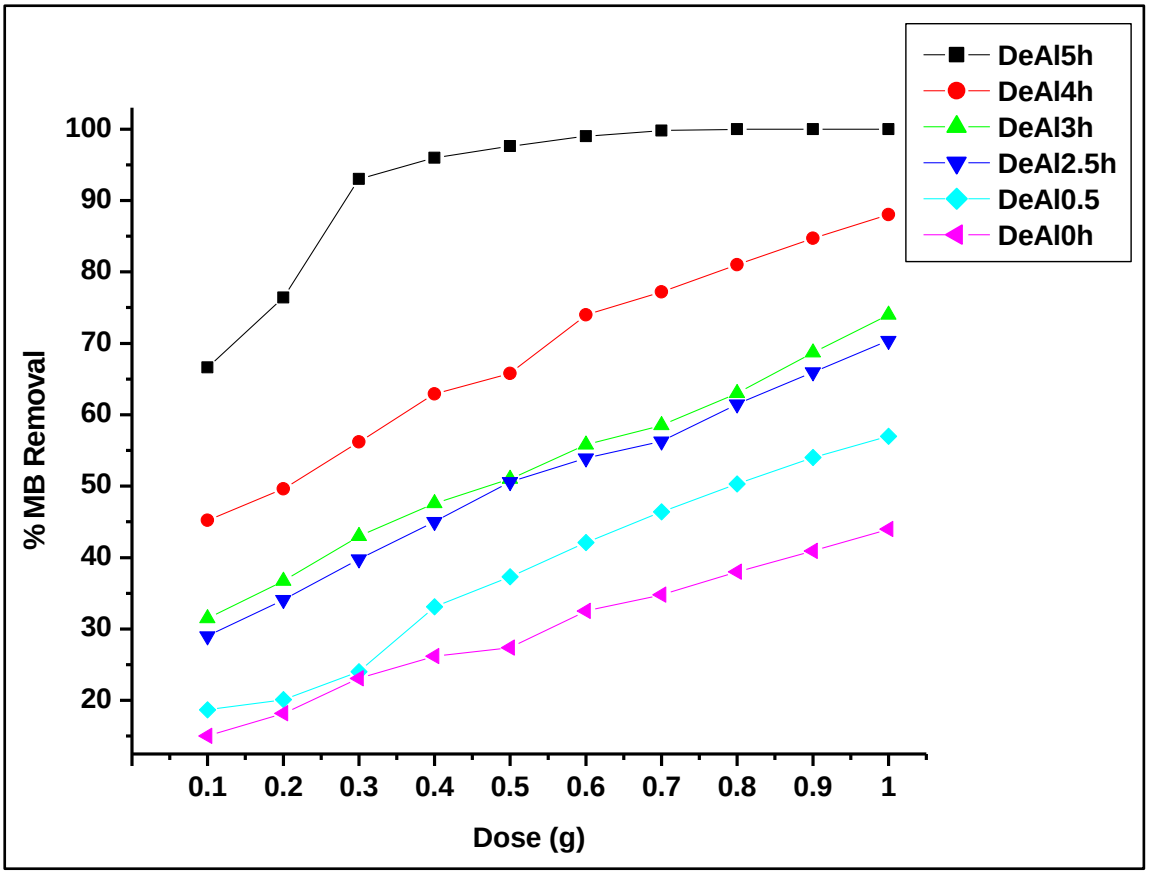

Figure 4.25: Variation of % MB removal with adsorbent dose for the ZSM-5(25) series of adsorbents. The designation DeAlYh means ZSM-5(25) dealuminated for Y hours and 0 h represents the parent material; conditions: contact time = 1 h, pH = 8).

The percentage removal of MB by the ZSM-5(25) series of adsorbents increases with the amount of zeolite used. This is expected because increasing the amount of adsorbent increases the number of adsorption sites for MB removal. The parent ZSM-5(25) shows the worst performance, while the derivative obtained upon a 5 h dealumination shows the highest performance, levelling off very close to 100 % MB removal within the dose range studied in this work. All the other materials would need adsorbent doses significantly larger than 1 g to achieve acceptable MB removal levels. The S_{BET}'s of the materials seem to be playing an important role in enhancing the

adsorptive performance, though the best material of the series may be assisted by the co-existence of a non-MFI phase in its matrix as confirmed by XRD patterns (Figure 4.1).

Figure 4.26 shows the corresponding variation of the adsorption capacity for MB on ZSM-5(25)-derived materials with adsorbent dose.

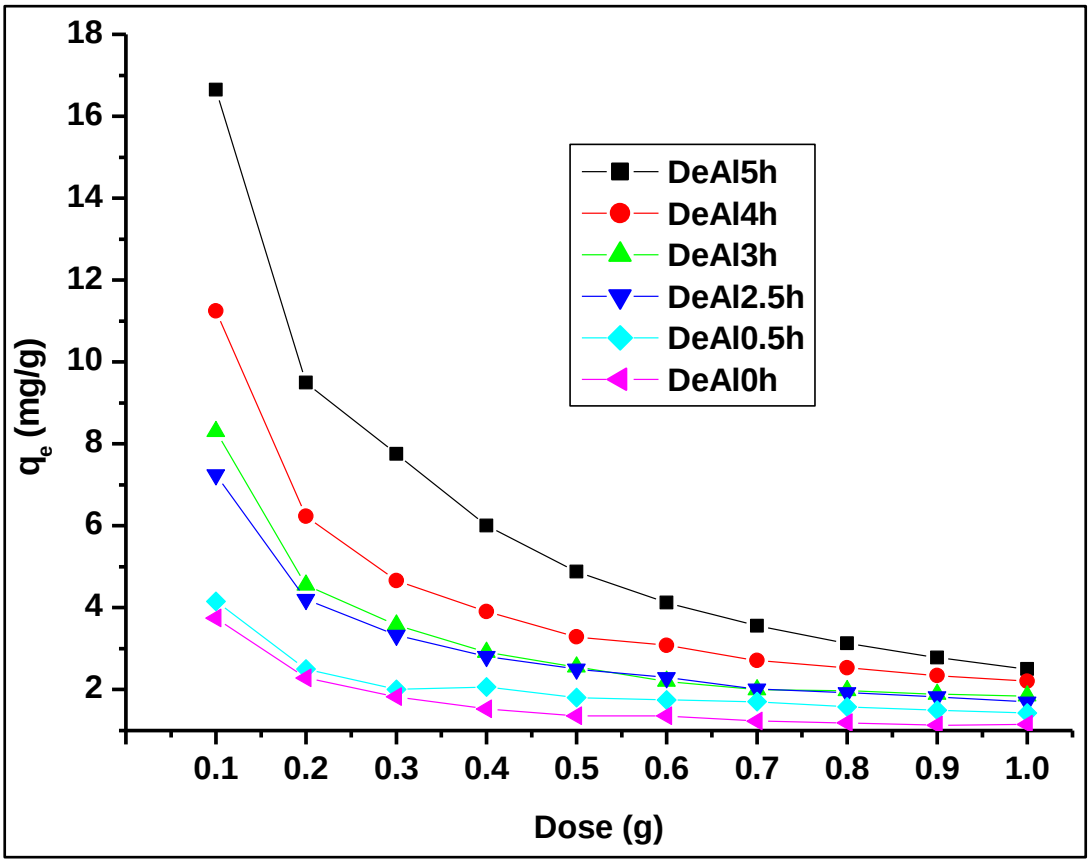

Figure 4.26: Variation of MB adsorption capacity with adsorbent dose for the ZSM-5(25) series of adsorbents. The designation DeAlYh means ZSM-5(25) dealuminated for Y hours and 0 h represents the parent material; conditions: contact time = 1 h, pH = 8).

The general trend in Figure 4.26 is similar to that observed in Figure 4.25 for the corresponding % MB removal. The observed decrease in q_e with adsorbent dose agrees well with the equation for determining it. Note that the two highly-performing adsorbents could have a contribution from the co-existing non-MFI phase in this material (inferred from XRD studies). The highest adsorption capacity reached by the best-performing zeolitic adsorbents was 16.95 mg/g.

The general trends in this study showed that the MB adsorption capacities decrease with increasing ZSM-5(25) adsorbent dose. Jin *et.al* [15] have reported similar trends

for MB adsorption by ZSM-5 zeolites. However, they reported significantly lower adsorption capacities for both the unmodified and modified ZSM-5 zeolites *i.e.*, 0.55 and ~14 mg/g.

4.5.3 Contact time

An investigation of the influence of contact time of the zeolitic adsorbents with dye solutions on the MB removal efficiency was carried out using a solution of initial concentration 50 mg/L, at pH ~8 and a dose of 0.3 g. The observed trends are illustrated in Figure 4.27.

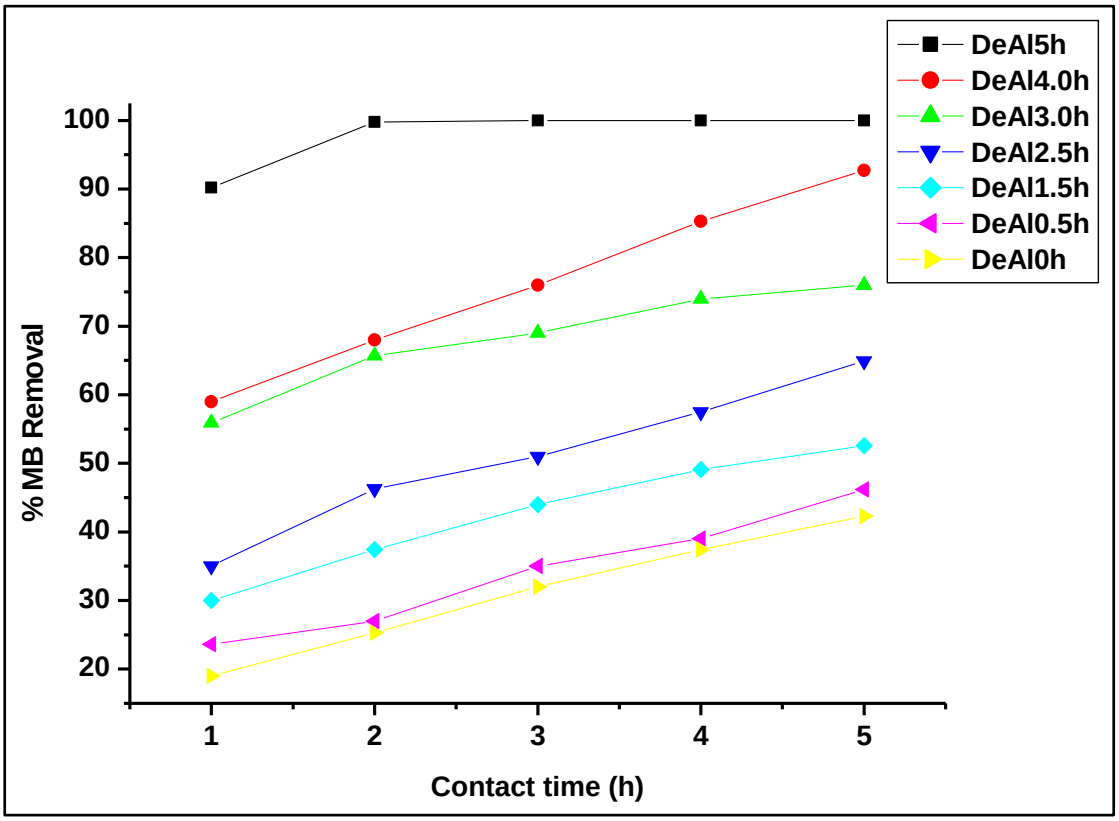

Figure 4.27 Variation of MB adsorption capacity with adsorbent dose for the ZSM-5(25) series of adsorbents. The designation DeAlYh means ZSM-5(25) dealuminated for Y hours and 0 h represents the parent material; conditions: contact time = 1 h, pH = 8).

The general trend in Figure 4.27 suggests that the removal of MB increases with the contact time for all adsorbents studied. Also, the poor performance shown by the parent ZSM-5(25) zeolite improves upon dealumination of this material, with the highest performance (close to 100 %) achieved by the material produced after dealuminating the parent material for 5 h. Again, this superior performance cannot be solely attributed to excellent textural properties (*i.e.* 301 m^2/g) of this sample, but also to a combined effect due to the co-existence of the non-MFI phase.

The corresponding MB adsorption capacity data for the ZSM-5(25) series of adsorbents is plotted in Figure 4.28.

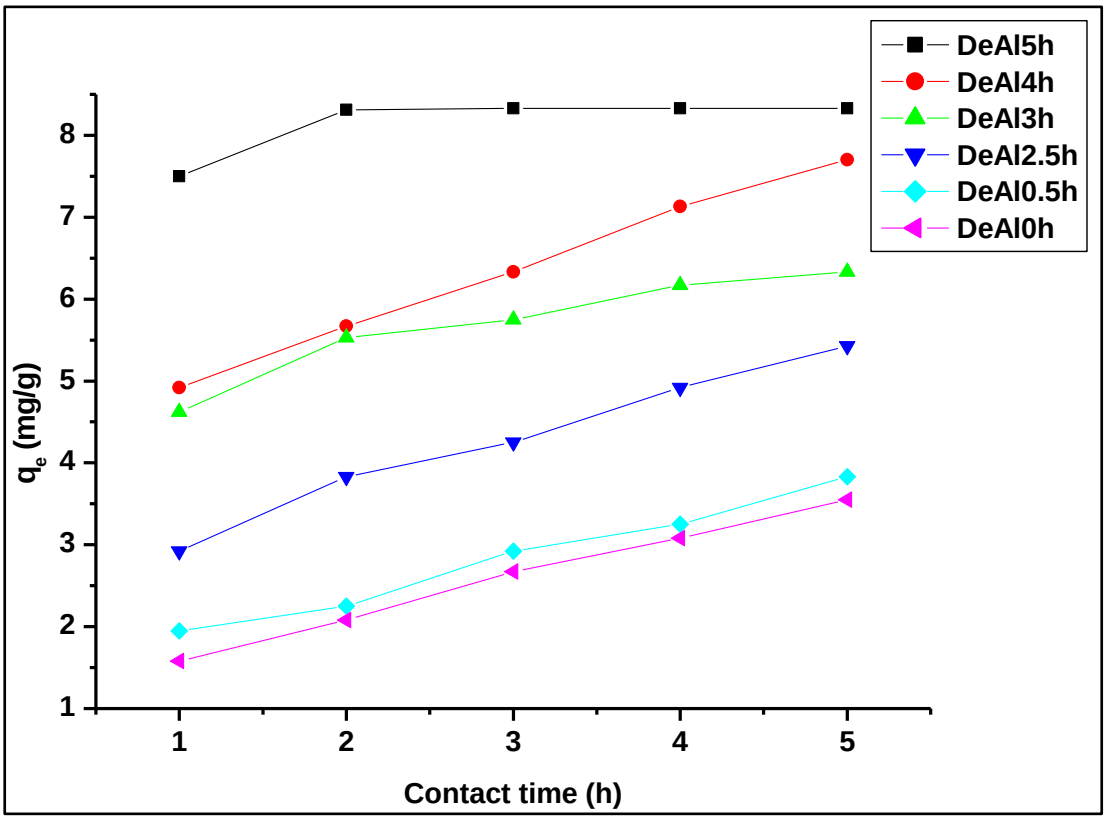

Figure 4.28: Influence of contact time of the ZSM-5(25) series of adsorbents with MB solutions on adsorption capacity. The designation DeAlYh means ZSM-5(25) dealuminated for Y hours and 0 h represents the parent material; conditions: pH = 8, dose = 0.3 g.

Figure 4.28 shows a similar pattern to the observation with the % MB removal efficiency (Figure 4.27), with the parent zeolite as the poorest performer, while its derivative obtained by dealuminating for 5 h as the best adsorbent in the series. The highest adsorption capacity achieved in this parameter is 8.33 mg/g.

The trends shown in this study illustrate a general increase of MB adsorption capacities with increasing contact time. A similar MB adsorption study by Jin *et al*. [15] showed a similar pattern for adsorption capacities, reporting MB adsorption capacities of 6.1 and 12.42 mg/g for both the unmodified and modified ZSM-5 adsorbents. This is slightly higher than the 8.33 mg/g value reported in this study for ZSM-5(25) obtained after 5 h dealumination.

4.5.4 Initial MB concentration

The influence of the initial MB concentration on the uptake from solution was investigated using the ZSM-5(25) series of adsorbents and the results are illustrated in Figure 4.29 below.

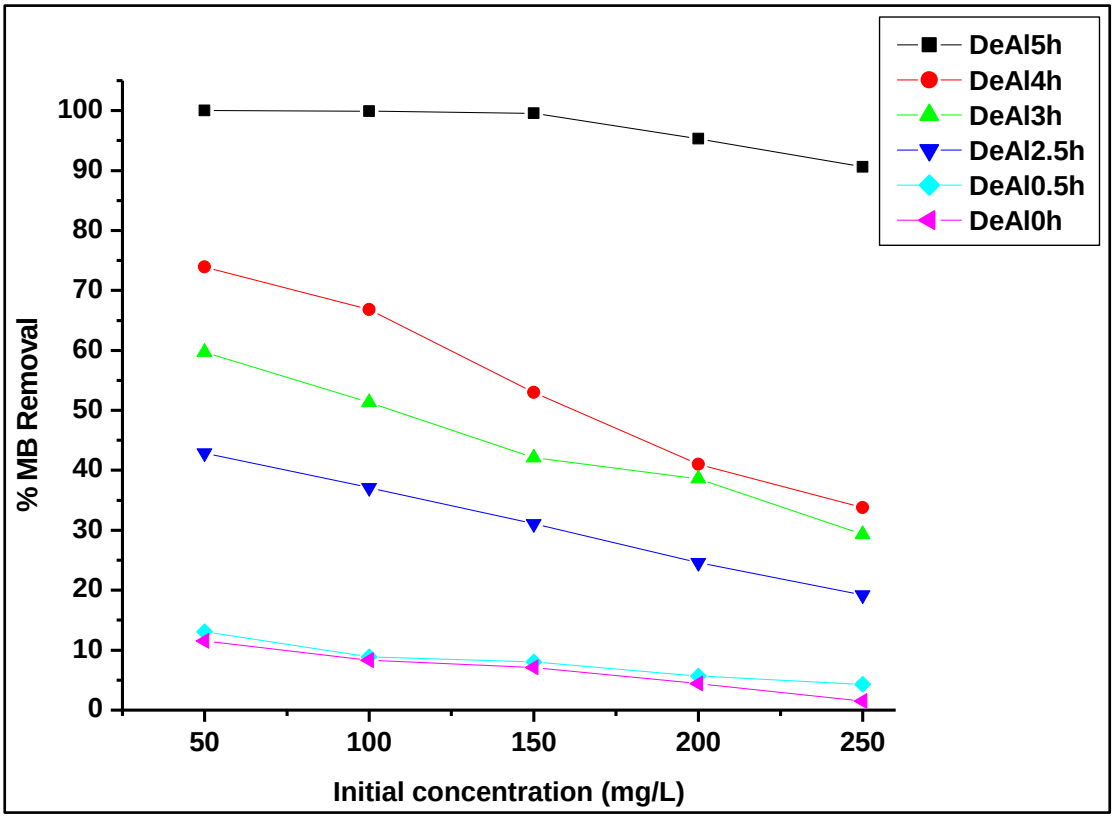

Figure 4.29: Variation of % MB removal by ZSM-5(25) series of zeolitic adsorbents with initial concentration. The designation DeAlYh means ZSM-5(25) dealuminated for Y hours and 0 h represents the parent material; conditions: pH = 8, contact time = 2 h, dose = 0.3 g.

A general observation from Figure 4.29 is a decrease in percentage MB removal with increasing initial MB concentration for the different adsorbents, with the exception of the sample dealuminated for 5 h. This sample shows an essentially constant MB removal efficiency in the concentration range 50 – 150 mg/L and a decrease thereafter. The decrease is, however, not abrupt. The decrease in the uptake is because the adsorbents have reached their carrying capacity for MB [13, 14, 16]. Increasing the initial MB concentration, leads to excess MB that can adsorb onto the limited number of adsorption sites of the ZSM-5(25) adsorbents. For a particular adsorbent, the total number of adsorption sites available is fixed, thus adsorbing a specific amount of MB [9, 10]. The parent material performed poorly in MB removal

even at lower concentrations, in agreement with the other reported studies [13, 14]. However, the dealumination treatment is observed to improve the MB removal efficiency of the parent zeolite remarkably, particularly for those materials obtained by dealuminating for > 0.5 h. For these zeolitic adsorbents, the increase in % MB correlates well with their BET surface areas.

The corresponding MB adsorption capacity data for the ZSM-5(25) series of adsorbents was determined and is plotted in Figure 4.30.

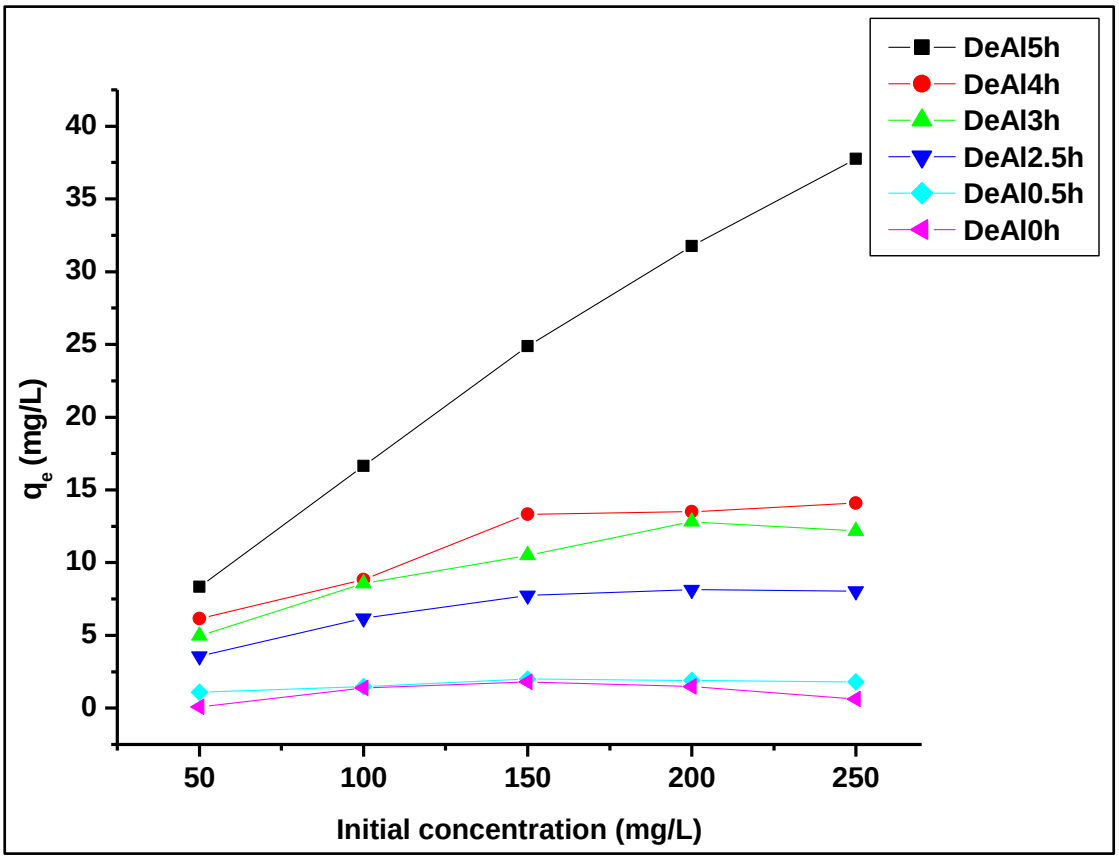

Figure 4.30: Variation of MB adsorption capacity of ZSM-5(25) series of zeolitic adsorbents with initial concentration. The designation DeAlYh means ZSM-5(25) dealuminated for Y hours and 0 h represents the parent material; conditions: pH = 8, contact time = 2 h, dose = 0.3 g.

As observed with the % MB removal trends (Figure 4.29) with respect to the initial concentration, the low-performing parent and its 0.5 h-dealuminated samples also show coinciding performances in their MB adsorption capacities. For the other samples, it can be seen that the adsorption capacity increases with increasing dealumination time, which tends to be the order of increasing BET surface area. It is worth remembering that the enhanced improvement in the adsorption capacity of the 5 h-dealuminated sample may be due to the presence of a non-MFI phase in this

material. The performance of adsorbent material dealuminated for 0 – 4 h tends to stabilise at higher initial concentration or go through a maximum.

4.6 Adsorption of MB on ZSM-5(50) adsorbents

Similar variables investigated for the ZSM-5(25)-based adsorbents were also investigated for this series of adsorbents.

4.6.1 Solution pH

The influence of the pH of MB solutions on the dye removal efficiency by ZSM-5(50) series of zeolites was evaluated. Evaluation of the pH of a solution is important because it determines the surface charge of the adsorbent material, thus affecting the adsorption affinity or preference for the adsorbate. Figure 4.31 summarises the results obtained on differently-treated ZSM-5(50) adsorbents.

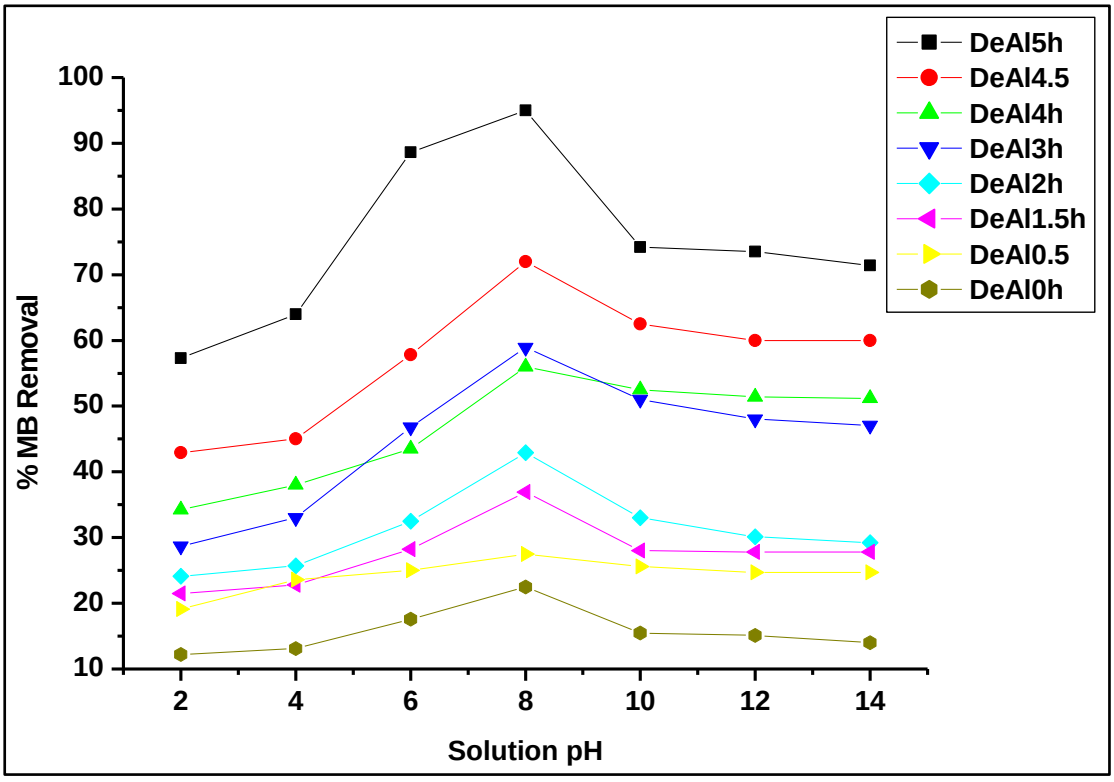

Figure 4.31: The effect of solution pH on MB removal by the dealuminated ZSM-5(50) series of zeolitic materials. The designation DeAlYh means ZSM-5(50) dealuminated for Y hours and 0 h represents the parent material; experimental conditions: dose = 0.1 g, contact time = 1 h, initial MB concentration = 50 mg/L.

Figure 4.31 shows a general increase in the percentage MB removal with solution pH up to a pH value of 8, beyond which it decreases. However, the decrease in percentage removal seems to remain essentially stable/constant above pH 10. This

performance pattern is observed for all the ZSM-5(50) series of zeolites investigated in this work. A similar pattern of performance was also observed by Hammed *et al*. [12] and Hassan *et al*. [14] in their studies. Interestingly, the adsorptive performance of the ZSM-5(50) derivatives increases with increasing dealumination time, with the largest improvement in MB removal exhibited by the derivative obtained by dealuminating the parent zeolite for 5 h. The enhanced MB adsorption by this material seems to agree with its high S_{BET} 275 m^2/g, but can also be arise from the mixed morphology observed for this derivative (Figure 4.22). This 5 h-dealumination sample attained the highest MB removal value of 95 %.

The accompanying MB adsorption capacity data was determined using the initial and equilibrium concentrations and is plotted in Figure 4.32 below.

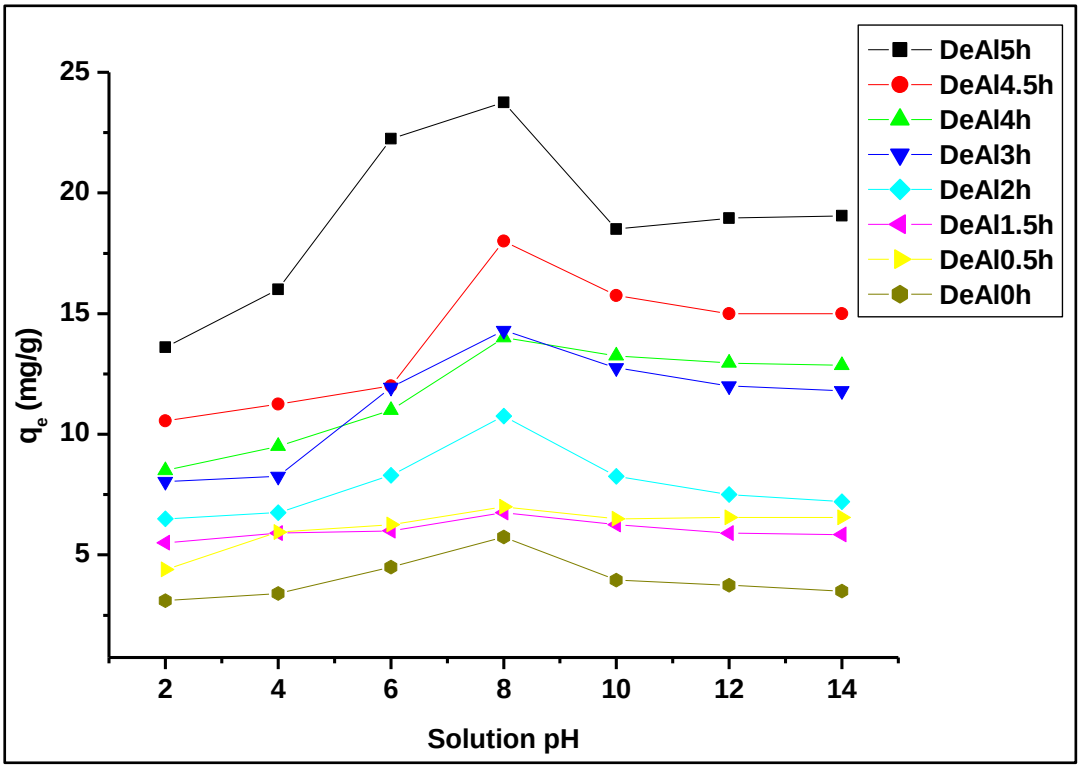

Figure 4.32: The effect of solution pH on MB adsorption capacity of the dealuminated ZSM-5(50) series of adsorbents. The designation DeAlYh means ZSM-5(50) dealuminated for Y hours and 0 h represents the parent material; experimental conditions: dose = 0.1 g, contact time = 1 h, initial MB concentration = 50 mg/L.

Figure 4.32 demonstrates an increase in MB adsorption capacity by the ZSM-5(50) adsorbents with solution pH up to a pH value of 8, beyond which it decreases. The increase in MB uptake with pH is aided by the decrease of electrostatic repulsions between the MB and the surface of the ZSM-5(50) adsorbents. Notably, the dealuminative treatment increases the adsorption capacity of ZSM-5(50) by a factor

of 4, from 5.75 mg/g in the parent zeolite to 23.75 mg/g in the derivative obtained after 5 h of dealumination. The slowdown of the uptake beyond pH 8 has been reported to be due to the precipitation of MB at basic range [12, 14]. It is worth noting that the 3 h-dealumination adsorbent shows an overlap in adsorption capacity at pH 8 with the sample obtained after dealuminating for 4 h. The larger surface area of the 3 h-derivative (335 m^2/g) compared to the 4 h-dealumination variant (268 m^2/g) could be aiding the adsorptive performance of this material. The pH of 8 was taken to be the ideal condition for MB removal and was used for the following studies.

Similarly to the trends observed for ZSM-5(25) adsorbents, dealumination of ZSM-5(50) zeolites improves the MB adsorption capacities of these materials 5-fold compared to the modifications reported by Jin *et al*. [15] on ZSM-5 zeolites.

4.6.2 Dose

Figure 4.33 below illustrates the variation of percentage MB removal with adsorbent dose. ZSM-5(50) and its dealuminated variants were explored as adsorbents.

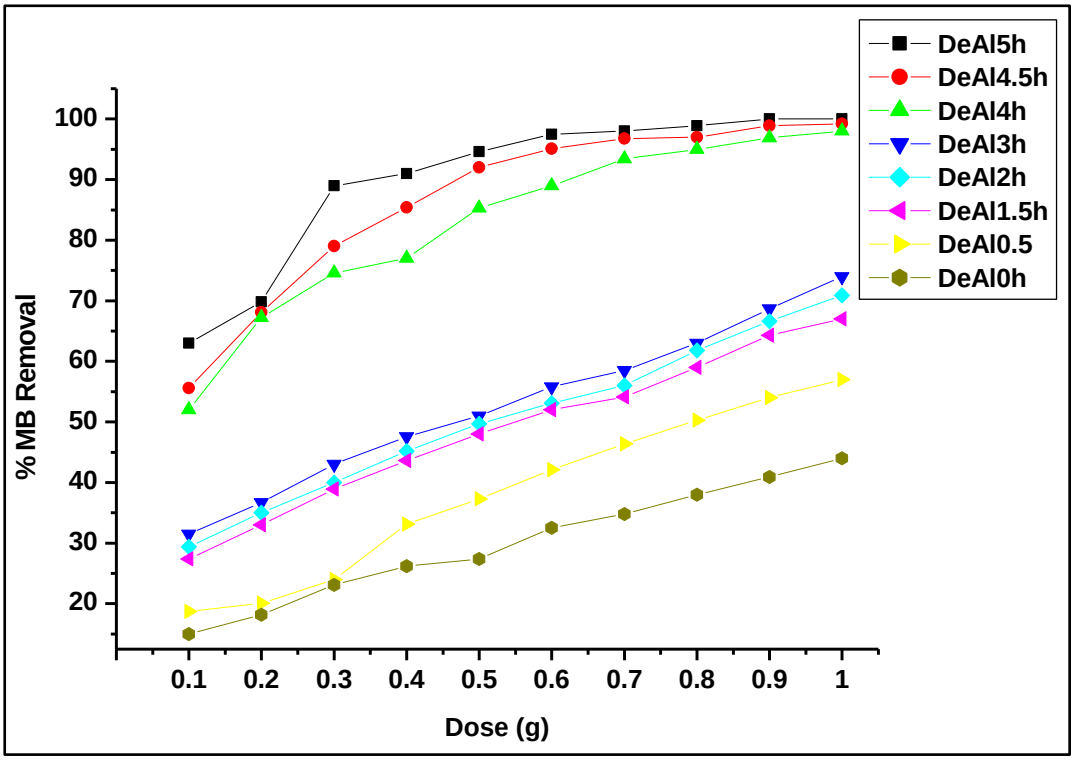

Figure 4.33: Variation of % MB removal with adsorbent dose for the ZSM-5(50) series of adsorbents. The designation DeAlYh means ZSM-5(50) dealuminated for Y hours and 0 h represents the parent material; experimental conditions: contact time = 1 h, pH = 8, initial MB concentration = 50 mg/L.

The percentage removal increases monotonically with adsorbent dose for all adsorbent materials obtained from pristine ZSM-5(50) through acid-mediated dealumination. This increase in percentage MB removal with increasing adsorbent dose can be attributed to the increase in the number of adsorption sites that become available when the amount of adsorbent is increased [12 – 14]. The parent ZSM-5(50) shows the most inferior performance, while the derivative obtained by a 5 h-long dealumination treatment shows the highest performance, with a tendency to level off very close to 100 % MB removal in the dose range studied in this work. Notably, the 4 h-, 4.5 h- and 5 h-dealumination derivatives were much more efficient for MB removal compared to the other adsorbents. The large S_{BET} of the materials play an important role in enhancing their adsorptive performance. The 5 h-dealumination derivative removed 89 % of MB at 0.3 g dose.

The corresponding data illustrating the variation of MB adsorption capacity with ZSM-5(50) adsorbent dose is plotted in Figure 4.34.

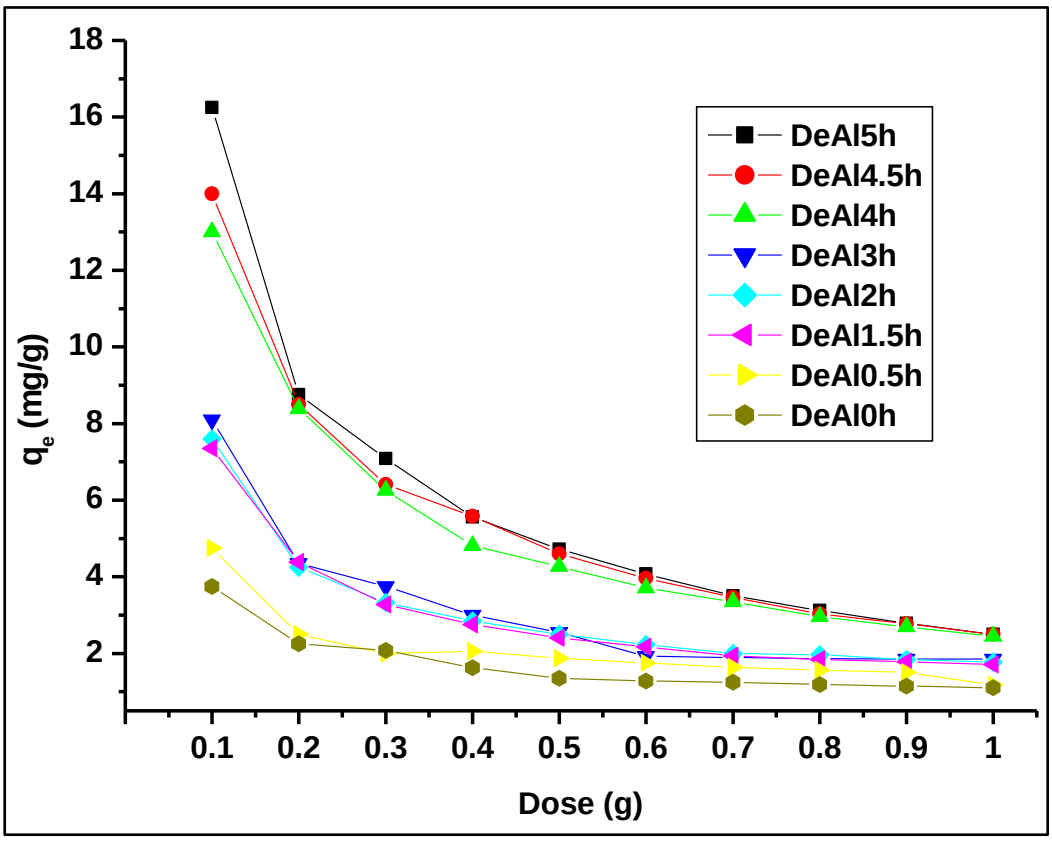

Figure 4.34: Variation of MB adsorption capacity with adsorbent dose for the ZSM-5(50) series of adsorbents. The designation DeAlYh means ZSM-5(50) dealuminated for Y hours and 0 h represents the parent material; experimental conditions: contact time = 1 h, pH = 8, initial MB concentration = 50 mg/L.

The general trend in Figure 4.34 suggests a decrease in MB adsorption capacity as the adsorbent dose increases, similar to the previous observation by Hassan *et al*. [14]. This is because a fixed initial MB concentration leads to equilibrium reached quickly with increasing adsorbent dose [12 – 14], as there are more adsorption sites than adsorbate species. It is worth noting that MB uptake by the 4.5 h- and 5 h-dealumination adsorbents could be aided by the large surface areas of the materials with 208 and 275 m^2/g, respectively. The highest adsorption capacity reached by the best performing zeolitic adsorbent was 16.25 mg/g. To be economical, a 0.3 g dose was used for following studies.

Similarly to the trends observed for ZSM-5(25) adsorbents, dealumination of ZSM-5(50) zeolites improves the MB adsorption capacities of these materials 4-fold compared to the modifications reported by Jin *et al*. [15] on ZSM-5 zeolites.

4.6.3 Contact time

The influence of contact time on percentage MB removal by ZSM-5(50) series of zeolites was evaluated and the results are illustrated in Figure 4.35.

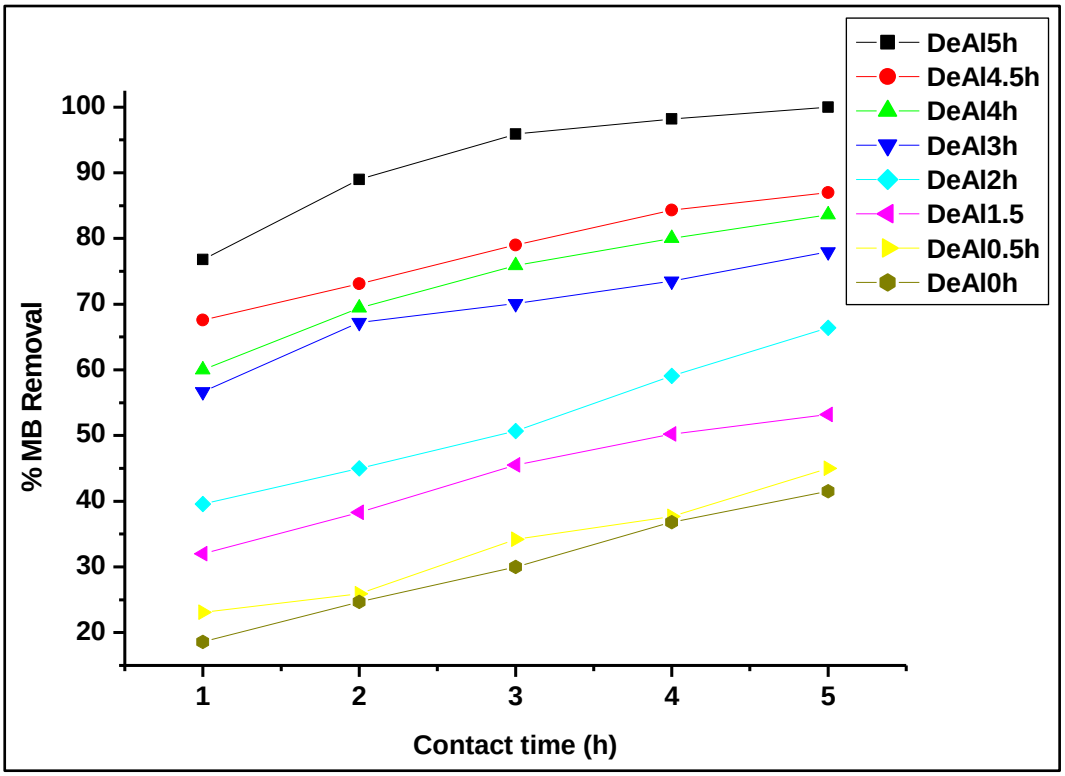

Figure 4.35: Variation of MB adsorption capacity with adsorbent dose for the ZSM-5(50) series of adsorbents. The designation DeAlYh means ZSM-5(50) dealuminated for Y hours and 0 h represents the parent material; experimental conditions: contact time = 1 h, pH = 8, initial MB concentration = 50 mg/L.

It is observed from Figure 4.35 that the removal of MB increases with the contact time for all adsorbents studied. A similar trend has also been reported by other researchers [12 - 14]. The poor performance shown by the parent ZSM-5(50) zeolite improves upon dealumination, with the highest performance achieved at a contact time of 5 h for the material produced after dealuminating for 5 h. Furthermore, the 5 h-dealumination adsorbent removed ~90 % MB at 2 h contact time, corresponding to the non-toxic final concentration of MB in water. The ideal contact time for efficient MB removal was then chosen to be 2 h.

The corresponding MB adsorption capacity data for the ZSM-5(50) series of adsorbents is plotted in Figure 4.36.

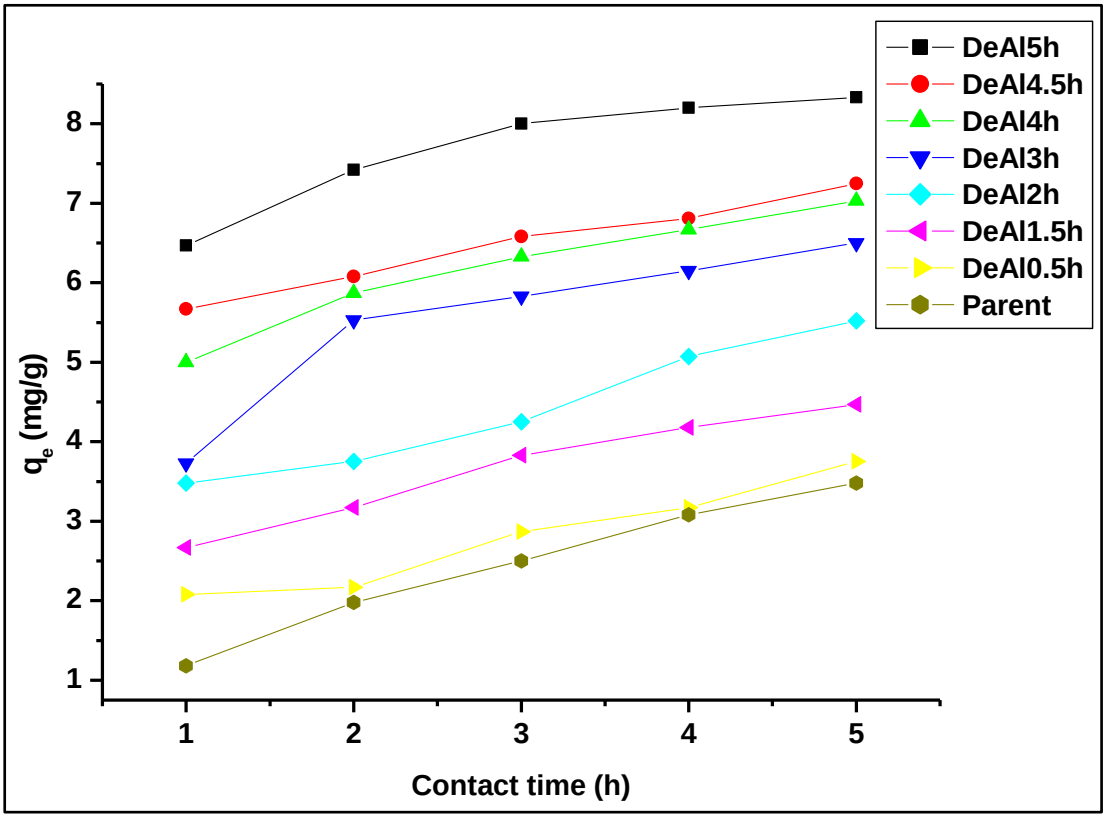

Figure 4.36: Influence of contact time of the ZSM-5(50) series of adsorbents with MB solutions on adsorption capacity. The designation DeAlYh means ZSM-5(50) dealuminated for Y hours and 0 h represents the parent material; experimental conditions: pH = 8, dose = 0.3 g, initial MB concentration = 50 mg/L.

Figure 4.36 shows a similar pattern to the observation with the percentage MB removal efficiency (Figure 4.35), with the parent adsorbent as the poorest performer, while its derivative obtained by dealuminating for 5 h is the best adsorbent in this series. The

adsorption capacity achieved in this parameter at 2 h contact time is 7.42 mg/g MB, rising to 8.32 mg/g at 5 h contact time. The contact time of 2 h was used for the following experiments.

Similarly to the trends observed for ZSM-5(25) adsorbents, dealumination of ZSM-5(50) zeolites improves the MB adsorption capacities of these materials 6-fold compared to the modifications reported by Jin *et al*. [15] on ZSM-5 zeolites.

4.6.4 Initial MB concentration

The influence of the initial MB concentration on the uptake from solution was investigated using the ZSM-5(50) series of adsorbents and the results are illustrated in Figure 4.37.

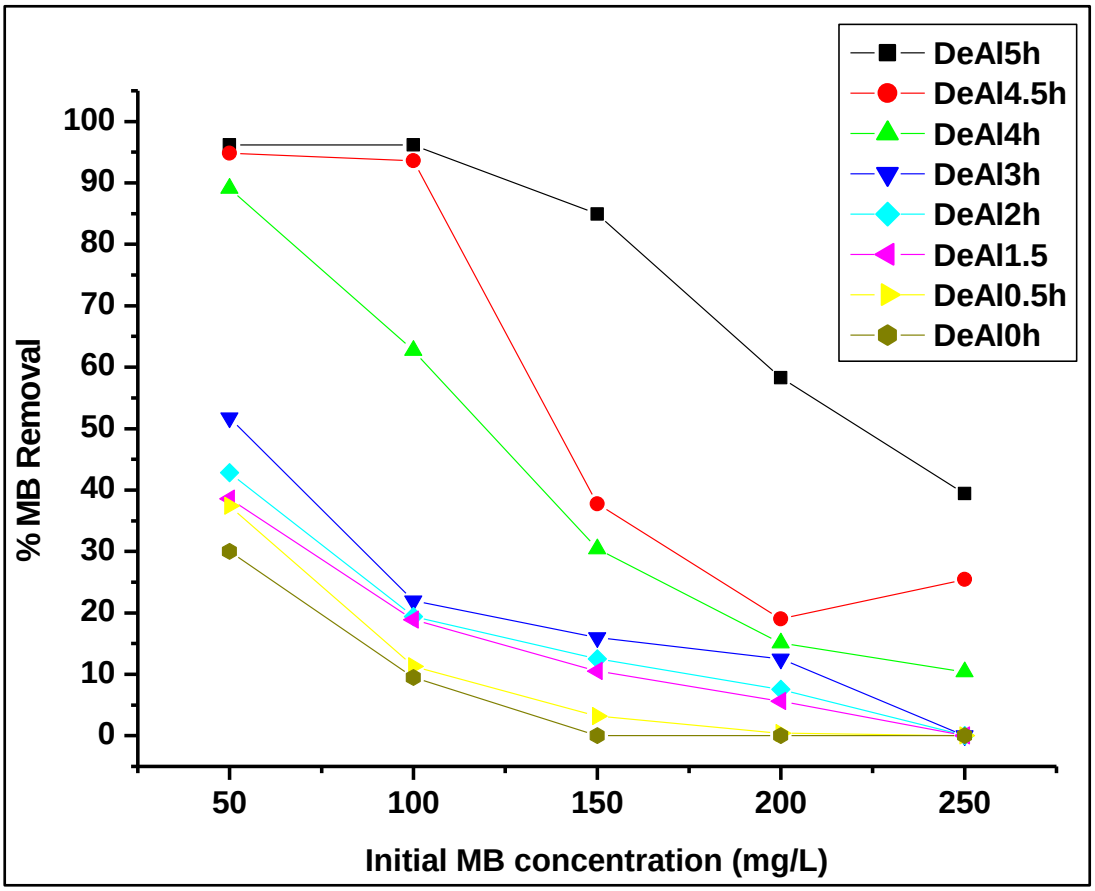

Figure 4.37: Variation of % MB removal by ZSM-5(50) series of zeolitic adsorbents with initial concentration. The designation DeAlYh means ZSM-5(50) dealuminated for Y hours and 0 h represents the parent material; experimental conditions: pH = 8, contact time = 2 h, dose = 0.3 g.

Figure 4.37 illustrates that percentage MB removal by the ZSM-5(50) series of adsorbents decreases with increasing initial concentration. This is because at a fixed adsorbent dose (e.g. 0.3 g), the total number of available adsorption sites is constant and can only remove a specific amount of adsorbate [12, 14]. Beyond this saturation point, no further MB adsorption takes place on the adsorbent surface, resulting in lower removal values. Also, for a specific initial MB concentration, the MB uptake increases with the dealumination time used in the preparation of the particular zeolitic adsorbent. This is because the S_{BET} of the parent ZSM-5(50) improved after dealumination for different durations (refer to Table A4 in Appenices), which aids the removal of MB by these adsorbents The highest MB removal value attained by this series of adsorbents is 96.2 % for the material produced by dealuminating for 5 h.

Figure 4.38 presents the variation of MB adsorption capacity for ZSM-5(50) series of adsorbents with initial MB concentration.

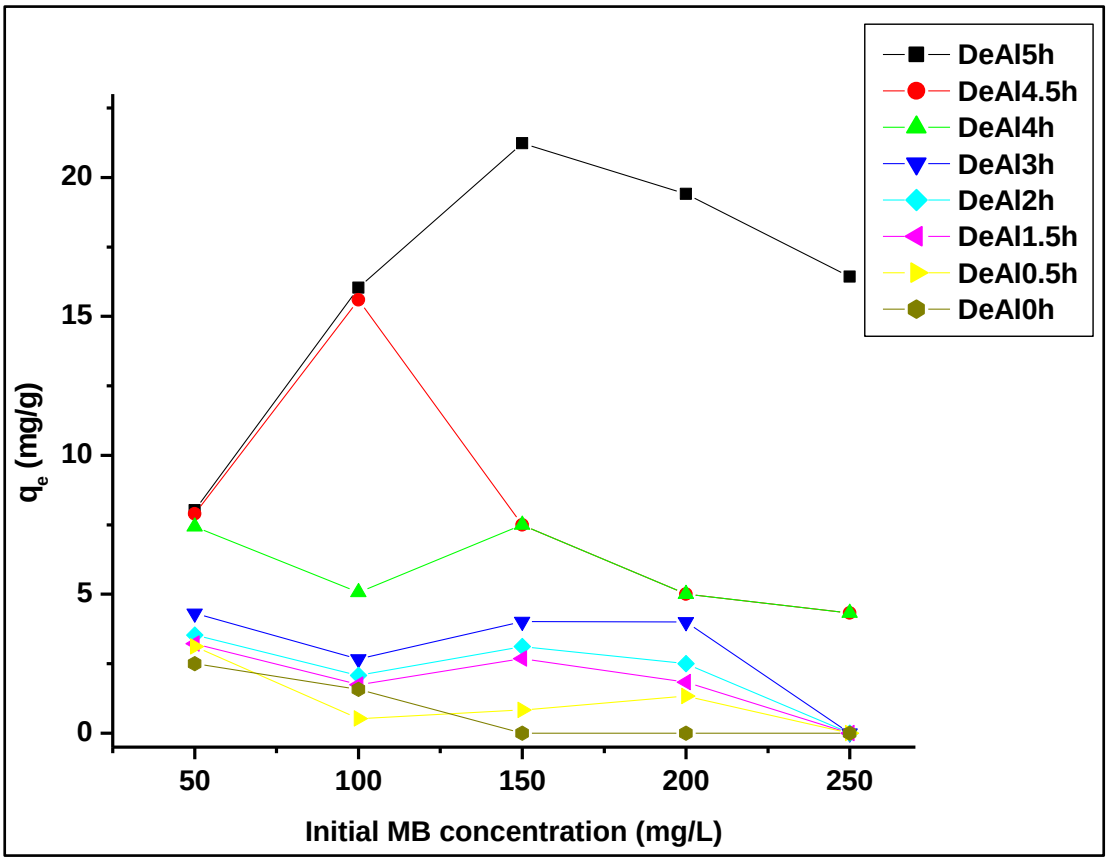

Figure 4.38: Variation of MB adsorption capacity of ZSM-5(50) series of zeolitic adsorbents with initial concentration. The designation DeAlYh means ZSM-5(50) dealuminated for Y hours and 0 h represents the parent material; experimental conditions: pH = 8, contact time = 2 h, dose = 0.3 g.

Zeolitic adsorbents produced by dealumination of ZSM-5(50) for ≤ 4 h show a decrease in adsorption capacity when the initial MB concentration is increased from 50 to 100 mg/L. At higher initial MB concentrations, the adsorption capacity increases through different maxima for the individual adsorbents, with the exception of the pristine zeolite. On the other hand, the materials obtained by dealumination for 4.5 h and 5 h showed an initial increase in adsorption capacity with increasing MB concentration up to their respective maxima, after which a decrease in adsorption capacity was observed at higher initial concentrations. Except for a few overlaps in the plots, the adsorption capacity seems to increase with increasing dealumination time during the preparation of these adsorbents. The highest adsorption capacity attained in this series was 21.23 mg/g at an initial MB concentration of 150 mg/L for the adsorbent obtained through a 5 h dealumination treatment time. This could be due to the large S_{BET} (275 m^2/g) of this adsorbent.

4.7 Adsorption isotherms

Equilibrium adsorption isotherms are fundamental in describing the interactions between adsorbates and adsorbents, and are therefore important in the design of adsorption systems [12, 16, 17]. These isotherms relate the amount of adsorbate (e.g., MB) in the solid to that remaining in solution, which allow calculation of the capacity of the adsorbent, as well as the affinity of the adsorbate for the adsorbent (e.g., zeolite) surface [16]. Several adsorption models are currently employed to describe adsorption phenomena, with the Langmuir and Freundlich isotherms being the most commonly used. The MB adsorption data in this study was experimentally obtained through a series of batch tests using ZSM-5 zeolites as adsorbents in aqueous environments. These zeolites, synthesised to two SARs of 25 and 50, were produced by direct hydrothermal synthesis, and were each dealuminated for different times by heating in HNO_3 solutions. Each of the resulting ZSM-5 derivatives were evaluated for efficiency in the adsorption of MB from aqueous solutions with various initial concentrations (C_0), *i.e*., 50, 100, 150, 200 and 250 mg/L. Adsorption data on representative adsorbents from each of the two SARs were further analysed using Langmuir and Freundlich isotherms. The expressions for the two forms of these isotherm models are summarised in Table 4.1:

Table 4.1: Forms of the Langmuir and Freundlich isotherm models [16].

Isotherm models	**Non-linear form**	**Linear form**
Langmuir	$q_e = q_m K_L \frac{C_e}{1 + K_L C_e}$	$\frac{C_e}{q_e} = \frac{1}{q_m} C_e + \frac{1}{K_L q_m}$
Freundlich	$q_e = K_F C_e^{1/n}$	*ln* (q_e) = *ln* (K_F) + $\frac{1}{n}$ *ln* (C_e)

where q_e is the equilibrium adsorption capacity (mg/g), C_e is the equilibrium solution concentration of MB (mg/L), q_m is the maximum adsorption capacity (mg/g), K_L is a constant related to adsorption energy, *n* is a Freundlich parameter giving an indication of favourability of the MB adsorption process and K_F is an adsorption constant for the amount of dye adsorbed by the adsorbents. The linear forms of the isotherm models enable the determination of adsorption parameters for the process. For the Langmuir isotherm, a plot of C_e/q_e against C_e gives a straight line with the slope of $1/q_m$ and intercept $1/K_L q_m$. Analogously, the Freundlich parameters n and K_F can be obtained from the slope and intercept, respectively, of the plot of *ln* (q_e) against *ln* (C_e) [16].

4.7.1 Langmuir model

The Langmuir isotherm assumes that adsorption only occurs on a finite number of homogeneous sites, and is based on monolayer surface coverage [12, 16]. Figure 4.39 depicts the two forms of the Langmuir isotherms plotted using experimental adsorption data collected for ZSM-5(25)-based adsorbents. The source data is tabulated in Table A21 in the Appendix section.

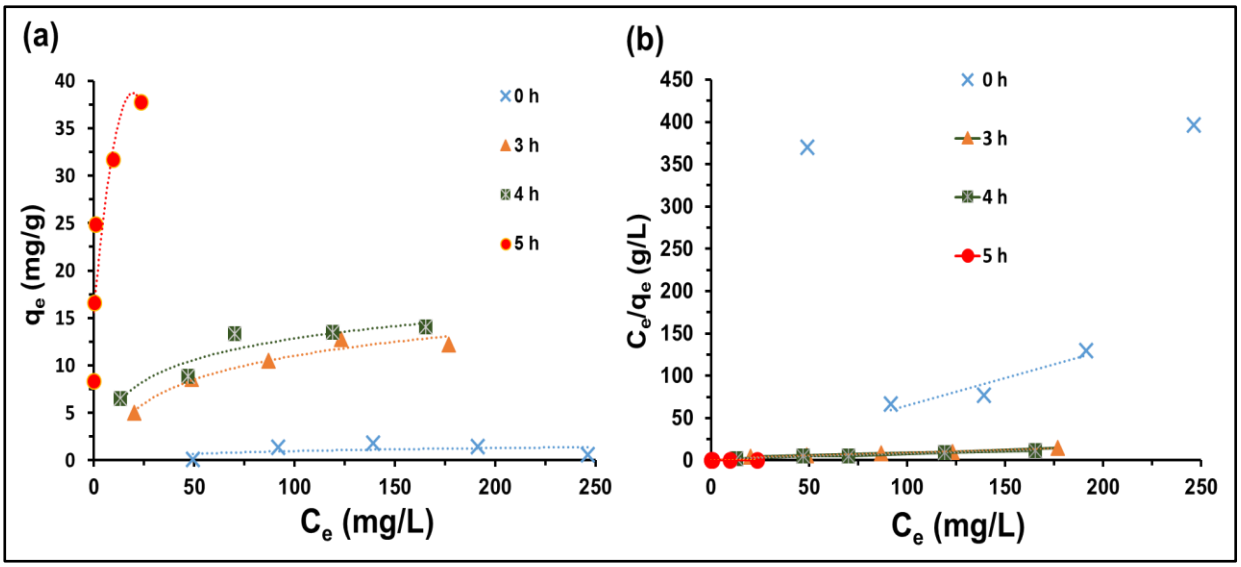

Figure 4.39: Langmuir adsorption isotherms for the adsorption of MB by ZSM-5(25) as affected by adsorbent dealumination time: (a) non-linear form, and (b) linear form. Adsorption conditions: dose = 0.5 g, pH 8, contact time = 2 h.

The plots in Figure 4.39(a) suggest trends that conform to the Langmuir model, *i.e.*, most data points lie on the trend line and the plot shapes suggest an initial increase in the adsorption capacity followed by a plateau (surface saturation). Such a trend is attributed to an adsorption process that involves a monolayer surface coverage by MB molecules [12]. The linear version of the Langmuir model fits the experiments data well, except for the parent ZSM-5(25) adsorbent, which shows a wide spread of data points. The values of the linear correlation coefficients (R^2), as well as the Langmuir adsorption parameters calculated from the linear Langmuir isotherms, are summarised in Table 4.2.Table 4.2: Langmuir adsorption parameters for the adsorption of MB by the ZSM-5(25)-based adsorbents.

Adsorbent	***Dealumination time (h)**	**Linear Langmuir**		
		R^2	**K_L (mg/g)**	**q_m (mg/g)**
ZSM-5(25)	0	0.891	0.032	2.10
	3	0.991	0.022	16.67
	4	0.996	0.010	20.00
	5	0.997	-	30.33

**Duration of acid dealumination time of pristine ZSM-5(25)*

The high R^2 values obtained from linear plots confirm adherence to the Langmuir mechanism and that the process proceeds *via* monolayer coverage. These correlation coefficients are accompanied by q_m values that are similar to the adsorption capacities (q_e) calculated from the experimental data (Table A21). Hammed *et al.* [12] reported similar trends in their study on the removal of MB using novel-modified ZSM-5. The values of K_L determined from the linear Langmuir isotherms in this study lie in the range $0 < K_L < 1$, indicating a favourable adsorption process. Furthermore, the inadmissible value of K_L for the 5 h dealumination derivative (indicated by a dash) shows that minimal energy is required for the adsorption of MB onto the adsorbent.

Similar studies were performed on the ZSM-5(50) series of zeolites, and the results are depicted in Figure 4.40.

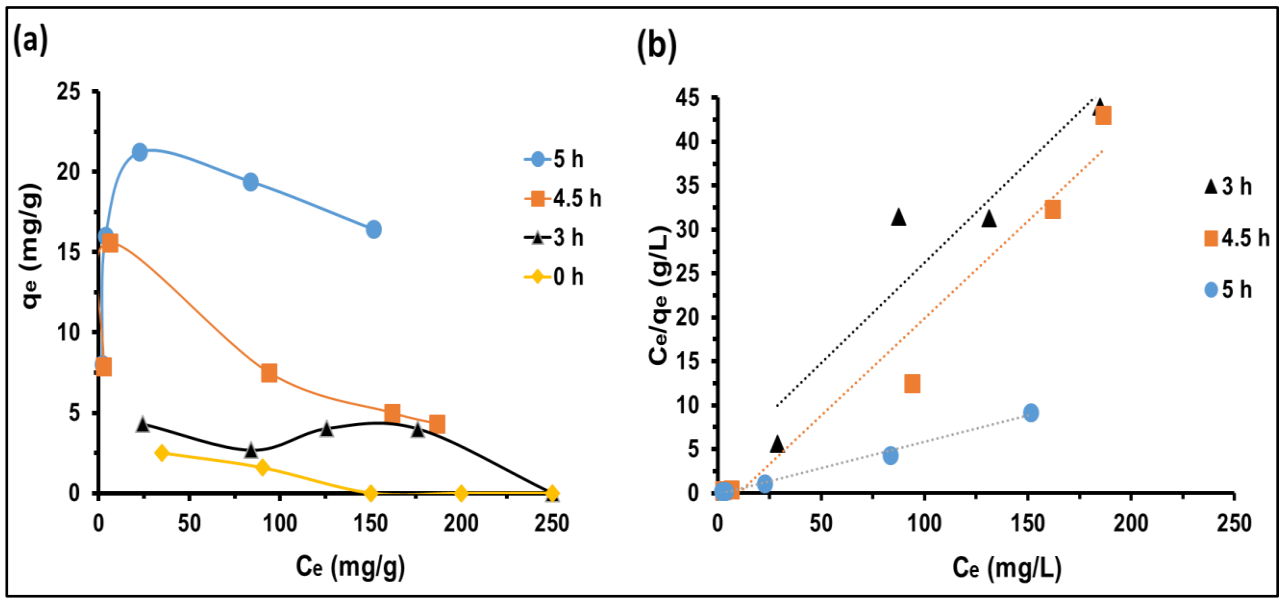

Figure 4.40: Langmuir adsorption isotherms for the adsorption of MB by ZSM-5(50) as affected by adsorbent dealumination: (a) non-linear form, and (b) linear form. Adsorption conditions: dose = 0.5 g, pH 8, contact time = 2 h.

The non-linear Langmuir isotherms adopt shapes that do not conform to that of the conventional Langmuir model, which is normally characterised by an initial increase in q_e followed by a plateau at higher equilibrium concentrations. The q_e values decrease with increasing initial concentration, thus deviating from the conventional model. This is due to equilibrium being reached rapidly since there are excess adsorbate molecules for a fixed number of adsorption sites [12, 17]. However, the MB adsorption

efficiency of ZSM-5(50) increases with increasing treatment time of the adsorbent. The adsorption parameters calculated from Figure 4.40(b) are summarised in Table 4.3.

Table 4.3: Langmuir adsorption parameters for the adsorption of MB by the ZSM-5(50)-based adsorbents.

Adsorbent	***Dealumination time (h)**	**Linear Langmuir**		
		R^2	**K_L (mg/g)**	**q_m (mg/g)**
ZSM-5(50)	3	0.8828	0.040	5.56
	4.5	0.9598	0.040	6.25
	5	0.9914	0.005	20.00

**Duration of acid dealumination time of pristine ZSM-5(50)*

Contrary to the observation in Figure 4.40(b), Table 4.3 suggests that the experimental data fits the linear Langmuir isotherm well, with high R^2 values suggesting that MB adsorption on ZSM-5(50) adsorbents proceeds *via* monolayer process. The q_m values determined from the linear Langmuir isotherms are similar to the adsorption capacities (q_e) calculated from the experimental data (Appendix, Table A20), and increase with prolonged zeolite dealumination period. The q_m values increase by 12.4% for the adsorbents dealuminated for 3 and 4.5 h, while increasing by 220% from the 4.5 to the 5 h dealumination adsorbents. This is due to the sharp decrease in S_{BET} from 3 to 4.5 h (335 – 208 m^2/g) dealumination treatment which is followed by an increase after dealumination from 4.5 to 5 h (208 – 275 m^2/g). The K_L constants determined for the ZSM-5(50)-based adsorbents lie in the range $0 < K_L < 1$, indicating a favourable adsorption process. Surprisingly, the ZSM-5(50) 5 h dealumination adsorbent does not show linear adsorption of MB in contrast to the sister derivative of the ZSM-5(25)-based adsorbents.

4.7.2 Freundlich model

The Freundlich isotherm is another popular model that describes heterogeneous adsorption, which applies to multilayer adsorption [16]. Figure 4.41 illustrates the two forms of Freundlich isotherm for MB uptake by ZSM-5(25) adsorbents.

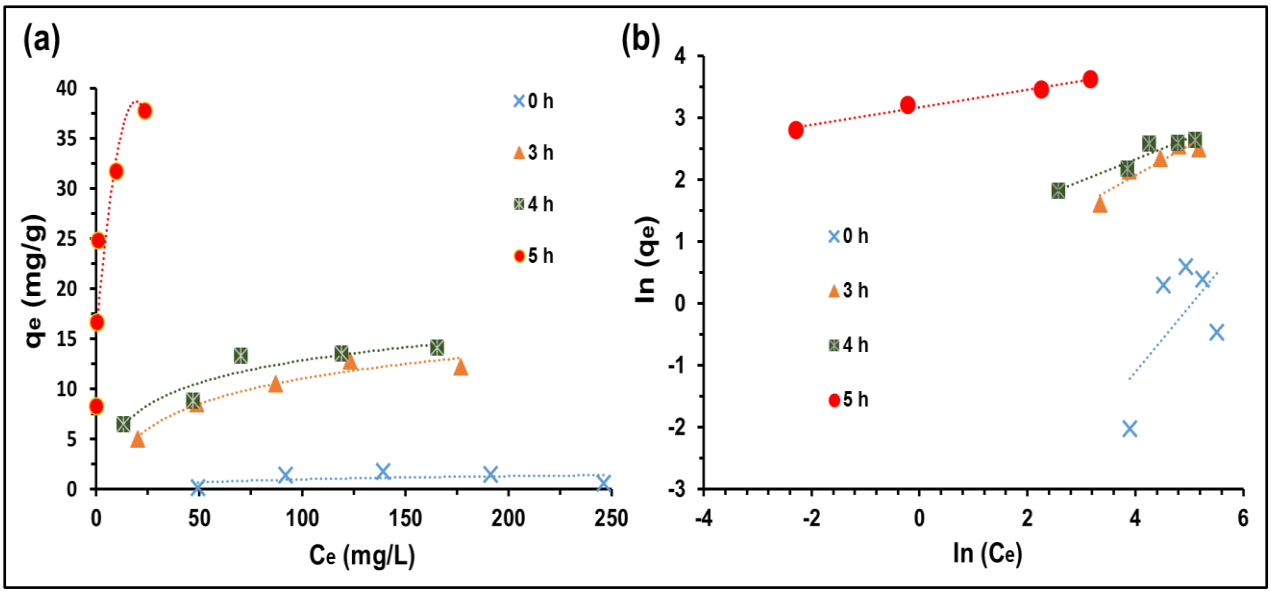

Figure 4.41: Freundlich isotherms for the adsorption of MB by ZSM-5(25) and its acid-dealuminated variants: (a) non-linear form, and (b) linear form. Adsorption conditions: dose = 0.5 g, pH 8, contact time = 2 h.

It follows from Figure 4.41 that the experimental data for MB adsorption by ZSM-5(25) adsorbents fits well in the non-linear form and not in the linear form of Freundlich isotherms. This suggests that the surface of the adsorbents is heterogeneous and MB removal by ZSM-5(25) adsorbents proceeds beyond monolayer adsorption [16, 17]. The heterogeneity of the ZSM-5(25) adsorbent surface accounts for the similar isotherm that was obtained in the Langmuir model, which conforms to the conventional form of that isotherm. Moreover, MB adsorption efficiency of ZSM-5(25) increases with increasing acid-treatment time of the adsorbent, *i.e.*, 0 < 3 < 4 < 5 h. Adsorption parameters for the Freundlich linear form were calculated and are displayed in Table 4.4:

Table 4.4: Freundlich adsorption parameters for the adsorption of MB by ZSM-5(25)-based adsorbents.

Adsorbent	***Dealumination time (h)**	**Linear Freundlich**		
		R^2	**K_F**	**n**
ZSM-5(25)	0	0.9814	2.72	1.74
	3	0.9114	1.77	0.62
	4	0.8799	7.69	0.66
	5	0.3879	6.29	0.48

**Duration of acid dealumination time of pristine ZSM-5(25)*

Table 4.4 suggests that the adsorption process is favourable, since the experimental data corresponds to high correlation coefficients. However, the R^2 values decrease with increasing adsorbent treatment times, suggesting that the experimental data does not fit well into the linear Freundlich form. A value of the slope $1/n < 1$ is associated with a chemisorption process that is more heterogeneous as the value gets closer to zero, while $1/n > 1$ is indicative of coorperative adsorption [17]. The *n* values calculated suggest that the adsorption of MB by the ZSM-5(25) dealumination derivatives proceeds through cooperative adsorption, *i.e*., unfavourable adsorption process. Hammed *et al.* [12] and Chen [16] have also reported unfavourable adsorption processes. However, the pristine ZSM-5(25) adsorbent removes MB by a favourbale adsorption process. This suggests that dealumination of the ZSM-5(25) material changes the mode of MB adsorption by the derivatives to unfavourable MB adsorption process. Moreover, the calculated K_F constants deviate from the adsorption capacities determined from experimental data, indicative of a poor fit by this isotherm model.

The Freundlich isotherm was also used to analyse experimental data from the adsorption of MB by ZSM-5(50) adsorbents, and the results are illustrated in Figure 4.46.

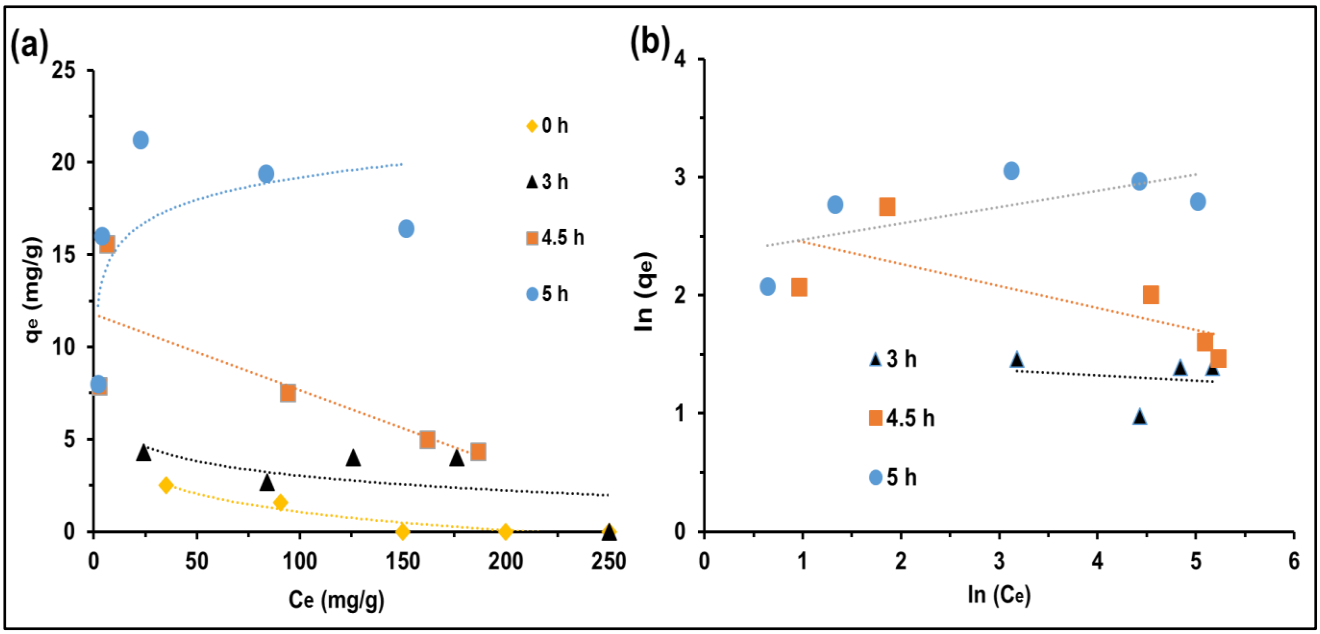

Figure 4.42: Freundlich isotherms for the adsorption of MB by ZSM-5(50) and its acid-dealuminated variants: (a) non-linear form, and (b) linear form. Adsorption conditions: dose = 0.5 g, pH 8, contact time = 2 h. Parent ZSM-5(50) is omitted in (b) because experimental data yields undefined results from analysis by the linear Freundlich equation.

The experimental data collected for MB adsorption using the ZSM-5(50)-based adsorbents does not fit either form of the Freundlich isotherms, because most of the data points do not lie on the trend lines. Furthermore, the inadequate fit of the experimental data into both forms of the model suggests that the surface of the ZSM-5(50) adsorbents is homogeneous even after dealumination. Surprisingly, the ZSM-5(25)-based adsorbents seem to have a heterogeneous surface [12], and the dealumination of this material changes the MB adsorption mode from favourable adsorption to a cooperative adsorption process. Moreover, adsorption efficiency of ZSM-5(50)-based adsorbents increases with dealumination time in agreement with what was found from the Langmuir analysis. Adsorption parameters were calculated from the linear Freundlich isotherms and are summarised in Table 4.5.

Table 4.5: Freundlich adsorption parameters for the adsorption of MB by ZSM-5(50)-based adsorbents.

Adsorbent	***Dealumination time (h)**	**Linear Freundlich**		
		R^2	**K_F**	**n**
ZSM-5(50)	3	0.4611	0.95	-1.340
	4.5	0.5466	0.83	-0.403
	5	0.9281	0.84	0.560

**Duration of acid dealumination time of pristine ZSM-5(50)*

The R^2 value of MB adsorption data by the 3 h dealumination adsorbent is low, while the correlation of the experimental data increases with the increase in zeolite dealumination time. Furthermore, 1/n < 1 indicates a sorption process that occurs on a homogeneous surface by favourable adsorption process [17], which agrees with the result from Langmuir analysis. The fitting of the experimental data generated from the 3 and 4.5 h dealumination adsorbents leads to negative values of n, which result from the negative slopes depicted on Figure 4.42 above. These negative n values suggest that the chemisorption process is heterogeneous. However, this is unique because n values usually range between 0 and 1. Moreover, the K_F values determined using this model deviate substantially from the data that was obtained experimentally.

4.8 Conclusions

The adsorption of MB by both the ZSM-5(25)- and ZSM-5(50)-based adsorbents proceeds *via* monolayer adsorption. The experimental data fits into the Langmuir model and not into the Freundlich isotherms, since higher R^2 values were found for both series of adsorbents by fitting into the linear Langmuir form. Pristine ZSM-5(25) is characterised by a homogeneous surface but, upon dealumination, the ZSM-5(25)-based derivatives were found to adsorb by cooperative adsorption. Furthermore, the ZSM-5(50) adsorbents were found to have a homogeneous surface even after acid dealumination. Importantly, MB adsorption by ZSM-5 adsorbents becomes more efficient as the acid dealumination period of the zeolites increases. The q_m values of 30.33 and 20 mg/g were calculated for the 5 h dealumination

derivatives of the ZSM-5(25) and ZSM-5(50) adsorbents, respectively, and are similar to the q_e values (38 and 21.23 mg/g) calculated from the experimental data.

4.9 References

1. R.J. Argauer, G.R. Landolt; Crystalline zeolite ZSM-5 and method of preparing the same, *US Patent* **3** 702-886, (1972).
2. C.S. Triatafillidis, A.G. Vlessidis, L. Nalbandian, N.P. Evmiridis; Effect of the degree and type of the dealumination method on the structural, compositional and acidic characteristics of H-ZSM-5 zeolites; *Journal of Microporous and Mesoporous Materials* **47**, 369-388, (2001).
3. Z.G.L.V. Sari, H. Younesi, H. Kazemian; Synthesis of nanosized ZSM-5 zeolite using extracted silica from rice husk without adding any alumina source; *Journal of Applied Nanoscience* **5**, 737-745, (2015).
4. Y. Fan, X. Bao, X. Lin, G. Lin, G. Shi, H. Liu; Acidity adjustment of HZSM-5 zeolites by dealumination and realumination with steaming and citric acid treatments; *Journal of Physical Chemistry B* **110**, 15411-15416, (2006).
5. M.J. Van Niekerk, J.C.Q. Fletcher, C.T. O'Connor; Characterisation of dealuminated large-pot mordenites; *Journal of Catalysis* **138**, 150-163, (1992).
6. M.D. Gonzalez, Y. Cesteros, P. Salagne; Comparison of dealumination of zeolites beta, mordenite and ZSM-5 by treatment with acid under microwave irradiation; *Journal of Microporous and Mesoporous Materials* **144**, 162-170, (2011).
7. S. Li, Y. Wang, B. Shi, J. Ren, X. Liu, Y. Wang, Y. Guo, Y. Guo; Synthesis of hierarchical MFI zeolite microspheres with stacking nanocrystals; *Journal of Microporous and Mesoporous Materials* **117**, 104-110, (2009).
8. R. Caicedo-Realpe, J. Perez-Ramirez; Mesoporous ZSM-5 zeolites prepared by a two-step route comprising sodium aluminate and acid treatments; *Journal of Microporous and Mesoporous Materials* **128**, 91-100, (2010).
9. S. Fujita, T. Kanai, Y. Oumi, T. Sano; Dealumination behaviour of ZSM-5-type zeolite containing alkaline earth metal; *Studies in Surface Science and Catalysis* **158**, 191-198, (2005).
10. J. Ahmadpour, M. Taghizadeh; Catalytic conversion of methanol to propylene over high-silica mesoporous ZSM-5 zeolites prepared by different combinations of mesogenous templates; *Journal of Natural Gas Science and Engineering* **23**, 184-194, (2015).

11. E. Mohiuddin, Y.M. Isa, M.M. Mdleleni, N. Sincadu, D. Key, T. Tshabalala; Synthesis of ZSM-5 from impure and beneficiated Grahamstown kaolin: Effect of kaolinite, crystallisation temperature and time; *Journal of Applied Clay Science* **119**, 213-221, (2016).
12. A.K. Hammed, N. Dewayanto, D. Du, M.H. Ab Rahim, M.R. Nordin; Novel modified ZSM-5 as an efficient adsorbent for methylene blue removal; *Journal of Environmental Chemical Engineering* **4**, 2607-2616, (2016).
13. Y. Dong, B. Lu, S. Zang, J. Zhao, X. Wang, Q. Cai; Removal of methylene blue from coloured effluents by adsorption onto SBA-15; *Journal of Chemical Technology and Biotechnology* **86**, 616-619, (2011).
14. A.F. Hassan, H. Elhadidy; Production of activated carbon from waste carpets and its application in methylene blue adsorption: Kinetic and thermodynamic studies; *Journal of Environmental Chemical Engineering* **5**, 955-963, (2017).
15. X.Y. Jin, M.Q. Jiang, X.Q. Shan, Z.G. Pei, Z. Chem; Adsorption of methylene blue and orange II onto unmodified and surfactant-modified zeolite; *Journal of Colloid and Interface Science* **328**, 243-247, (2008).
16. X. Chen; Modelling of experimental adsorption isotherm data; *Information* **6**, 14-22, (2015).
17. A.O. Dada, A.P. Olalekan, A.M. Olatunya, O. Dada; Langmuir, Freundlich. Temkin and Dubnin-Radushkevich isotherms studies of equilibrium sorption of Zn^{2+} unto phosphoric acid modified rice husk; *Journal of Applied Chemistry* **3**, 38-45, (2012).

CHAPTER 5

5.1 Summary and conclusions

The aim of this work was address the water contamination problem arising from textile effluents through the development of MFI-based zeolitic adsorbents with improved efficiency in the removal of methylene blue (MB) from aqueous solutions. First, parent ZSM-5 zeolites were prepared by a hydrothermal method to two levels of silica-to-alumina ratio (SAR), *viz*., 25 and 50. Then, these zeolites were further dealuminated by post-synthesis treatment using an aqueous 1 M solution of HNO_3 at 90 °C for different lengths of time. Physicochemical characterisation of the parent zeolites and their post-synthesis treated derivatives was carried out using X-ray powder diffraction (XRD), N_2 adsorption/desorption, scanning electron microscopy (SEM) and Fourier transform infrared (FTIR) spectroscopy. MB was chosen as a model basic cationic dye to study the performance of the synthesised zeolites in its adsorptive decontamination from water. The MB adsorption performance of the ZSM-5 zeolites prepared in this study was investigated *via* batch experimentation.

For the parent ZSM-5(25), the successful synthesis of a phase-pure material was immediately confirmed using XRD. Dealumination of the parent ZSM-5(25) was found to influence the crystal structure, resulting in mixed-phase MFI/analcime-type structure at dealumination times longer than 3 h as suggested by XRD. The percentage XRD crystallinity of this zeolite was found to decrease with increasing dealumination treatment time. A gradual decrease of the ZSM-5(25) crystallite sizes was also observed with the increasing HNO_3 treatment time relative to the parent material. In addition, the synthesis of ZSM-5(25) was also corroborated by FTIR spectroscopy, with bands in the infrared skeletal vibration at ~1225 cm-1, 1064 cm^{-1} and ~800 cm^{-1} characteristic of MFI materials. The Si-O-Al bands were observed to decrease in intensity and shift to lower wavenumbers with prolonged dealumination treatment, confirming the extraction of framework aluminium from this zeolite. The parent ZSM-5(25) showed a Type I N_2 adsorption isotherm, suggestive of a purely microporous character. Nitrogen adsorption-desorption isotherms of the dealuminated derivatives revealed the presence of mesopores in the intrinsically microporous ZSM-5(25) zeolite framework consequent to the dealumination treatment. This was demonstrated by combined Type I and Type IV adsorption isotherms with a broader step in the

adsorption branch and a pronounced hysteresis loop. The BET surface area (S_{BET}) and porosity data improved significantly following the dealumination treatment, and ranged from 109 m^2/g in the parent to 301 m^2/g in the highest S_{BET} derivative, *i.e*., a 3-fold increase in S_{BET}. Pore sizes of the ZSM-5(25)-derived series of zeolites were not significantly affected by the acid treatment. Adsorption of MB on ZSM-5(25) zeolites was found to be influenced by experimental variables such as pH, adsorbent dose, contact time and initial MB concentration. The adsorptive removal of MB was highest at pH 8, and significantly lower in the more basic and acidic range. MB uptake by ZSM-5(25) series of adsorbents was found to increase with the amount of zeolite used. This is due to the abundance of adsorption sites in the larger doses. The MB uptake by ZSM-5(25) zeolites decreased with increasing initial MB concentration for this series of adsorbents because the adsorbents reached equilibrium quickly at higher concentration. Amongst these materials, the sample obtained after 5 h of dealumination showed the highest MB adsorption performance (37.75 mg/g) compared to the other samples in the ZSM-5(25) series. This could be attributed to either the high surface area of this material relative to other members of this series, or to the co-existence of an additional non-MFI phase in this sample that was suggested by XRD.

The successful synthesis of phase-pure parent ZSM-5(50) was also confirmed using XRD, which further indicated that ZSM-5(50) was resistant to structural destruction by acid treatment. That is, phase-pure MFI-derivatives were obtained even after 5 h of dealumination. The percentage XRD crystallinity decreased with increasing dealumination time. This decrease could be associated with lattice contractions as Al species are extracted from the parent zeolite framework. The crystallite sizes of the ZSM-5(50) also decreased with increasing acid treatment time. In addition to XRD findings, successful synthesis of the ZSM-5(50) series was also corroborated by FTIR spectra, with bands in the infrared skeletal vibration at ~1224 cm^{-1}, ~1073 cm^{-1} and ~801 cm^{-1}. The IR bands corresponding to the Si-O-Al vibrations decreased in intensity with prolonged dealumination time, confirming the leaching of Al from the zeolite lattice through this treatment. The N_2 adsorption isotherm of the parent ZSM-5(50) changed from Type I to Type IV consequent to the dealumination treatment, suggesting the co-generation of mesopores in the zeolite matrix. A pronounced hysteresis loop in the N_2 adsorption isotherms of these dealuminated products also signalled the presence of

mesoporosity. The corresponding S_{BET} values were generally increased by the HNO_3 treatment, and ranged from 105 m^2/g in the parent ZSM-5(50) to the highest value of 335 m^2/g in the 3 h-dealumination sample. SEM morphological studies revealed that pristine ZSM-5(50) synthesised through this method is dominated by a previously-unobserved morphology, consisting of deltoidal icositetrahedral crystals, similar to that normally found in zeolite analcime. The dealuminative treatment of this material completely altered the observed icositetrahedral morphology of the parent, producing a range of other morphologies at different treatment times. A spectacular morphology was observed in the ZSM-5(50) zeolite after a 4.5 h dealumination treatment: In addition to agglomerated particles with ill-defined grain boundaries, and coffin-shaped as well as prismatic structures conventionally found in ZSM-5, this ZSM-5(50) derivative showed a cylindrical stack of self-assembled longitudinally-packed nanorods, which seems to be absent in the other derivatives. Similarly to the ZSM-5(25) series of zeolitic adsorbents, the adsorption of MB by ZSM-5(50) materials was influenced by pH, adsorbent dose, contact time and initial MB concentration. The ZSM-5(50) series of zeolites also performed best in the adsorptive removal of MB at pH 8. MB uptake by ZSM-5(50) series of adsorbents also increased with the amount of zeolite used due to the abundance of adsorption sites at larger doses, while it decreased with increasing initial MB concentration because equilibrium between the adsorbate and the materials is reached quicker at high concentrations. Again, the zeolitic adsorbent obtained by dealuminating ZSM-5(50) for 5 h showed the highest performance in the removal of MB from aqueous systems (21.23 mg/g). This performance can be attributed solely to the high S_{BET} of this phase-pure material, in contrast with the observation in the corresponding adsorbent derived from ZSM-5(25), whose activity could also be attributed to its analogue mixed-phase nature.

5.2 Recommendations

The following recommendations are suggested for future studies:

- Dealumination of ZSM-5 zeolites could be carried out beyond 5 hours to obtain materials with larger surface areas and having better adsorption capacities.

APPENDICES

Table A1: Effect of dealumination on the physicochemical properties of dealuminated ZSM-5(25) zeolites.

Sample	**Dealumination time (h)**	**Relative Crystallinity (RC)**	**Scherrer crystallite size (μm)**
Parent	0	96.40	0.22
1	0.5	75.85	0.21
2	1	56.91	0.14
3	1.5	52.63	0.14
4	2	81.74	0.13
5	2.5	61.60	0.13
6	3	55.97	0.13
7	3.5	60.81	0.12
8	4	61.49	0.12
9	4.5	58.29	0.11
10	5	69.26	0.10
11	5.5	50.79	0.21
12	6	35.85	0.22

Table A2: Textural properties of ZSM-5(25) samples.

Sample	**Treatment (h)**	**S_{BET} (m^2/g)**	**t-plot Micropore area (m^2/g)**	**t-plot Micropore volume (cm^3/g)**
Parent	0	109.620	89.78	0.04
DZM-01	0.5	154.327	77.691	0.04
DZM-02	1.5	190.095	95.577	0.05
DZM-03	2	230.324	110.39	0.04
DZM-04	2.5	228.304	115.112	0.06
DZM-05	3.5	215.796	126.82	0.04
DZM-06	4	292.129	154.71	0.04
DZM-07	5	301.490	159.68	0.09

Table A3: Effect of dealumination on the physicochemical properties of ZSM-5(50) products.

Sample	**Dealumination Time (h)**	**Relative Crystallinity (RC)**	**Scherrer Crystallite sizes (μm)**
Parent	0	100	0.226
1	0.5	94.03	0.259
2	1	90.61	0.211
3	1.5	82.32	0.208
4	2	81.74	0.201
5	2.5	75.90	0.181
6	3	78.83	0.164
7	3.5	74.89	0.158
8	4	62.27	0.179
9	4.5	59.35	0.151
10	5	47.35	0.111
11	5.5	51.68	0.102

Table A4: Textural properties of the parent and treated ZSM-5(50) zeolites.

Sample	Treatment (h)	S_{BET} (m^2/g)	t-plot Micropore area (m^2/g)	t-plot Micropore volume (cm^3/g)
Parent	0	105.45	89.780	0.04
DZM-01	0.5	115.45	88.612	0.04
DZM-02	1	270.12	187.04	0.09
DZM-03	1.5	283.06	217.31	0.11
DZM-04	2	310	223.58	0.11
DZM-05	2.5	228.66	158.15	0.08
DZM-06	3	335.18	215.49	0.10
DZM-07	4	268.36	179.49	0.09
DZM-08	4.5	208.33	97.10	0.05
DZM-09	5	275.02	176.58	0.09
DZM-09	5.5	301.86	194.28	0.09

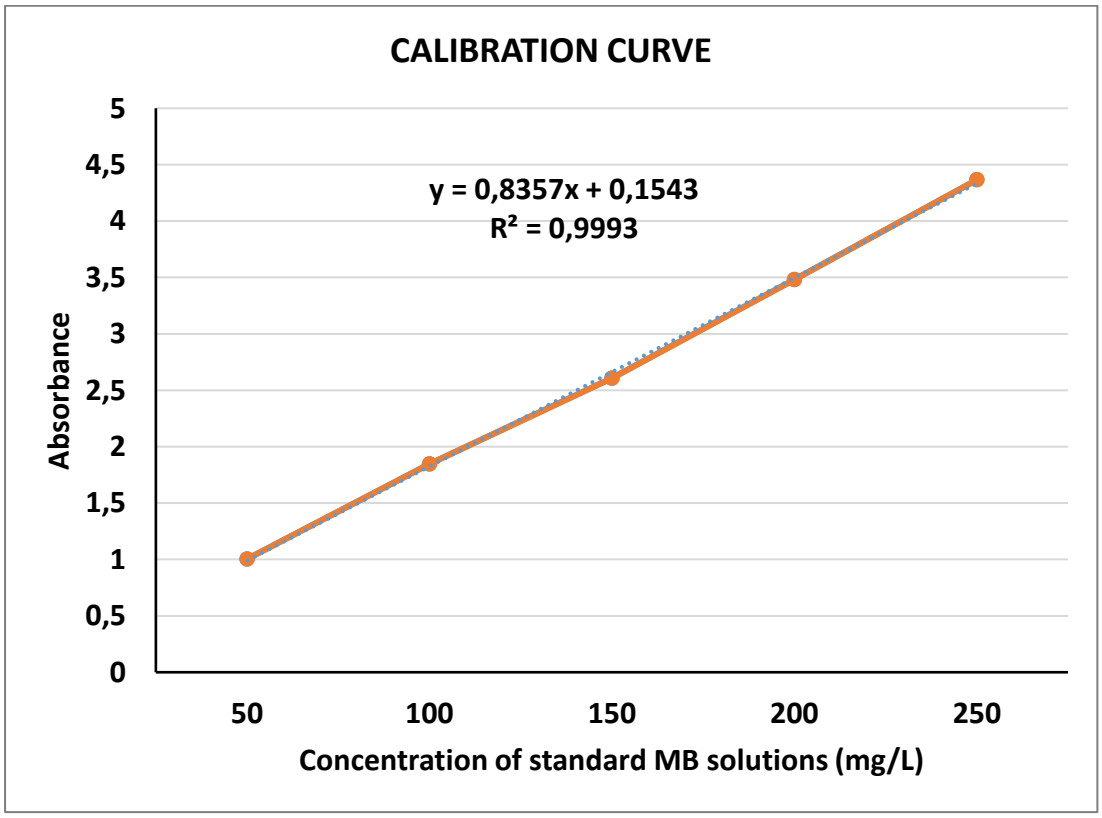

Figure A1: Calibration curve of standard MB solutions.

Table A5: Equilibrium concentrations (mg/L) of MB removal by ZSM-5(25) with increasing pH.

pH	**Dealumination time (h)**							
	5	**4.5**	**4**	**3**	**2.5**	**1.5**	**0.5**	**0**
2	16.5	25.6	34.5	35.8	38	39.3	40.4	44.4
4	11	22.5	32	33.5	36.9	38.1	38	44
6	8.3	16.2	24.3	26.8	33.3	35.9	37.5	41.5
8	2.2	14	19.7	20.6	21.8	31.7	36.2	38.7
10	8	18.8	23.4	24.5	33.5	35.5	37.5	40.4
12	8.6	20	23.6	26	35.3	34	37.6	40.4
14	8.5	20	24	26.2	35.6	34.3	37.6	40.5

Table A6: Percentage MB removal by ZSM-5(25) with increasing pH.

pH	**Dealumination time (h)**							
	5	**4.5**	**4**	**3**	**2.5**	**1.5**	**0.5**	**0**
2	67.6	48.9	31	28.7	24.1	21.6	19.1	12.2
4	78	55	36.30	33	25.7	23.9	23.6	13.1
6	83.8	67.8	51.59	46.8	32.5	28.7	25	17.6
8	95.6	72	60.56	58.9	42.9	36.54	27.5	22.5
10	84.2	62.5	53.10	51	33	29	25.6	19.2
12	83.4	60	52.81	48	30.1	28.13	24.7	19.1
14	83	60	52	47.1	29.2	27.8	24.7	19

Table A7: Equilibrium concentrations (mg/L) of MB removal by ZSM-5(25) with increasing adsorbent dose.

Dose (g)	**Dealumination time (h)**							
	5	**4.5**	**4**	**3**	**2.5**	**1.5**	**0.5**	**0**
0.1	16.7	24	27.5	33.4	35.5	36.7	41.7	42.5
0.2	12	16.2	25.1	31.8	33.2	32.5	40	40.9
0.3	3.5	12.2	22	28.5	30	30.3	38	39
0.4	2	11.5	18.8	26.7	27.5	28.4	33.5	36.8
0.5	1.2	7.1	17.1	24.5	25	26	31.9	36.4
0.6	0.5	5.5	13	23.6	22.5	24	29	33.7
0.7	0.2	3.2	12.1	22.1	21.8	23	26.1	32.8
0.8	0	2.6	9.5	18.5	19.1	19.6	24.8	31
0.9	0	1.6	7.8	15.9	17	18	23	29.7
1.0	0	1	6	13	16.1	16.5	21.5	27

Table A8: Percentage MB removal by ZSM-5(25) with increasing dose.

Dose (g)	**Dealumination time (h)**							
	5	**4.5**	**4**	**3**	**2.5**	**1.5**	**0.5**	**0**
0.1	66.6	52	45.2	31.5	29	27.4	18.7	15
0.2	76.4	67.2	49.6	36.7	34.1	33	20.1	18.2
0.3	93	74.6	56.2	43	39.8	38.9	24	23.1
0.4	96	77	62.9	47.6	45	43.6	33.1	26.2
0.5	97.6	85.3	65.8	51	50.6	48	37.3	27.4
0.6	99	89	74	55.8	53.9	52	42.1	32.5
0.7	99.8	93.4	77.2	58.5	56.3	54.1	46.4	34.8
0.8	100	95	81	63	61.5	59	50.3	38
0.9	100	96.9	84.7	68.7	66	64.3	54	40.9
1	100	98	88	74	70.4	67	57	44

Table A9: Equilibrium concentrations (mg/L) of MB removal by ZSM-5(25) with varying contact time.

Contact time (h)	**Dealumination time (h)**							
	5	**4.5**	**4**	**3**	**2.5**	**1.5**	**0.5**	**0**
1	5	5.5	20.5	22.3	32.5	35	38.3	40.5
2	0.1	1.5	16	16.8	27	32.8	36.5	37.5
3	0	0.3	12	15.5	24.5	28	32.5	34
4	0	0	7.2	13	20.5	25.5	30.5	31.5
5	0	0	3.8	12	17.4	23.5	27	28.7

Table A10: Percentage MB removal by ZSM-5(25) at different contact time.

Contact time (h)	Dealumination time						
	5 h	**4 h**	**3 h**	**2.5 h**	**1.5 h**	**0.5 h**	**Parent (0 h)**
1	90.2	59	55.9	35	30	23.6	19
2	99.8	68	65.7	46.3	37.4	27	25.3
3	100	76	69	51	44	35	32
4	100	85.3	74	57.5	49.1	39	37.4
5	100	92.7	76	64.9	52.6	46.2	42.3

Table A11: Equilibrium concentrations (mg/L) of MB removal by ZSM-5(25) with increasing initial concentration.

MB Concentration (mg/L)	Dealumination time (h)							
	5	**4.5**	**4**	**3**	**2.5**	**1.5**	**0.5**	**0**
50	0	0	13.1	20.1	28.6	40	43.4	49.3
100	0.1	2.1	47	48.7	62.9	87.6	91.1	91.7
150	0.8	2.9	70	86.9	103.4	127	138	139.2
200	9.53	15.4	119	123.1	151.1	175.3	188.6	191.2
250	23.5	58.9	165.5	176.9	201.7	231.5	239.2	246.2

Table A12: Influence of initial concentration on MB uptake by ZSM-5(25).

MB Concentration (mg/L)	Dealumination time (h)							
	5	**4.5**	**4**	**3**	**2.5**	**1.5**	**0.5**	**0**
50	100	85	73.9	59.7	42.9	25.7	13.1	11.5
100	99.90	77	66.8	51.3	37.1	17.4	8.9	8.3
150	99.55	71.3	53	42,1	31.1	15.8	8	7.1
200	95.28	67	41	38.6	24.6	12.3	5.7	4.4
250	90.60	60.1	33.8	29.3	19.2	10.2	4.3	1.5

Table A13: MB adsorption capacity for ZSM-5(25) as a function of pH.

pH	Dealumination time (h)							
	5	**4.5**	**4**	**3**	**2.5**	**1.5**	**0.5**	**0**
2	16.75	12.20	7.75	7.10	6	5.35	4.80	2.80
4	19.50	13.75	9	8.25	6.55	5.95	5.95	3
6	20.85	16.90	12.85	11.60	8.35	7.05	6.25	4.25
8	23.90	18	15.15	14.70	14.10	9.15	6.90	5.65
10	21	15.60	13.30	12.75	8.25	7.25	6.25	4.80
12	20.70	15	13.20	12	7.55	8	6.20	4.80
14	20.75	15	13	11.90	7.20	8.10	6.20	4.75

Table A14: MB adsorption capacities for ZSM-5(25) as a function of dose.

Dose (g)	Dealumination time (h)							
	5	**4.5**	**4**	**3**	**2.5**	**1.5**	**0.5**	**0**
0.1	16.65	13	11.25	8.30	7.25	6.65	4.15	3.75
0.2	9.50	8.45	6.23	4.55	4.20	4.38	2.50	2.28
0.3	7.75	6.30	4.66	3.58	3.33	3.28	2	1.83
0.4	6	4.81	3.90	2.91	2.81	2.70	2.06	1.53
0.5	4.88	4.29	3.29	2.55	2.50	2.40	1.81	1.36
0.6	4.13	3.71	3.08	2.20	2.29	2.17	1.75	1.36
0.7	3.56	3.34	2.71	1.99	2.01	1.93	1.71	1.23
0.8	3.13	2.96	2.53	1.97	1.93	1.90	1.58	1.19
0.9	2.78	2.69	2.34	1.89	1.83	1.78	1.50	1.13
1.0	2.50	2.45	2.20	1.85	1.70	1.68	1.43	1.15

Table A15: MB adsorption capacities for ZSM-5 (25) as a function of contact time.

Contact time (h)	Dealumination time (h)							
	5	**4.5**	**4**	**3**	**2.5**	**1.5**	**0.5**	**0**
1	7.50	5	4.92	4.62	2.92	2.50	1.95	1.58
2	8.31	5.65	5.67	5.53	3.83	2.87	2.25	2.08
3	8.33	5.78	6.33	5.75	4.25	3.67	2.92	2.67
4	8.33	6.42	7.13	6.17	4.92	4.08	3.25	3.08
5	8.33	7.42	7.70	6.33	5.43	4.42	3.83	3.55

Table A16: MB adsorption capacities on ZSM-5(25) as a function of initial concentration.

MB Concentration (mg/L)	Dealumination time (h)					
	5	**4**	**3**	**2.5**	**0.5**	**0**
50	8.33	6.15	4.98	3.57	1.10	0.133
100	16.65	8.83	8.55	6.18	1.48	1.38
150	24.87	13.33	10.51	7.76	2	1.80
200	31.75	13.50	12.81	8.15	1.90	1.47
250	37.75	14.08	12.18	8.05	1.80	0.63

Table A17: Equilibrium concentrations (mg/L) of MB removal by ZSM-5(50) with increasing pH.

pH	Dealumination time (h)							
	5	**4.5**	**4**	**3**	**2**	**1.5**	**0.5**	**0**
2	22.8	28.9	33	33.9	38	39	41.2	43.3
4	18	27.5	31	33.5	37	38.2	38.1	43.2
6	5.5	26	28	26.1	33.4	38	37.5	41
8	2.5	14	22	22.4	28.5	36.5	36	38.5
10	13	18.5	23.5	24.5	33.5	37.5	37	42.1
12	12.1	20	24.1	26	35	38.2	36.9	42.5
14	11.9	20	24.3	26.5	35.6	38.3	36.9	43

Table A18: Percentage MB removal at different pH by ZSM-5(50).

pH	Dealumination time (h)							
	5	**4.5**	**4**	**3**	**2**	**1.5**	**0.5**	**0**
2	57.3	42.9	34.2	28.7	24.1	21.5	19.1	12.2
4	64	45	38	33	25.7	22.8	23.6	13.1
6	88.6	57.8	43.5	46.8	32.5	24.2	25	17.6
8	95	72	56	58.9	42.9	26.9	27.5	22.5
10	74.2	62.5	52.5	51	33	25	25.6	15.5
12	73.5	60	51.4	48	30.1	23.8	24.7	15.1
14	71.4	60	51.2	47.1	29.2	23.5	24.7	14

Table A19: Equilibrium concentrations (mg/L) of MB removal by ZSM-5(50) with increasing dose.

Dose (g)	Dealumination time (h)							
	5	**4.5**	**4**	**3**	**2**	**1.5**	**0.5**	**0**
0.1	17.5	22	24	33.8	34.8	35.3	40.5	42.5
0.2	15	16	16.5	32.6	33	32.5	40	41
0.3	7.5	11.5	12.5	27.5	30	30.3	38	37.5
0.4	5.5	5.4	11.5	26	27.3	28	33.5	37
0.5	2.8	4	7.3	24.5	25	26	31.3	36.5
0.6	1.2	2.5	5.5	23.9	23.2	24	29	34.7
0.7	1	1.5	3.1	23.5	22	23	27	32.5
0.8	0.1	1.5	2.5	17.5	18.7	20.5	24.9	31
0.9	0	0.1	1.6	16.7	16.9	18	23	29.5
1.0	0	0.1	1	13	14.7	15.9	26.5	28

Table A20: Percentage MB removal with varying ZSM-5(50) dose.

Dose (g)	Dealumination time (h)							
	5	4.5	4	3	2	1.5	0.5	0
0.1	63	55.6	52	31.5	29.4	27.4	18.7	15
0.2	69.8	68.1	67.2	36.7	35	33	20.1	18.2
0.3	84.5	79	74.6	43	40	38.9	24	23.1
0.4	89	85.4	77	47.6	45.2	43.6	33.1	26.2
0.5	94.6	92	85.3	51	49.7	48	37.3	27.4
0.6	97.5	95.1	89	55.8	53.1	52	42.1	32.5
0.7	98	96.8	93.4	58.5	56	54.1	46.4	34.8
0.8	98.9	97	95	63	61.8	59	50.3	38
0.9	100	98.9	96.9	68.7	66.6	64.3	54	40.9
1	100	99.2	98	74	70.9	67	57	44

Table A21: Equilibrium concentrations (mg/L) of MB removal by ZSM-5(50) with varying contact time.

Contact time (h)	Dealumination time (h)							
	5	4.5	4	3	2	1.5	0.5	0
1	11.2	16	20	27.6	32.9	34	37.5	42.9
2	5.5	13.5	14.8	16.8	27.5	31	37	38.1
3	4.2	10.5	12	15	24.5	27	32.8	35
4	0.8	9.1	10	13.1	19.6	24.9	31	31.5
5	0	6.5	7.8	11	16.9	23.2	27.5	29.1

Table A22: Percentage MB removal by ZSM-5(50) with increasing contact time.

Contact time (h)	Dealumination time (h)							
	5	4.5	4	3	2	1.5	0.5	0
1	76.8	67.6	60	56.7	39.6	32	23.1	18.6
2	89	73.1	69.4	67.2	45	38.3	25.9	24.7
3	95.9	79	75.9	70.1	50.7	45.5	34.2	30
4	98.2	84.3	80	73.5	59.1	50.2	37.7	36.8
5	100	87	83.6	78	66.4	53.2	45	41.5

Table A23: Equilibrium concentrations (mg/L) of MB removal by ZSM-5(50) with increasing initial concentrations.

MB Concentration (mg/L)	Dealumination time (h)							
	5	4.5	4	3	2	1.5	0.5	0
50	1.9	2.6	5.4	24.1	28.8	30.7	31.3	35
100	3.8	6.4	69.6	84	87.5	89.5	96.8	90.5
150	22.6	94	105	125.9	131.3	133.9	145	150
200	83.5	161.8	170	176	185	189	192	200
250	151.4	186.4	224	250	250	250	250	250

Table A24: Percentage MB removal by ZSM-5(50) with increasing initial concentration.

MB Concentration (mg/L)	Dealumination time (h)							
	5	4.5	4	3	2	1.5	0.5	0
50	96.2	94.8	89.1	51.8	42.8	38.6	37.4	30
100	96.2	93.6	62.7	22	19.4	18.9	11.3	9.5
150	84.93	37.73	30.4	16	12.5	10.5	3.2	0
200	58.25	19	15.1	12.5	7.58	5.6	0.4	0
250	39.44	25.44	10.4	0	0	0	0	0

Table A25: MB adsorption capacities for ZSM-5(50) as a function of pH.

pH	Dealumination time (h)							
	5	4.5	4	3	2	1.5	0.5	0
2	13.6	10.55	8.50	8.05	6.5	5.5	4.4	3.10
4	16	11.25	9.50	8.25	6.75	5.9	5.95	3.40
6	22.25	12	11	11.95	8.3	6	6.25	4.50
8	23.75	18	14	14.3	10.75	6.75	7	5.75
10	18.5	15.75	13.25	12.75	8.25	6.25	6.5	3.95
12	18.95	15	12.95	12	7.5	5.9	6.55	3.75
14	19.05	15	12.85	11.8	7.2	5.85	6.55	3.50

Table A27: MB adsorption capacity for ZSM-5(50) as a function of dose.

Dose (g)	Dealumination time							
	5	4.5	4	3	2	1.5	0.5	0
0.1	16.25	14	13	8.1	7.6	7.35	4.75	3.75
0.2	8.75	8.50	8.38	4.35	4.25	4.38	2.50	2.25
0.3	7.08	6.41	6.25	3.75	3.33	3.28	2	2.08
0.4	5.56	5.58	4.81	3	2.84	2.75	2.06	1.63
0.5	4.72	4.60	4.27	2.55	2.50	2.40	1.87	1.35
0.6	4.07	3.96	3.71	1.92	2.23	2.17	1.75	1.28
0.7	3.50	3.46	3.35	1.89	2	1.93	1.64	1.25
0.8	3.12	3.03	2.96	1.86	1.96	1.84	1.57	1.19
0.9	2.78	2.77	2.69	1.85	1.84	1.78	1.50	1.14
1.0	2.50	2.50	2.45	1.85	1.77	1.71	1.18	1.10

Table A28: MB adsorption capacity for ZSM-5(50) as a function of contact time.

Contact time (h)	Dealumination time (h)							
	5	4.5	4	3	2	1.5	0.5	0
1	6.47	5.67	5	3.73	3.48	2.67	2.08	1.18
2	7.42	6.08	5.87	5.53	3.75	3.17	2.17	1.98
3	8	6.58	6.33	5.83	4.25	3.83	2.87	2.5
4	8.2	6.81	6.67	6.15	5.07	4.18	3.17	3.08
5	8.33	7.25	7.03	6.5	5.52	4.47	3.75	3.48

Table A29: MB adsorption capacity of ZSM-5(50) as a function of increasing initial concentration.

MB Concentration (mg/L)	Dealumination time (h)							
	5	4.5	4	3	2	1.5	0.5	0
50	8.02	7.90	7.43	4.31	3.53	3.22	3.12	2.50
100	16.03	15.60	5.07	2.67	2.08	1.75	0.53	1.58
150	21.23	7.50	7.50	4.02	3.12	2.68	0.83	0
200	19.41	5	5	4	2.50	1.83	1.33	0
250	16.43	4.33	4.33	0	0	0	0	0

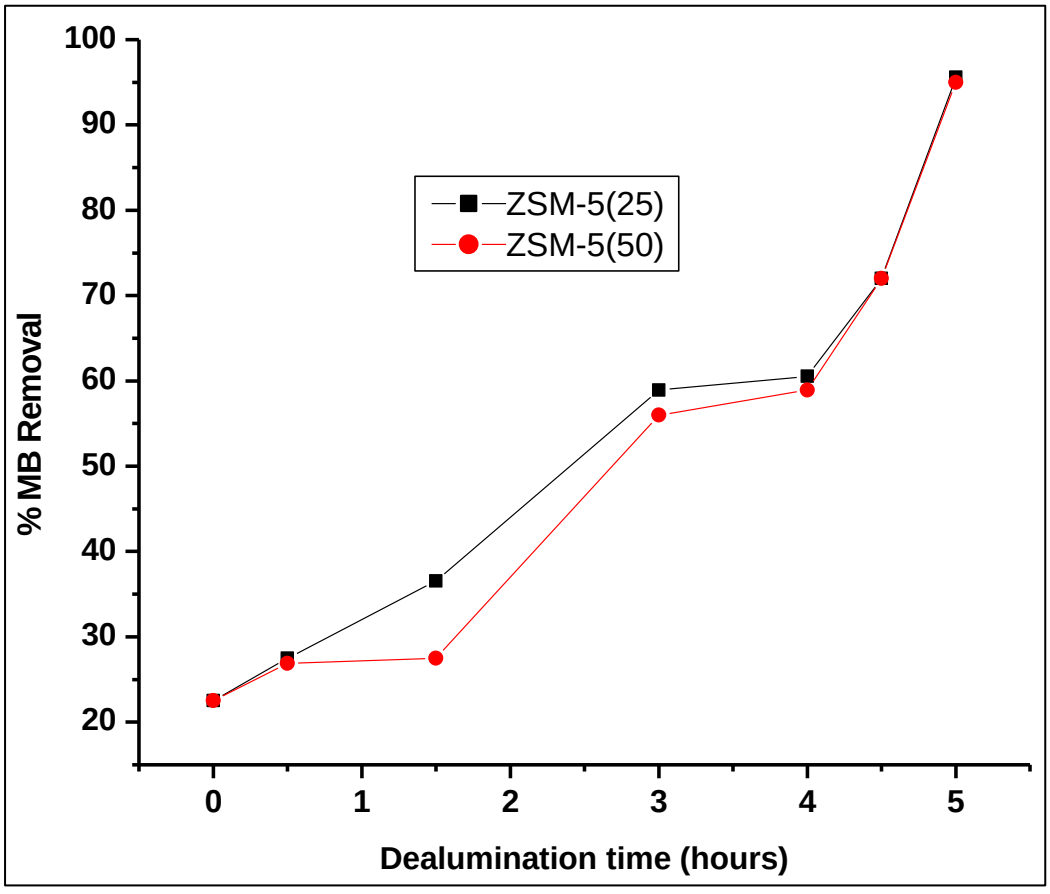

Figure A2: Comparison of MB uptake by ZSM-5(25) and ZSM-5(50) zeolites at pH 8 obtained after dealumination for 5 h.